Nano-Micro Letters

e-ISSN 2150-5551
CN 31-2103/TB

REVIEW

https://doi.org/10.1007/s40820-026-02178-9

Cite as
Nano-Micro Lett.
(2026) 18:331

Received: 5 January 2026
Accepted: 16 March 2026

Electrochemical Corrosion and Safety Hazards in Sustainable Batteries: Corrosion Mechanisms, Safety Challenges, and Protection

Chandrabhan Verma[1,2] ✉, Imad Barsoum[2,3], Akram Alfantazi[1], Kyong Yop Rhee[4] ✉

HIGHLIGHTS

- This review provides the first comprehensive collection of electrochemical corrosion mechanisms in Zn-, Al-, Mg-, Na-, organic-, and bio-based batteries, highlighting their safety and hazardous effects of corrosion in sustainable batteries.
- This review uniquely presents the connection of electrochemical corrosion with dendrite formation, hydrogen evolution, impedance growth, recycling challenges, capacity fading, and safety hazards.
- This provides a next-generation solution, such as corrosion inhibitors, bio-derived additives, metal–organic frameworks, deep eutectic solvents, ionic liquids, gel electrolytes, and interfacial and surface engineering approaches.

ABSTRACT The swift transition to sustainable energy has heightened demand for high-performance, safe, and environmentally responsible battery technologies. Zn–, Mg–, Na–, Al–, Fe–, organic, and bio-based systems offer several advantages over traditional resource-intensive and toxic alternatives. However, their practical implications are significantly challenged by their susceptibility to electrochemical corrosion, which adversely affects their efficiency, longevity, safety, recyclability, and reversibility. Corrosion is one of the most significant and persistent barriers to the development of next-generation energy storage systems. This review comprehensively presents unified mechanisms of corrosion across diverse sustainable battery systems, with a detailed account of pitting, uniform, galvanic, intergranular, and passivation-related degradation pathways. The article presents a unique comparison of the degradation mechanisms of Zn, Al, Mg, and other anodes in different electrolytes. Corrosion mitigation strategies, including surface passivation, surface engineering, alloying, use of surfactants and polymer-based films, ionic liquids, deep eutectic solvents, metal–organic frameworks, heterocycles, and bio-based multifunctional corrosion inhibitors, have been comprehensively surveyed. These inhibitors suppress the increase in cycle life, achieving inhibition efficiencies of over 90%. Lastly, the review highlights the design of molecular-level corrosion inhibitors, interfacial engineering, real-time corrosion testing, advanced electrolytes, and forward-looking directions, all of which are essential to the development of sustainable, stable energy storage systems.

KEYWORDS Electrochemical corrosion; Sustainable energy storage; Metal-anode batteries; Interfacial engineering; Corrosion inhibitors

✉ Chandrabhan Verma, chandraverma.rs.apc@itbhu.ac.in; Kyong Yop Rhee, rheeky@khu.ac.kr
[1] Department of Chemical and Petroleum Engineering, Khalifa University of Science and Technology, P.O. Box 127788, Abu Dhabi, United Arab Emirates
[2] Emirates Nuclear Technology Center (ENTC), Khalifa University, 12788 Abu Dhabi, United Arab Emirates
[3] Department of Mechanical and Nuclear Engineering, Khalifa University of Science and Technology, Abu Dhabi 12788, United Arab Emirates
[4] Department of Mechanical Engineering, College of Engineering, Kyung Hee University, Yongin 445-701, South Korea

Published online: 15 April 2026

Shanghai Jiao Tong University Press

Springer

1 Introduction

1.1 Safe and Sustainable Batteries: Need for Clean and Green Energy Transition

Batteries are electrochemical devices that change stored chemical energy into electrical energy through redox reactions [1, 2]. They consist of negative (anode) and positive (cathode) electrodes, a separator that prevents direct electrical contact between the electrodes, and an electrolyte that allows ions to move between the electrodes during charging and discharging. By storing wind and solar energy, they serve as renewable energy resources for on-demand use. They are widely used in electric vehicles (EVs) to minimize greenhouse gas emissions from transport and achieve a net-zero emissions (NZE) target by 2050 [3, 4]. The urgent climate goals, such as reducing CO_2 emissions, fossil fuel use, and improving the economy, have driven research and development (R&D) into battery technology. In the power sector, to achieve NZEs by 2050, global energy storage capacity needs to be increased sixfold to 1,500 GW, with batteries accounting for approximately 90% of this increase [5]. They have also reduced the reliance on fossil fuels and enhanced energy security. According to the IEA's 2024 report, the development of batteries alone in the transport sector could increase battery demand by nearly sevenfold by 2030, representing a significant shift that could displace over 8 million barrels of oil/day compared to the fossil fuel baseline. According to this report, the worldwide battery manufacturing size stood at nearly ~ 3 TWh in 2024 and is projected to reach ~ 6.5 TWh by 2030. Despite significant progress, scientists and engineers continue to work diligently to develop more affordable, energy-efficient, and environmentally friendly substitutes. This surge has led to noticeable improvements in charging speed, battery lifespan, and energy density.

Although traditional batteries have been widely used for decades, they pose significant health and environmental challenges due to their toxic materials (Fig. 1) [6, 7]. Lead-acid batteries, which are among the oldest, most reliable, and least expensive types of batteries, contain a highly poisonous lead electrode and a corrosive H_2SO_4 electrolyte [8]. If they are not suitably recycled or processed, they contaminate and adversely affect aquatic and soil life. Besides the toxicity concerns of lead, the spillage or leakage of highly corrosive acid causes metallic corrosion, skin burns, and damages the ecosystem by altering the pH of soil and water. Likewise, nickel–cadmium (Ni–Cd or NiCd) batteries are associated with several serious environmental and health issues, although they are relatively durable and can withstand many charge–discharge cycles [9, 10]. Cd is a highly toxic and cancer-causing element, adversely affecting the aquatic and soil life, and it accumulates in plants and animals after entering the food chain [11]. Cd also causes kidney and lung damage. Nickel-metal-hybrid (NiMH) batteries are relatively safer than Pb- and Cd-based batteries; nevertheless, they pose significant environmental challenges [10, 12].

The extraction, processing, and purification of the rare earth and Ni elements can cause severe ecosystem damage through mining waste contamination of soil and water, causing deforestation and soil erosion [13, 14]. The mining process is energy- and water-consuming, contributing to greenhouse gas emissions. Conventional Li-ion batteries, mainly composed of Ni, Mg, and Co (NMC) or Ni, Co, and Al (NCA), have undergone a remarkable transformation in current knowledge, powering laptops, EVs, and smartphones. However, they are associated with serious sustainability challenges, as mining-based extraction and processing of Co and Li result in water and soil pollution [15, 16]. Li-ion batteries also pose safety risks, as they can catch fire, explode, and overheat. Zinc-carbon (ZnC) batteries are frequently used in small household electronics such as flashlights. The toxicity concerns of ZnC batteries arise from corrosive chemicals and toxic metals, including NH_4Cl, MnO_2, and Zn. These substances can leak, especially after disposal, to cause aquatic and oil pollution. The environmental challenges and their short lifespan make them unsuitable alternatives for modern sustainability goals, despite the convenience and inexpensiveness.

Recently, demand for environmentally friendly and sustainable energy storage technologies has increased significantly as the shift toward renewable energy systems continues [17, 18]. Efforts are underway to minimize the carbon footprint, promote recycling, and encourage EV adoption, thereby enabling the emergence of eco-friendly, socially responsive, economically and technically viable alternatives. Sustainable battery strategies utilize renewable materials, energy-efficient and eco-conscious syntheses, and non-toxic components. These strategies promote biodegradability, recyclability, the circular economy, and sustainable sourcing, with enhanced renewability, safety, performance, and

https://doi.org/10.1007/s40820-026-02178-9

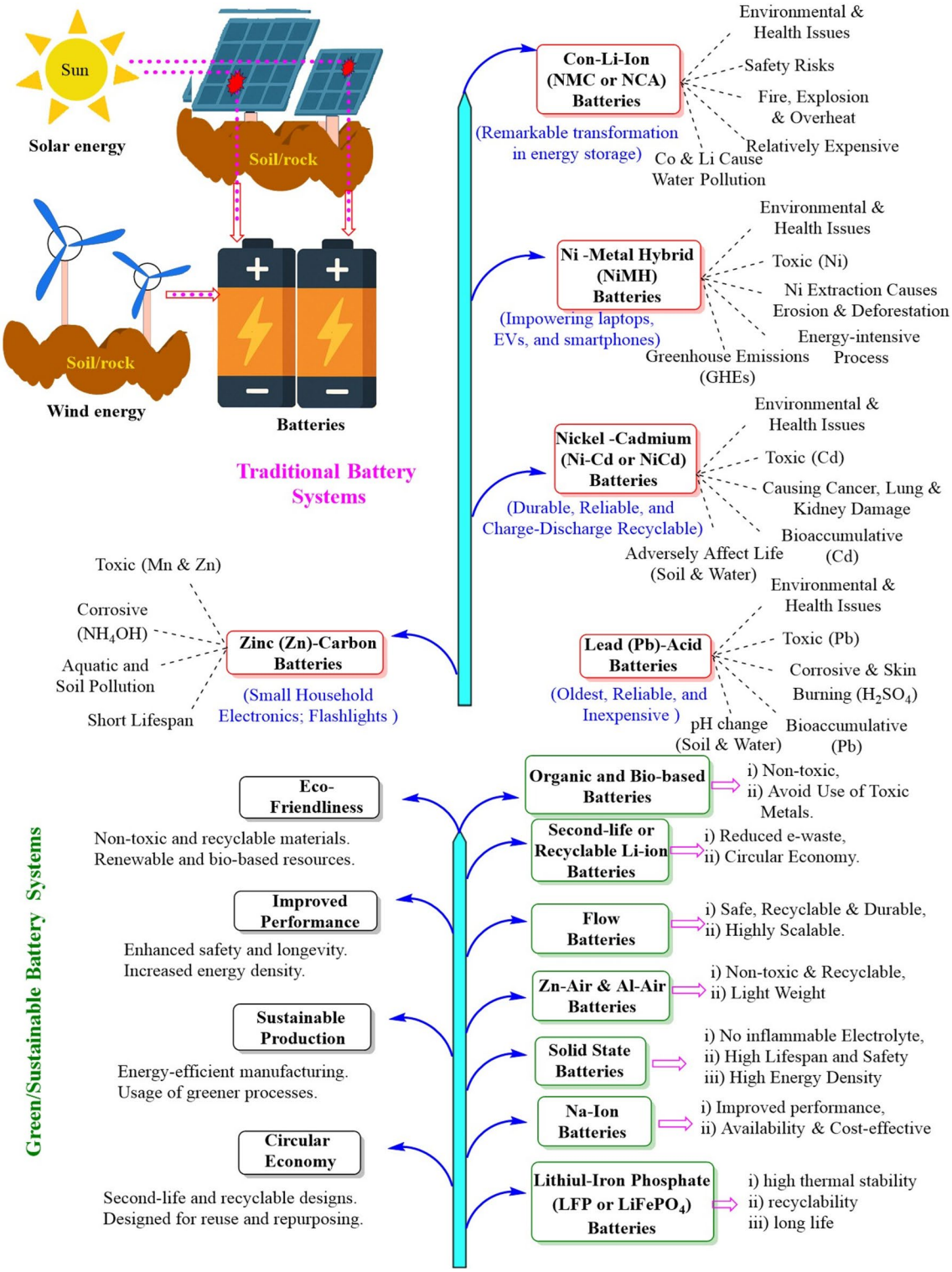

Fig. 1 Schematic illustration of challenges and drawbacks of traditional battery systems and opportunities of sustainable battery systems. The figure represents the comparative representation of (upper) conventional battery systems, including Ni–Cd, Pb-acid, Co/Ni-rich Li-ion, and NiMH, with particular emphasis on main challenges such as environmental burden, toxicity, dependence on raw materials, mining and disposal, limited recycling, and safety risks; and (lower) emerging (next-generation) battery systems, such as Zn-, Al-, Mg-, Fe-, Na-based, and organic/bio-based, with particular advantages of reduced toxicity, high compatibility, resource abundance, scalability and improved safety. The figure also shows that, despite several advantageous features of emerging battery systems, corrosion-mediated electrode degradation remains a significant challenge that adversely affects battery durability, stability, and performance

sustainability. The use of bio-inspired systems has shown great potential in bio-electrochemical and biomolecule-based batteries, imitating biological energy conversion [19–21]. These safe, biodegradable, and sustainable substitutes have already demonstrated great potential in wearable devices, environmental monitoring, biomedical applications, and agricultural systems. Recent studies have explored the use of promising biomolecules, such as lawsone, juglone, and flavins, as sustainable redox-active agents [22]. These naturally derived renewable biomasses eliminate toxic metals and deliver high energy density with excellent sustainability and biodegradability. The use of efficient and sustainable electrolytes, such as deep eutectic solvents (DESs), ionic liquids (ILs), renewable and bio-based polymers, additive-free water-based systems, and gel-based systems, has emerged as another sustainable strategy (Fig. 2) [23, 24]. Recently, the use of lignocellulose-based polymer electrolytes derived from biomass has also advanced substantially, owing to their enhanced interfacial compatibility, mechanical integrity, and controlled ion transport [25]. As illustrated in Fig. 2, the transition from convectional to next-generation sustainable batteries can be understood through a structured framework (Table 1): Challenges and shortcoming of traditional batteries (safety risks, toxicity, environmental burden, limited recyclability) motivate specific green or sustainable design principles (circular economy compatibility, recyclability, resource abundance, ecological safety, reduced risks and toxicity) which are then implemented through the targeted material-level strategies such as advanced electrolytes (e.g., ILs, DESs, and gel systems), sustainable electrodes (Zn, Al, Mg, Na, Fe, and organic systems), and nanostructured and bio-based separators. Nevertheless, despite these improvements, corrosion remains a critical shortcoming that affects the durability, stability, and performance of sustainable batteries.

These strategies also include using green and sustainable separators, especially those derived from natural resources, such as chitosan- and cellulose-based membranes, bio-based separators, and advanced nanostructured separators [26, 27]. Nowadays, lithium iron phosphate (LFP or $LiFePO_4$) batteries, which feature Co- and Ni-free compositions, offer numerous benefits, including high thermal stability, recyclability, and long life [28, 29]. Similarly, Na-ion batteries improve environmental performance due to their significant availability, non-toxicity, reduced production costs, especially at large scale, which minimizes resource strain and affordability [30]. Solid-state batteries eliminate the use of flammable liquid-based electrolytes, thereby increasing lifespan, energy density, and safety [31, 32]. These properties make them useful alternatives for next-generation EV batteries. Zn-air and Al-air batteries, which utilize oxygen from the air as a reactant, produce non-toxic, recyclable, and lightweight power sources useful for storage and backup systems [33, 34]. Flow batteries (organic or vanadium) offer safe, recyclable, durable, and highly scalable alternatives for renewable energy grids. Second-life or recyclable Li-ion batteries reduce adverse effects by supporting the circular economy and extending the usefulness of EV batteries, thereby reducing e-waste [35, 36]. Organic and bio-based batteries are composed of carbon and bio-based polymers, thereby avoiding the use of toxic heavy metals [37]. For the second-life use and safe recycling of Li-ion batteries, efficient discharge methods are essential. The redox-couple electrolytes, such as Fe(II)/Fe(III) systems, can be fully discharged without producing toxic gases. Obviously, this approach reduces the hazards and reasonably protects recycling workers. In the present article, the term "sustainable batteries" refers to emerging battery technologies that have emerged as alternatives to conventional toxic and critical-material-intensive battery systems such as Ni–Cd, Pb-acid, and Co-/Ni-rich Li-ion (NMC/NCA) batteries. The sustainable battery systems include aqueous and metal-anode batteries based on earth-abundant elements, such as Al, Zn, Mg, Na, and Fe, as well as selected organic or bio-based electrode systems. The sustainable battery systems offer several advantages over traditional alternatives, including safety, resource availability, and large-scale compatibility. This article aims to understand the corrosion mechanisms in sustainable battery systems, their associated challenges, consequences, and mitigation strategies.

1.2 Electrochemical Corrosion in Sustainable Batteries: Significance, Mechanisms, and Environmental Factors

Corrosion is defined as the degradation of metallic materials due to their interactions with environmental constituents [38]. In battery systems, corrosion poses a severe problem to the safety, long-term performance, and cost efficiency of the energy storage technologies, which are the most significant pillars of NZE 2050 [39, 40]. Corrosion adversely affects

https://doi.org/10.1007/s40820-026-02178-9

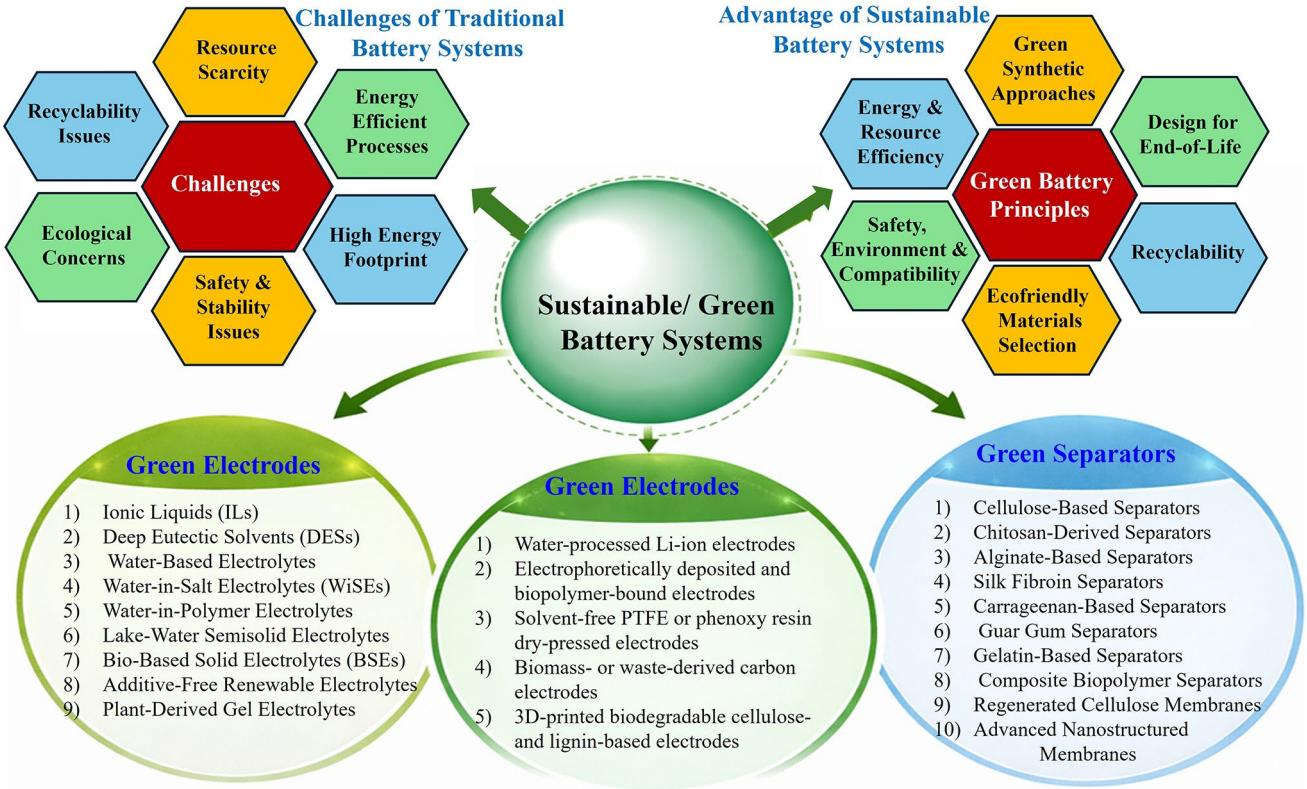

Fig. 2 Schematic presentation of the conceptual framework linking (i) main challenges and shortcomings of traditional batteries, such as safety risks, toxicity, environmental burden, and limited recyclability; (ii) green battery design principles, including circular economy compatibility, recyclability, resource abundance, environmental safety, reduced risks and toxicity; (iii) material-level use strategies such as advanced electrolytes (e.g., ILs, DESs and gel systems), sustainable electrodes (Zn, Al, Mg, Na, Fe, and organic systems), and nanostructured and bio-based separators. This figure shows that corrosion remains a critical shortcoming affecting the durability, stability, and performance of sustainable batteries

efficiency and lifespan, leading to undesirable replacement. This could increase the material cost and consumption, raise the carbon footprint, and reduce recyclability. Corrosion-related damages or failures can compromise the integrity and stability of the grid, as well as its reliability, discouraging confidence in clean energy transformations. Numerous battery components, including metallic connectors (e.g., Al in cathodes and Cu in anodes) and current collectors, are highly susceptible to electrochemical corrosion, particularly in humid, high-voltage conditions [41, 42]. Corrosion-related failures can cause short circuits, increase internal resistance, and promote the decomposition of electrodes and electrolytes. Electrochemical corrosion directly affects the performance of battery systems by reducing specific capacity and active material utilization due to continuous metal dissolution. The formation of unstable passive films and corrosion products increases interfacial resistance, thereby reducing the rate capacity and causing greater polarization. Unfavorable electrochemical corrosion directly affects key battery performance parameters. The dissolution of active metals at the anode reduces their capacity and lowers the energy density. The formation of passive films of oxides, hydroxides, or corrosion inhibitors increases interfacial charge transfer resistance, thereby reducing power output and increasing polarization. At the same time, excessive H_2 evolution reactions utilize electrolyte components and electrons without contributing to applicable charge (energy) storage. This leads to a decrease in Coulombic efficiency and accelerates self-discharge. Uneven metal dissolution and localized corrosion accelerate the risks of dendrite growth in rechargeable batteries. Dendrite growth not only reduces reversibility but also increases the risk of rapid capacity fading and internal short circuits. Therefore, in battery systems, corrosion is not just a problem of material (electrode) degradation but a

Table 1 A comparative summary of challenges of traditional battery systems, sustainability of green design principles, sustainable alternatives, and their advantages

S/N	Traditional battery challenges	Green/ sustainable design principles	Sustainable alternatives	Advantages of sustainable alternatives
1	Toxic electrodes (Co, Pd, Cd)-environmental and health risks	Replace with more sustainable alternatives	Zn, Al, Mg, Na, Fe-based metals, organic and bio-based systems	Improved environmental computability, reduced toxicity, and risks
2	Dependence on dangerous raw materials (rare earth elements, Ni, Co)	Replace with more abundant metal chemistries	Co/Ni-free cathodes, Zn-ion, Na-ion, Fe-ion, etc	Supply chain stability and resource abundance
3	High carbon footprint (due to mining-related processes)	Avoid mining-related processes to reduce the environmental impact	Recyclable separators, aqueous systems, and second-life battery uses	Circular economy mixing and minimizing ecological risks
4	Traditional organic electrolytes: flammability and thermal runway risks	Replace flammable electrolytes with less volatile ones	Solid-battery systems, aqueous systems, polymer gel electrolyte, and DESs/ILs electrolyte	Enhanced thermal and intrinsic safety
5	Disposal problem (hazardous) and limited recyclability	Focusing on metal recovery strategies	Recyclable electrodes (Metal) in an aqueous system	Enhanced material recovery and cycling
6	Performance in stability-side reactions and corrosion	Material design, surface engineering, and electrolyte modification	Alloying, corrosion inhibitors, functional additives, protective coatings, etc	Improved stability, cycle life, and performance

fundamental factor affecting battery efficiency, safety, cycle life, and rate capability. Corrosion-related shortcomings can pose environmental, health, and safety risks through interfacial corrosion and subsequent leakage.

Zhang et al. observed and reported that in Li-ion batteries, corrosion of Al (cathode) and Cu (anode) collectors results in contact loss, reduced power, short circuits, and increased resistance under stress [43]. High voltage and over-discharging cause Al and Cu to dissolve, respectively. During recharging, these processes pose safety risks, cause capacity loss, and lead to short circuits. Ruetschi proposed that corrosion is one of the main factors determining the batteries' lifespan [44]. The corrosion rate in battery electrolytes depends on temperature, voltage, and the metals (anodes and cathodes). The author proposed that the lifespan of batteries can be reduced by 50–75% if these factors are not adequately controlled or managed. Valve-regulated lead-acid batteries (VRLA) employed in UPS systems fail only in 3–5 years, much before their 10-year design life. Corrosion significantly reduces life expectancy. Interfacial interactions between electrodes and subsequent corrosion can reduce Li-ion battery performance by up to 20% [45, 46]. In EV lead-acid batteries, 30%-50% failures resulted from corrosion of the lead grids.

In batteries, Al, Zn, and Mg are frequently used as anodes due to their compatibility and high energy densities; however, they face significant corrosion challenges, especially in aqueous electrolytes [47, 48]. In these systems, corrosion is mediated by redox reactions that lead to undesirable and irreversible loss of metallic material, as well as adverse effects on battery performance, including shortened lifespan and reduced capacity. Mechanistically, corrosion can be classified into two types: general (uniform) and localized [49]. General corrosion occurs uniformly throughout the anode surface, causing uniform surface thinning or loss. On the other hand, in localized corrosion, some specific areas of the electrode surface experience more severe corrosion than the adjacent areas. The diffusion of electrolyte components (e.g., Cl^- and H_2O) and oxygen (O_2) or other active oxidants into the defective regions results in the formation of a pitting nucleus. Most localized corrosion occurs through the formation of aeration concentration cells, i.e., O_2-rich cathode and O_2-deficient anode regions. Corrosion can also initiate and propagate along grain boundaries [50, 51]. Obviously, the diffusion of corrosive or active species

https://doi.org/10.1007/s40820-026-02178-9

will be relatively easy in grain boundaries due to the high surface defect density. This results in easy setting of electrochemical cells, mainly through the aeration concentration mechanism. After initiation, corrosion may propagate along grain boundaries (intergranular corrosion) or through grains (intragranular corrosion). The dissolution mechanism can involve galvanic corrosion if the anodes contain metallic impurities [52, 53]. The mechanisms of uniform (general) and localized corrosion are schematically presented in Fig. 3. Figure 3a illustrates the anodic metallic dissolution and cathodic reduction reactions occurring in the aqueous electrolytes. Notably, in anode dissolution, a single anodic reaction (oxidation) occurs, whereas several cathodic reactions are possible depending on the electrolyte composition. Hydrogen evolution and oxygen reduction are significant cathodic reactions in proton- and oxygen-based electrolytes, respectively. Figure 3b depicts the development of the electric double layer at the interface of the metal and electrolyte. This schematic illustrates the formation of the inner Helmholtz plane (IHP), the outer Helmholtz plane (OHP), and the diffuse layer (bulk solution), showing the interfacial potential distribution and charge separation. The general or uniform corrosion of the anode in the battery electrolyte is illustrated in Fig. 3c, which shows a homogeneous material loss throughout the surface. Localized corrosion mechanisms, including pitting, intergranular, and galvanic corrosion, are described in Fig. 3d–f. Lastly, the formation of oxygen gradient cells, or concentration cells, due to different oxygen concentrations at the anode and cathode regions, and the subsequent corrosion, is schematically presented in Fig. 3g.

The corrosion mechanisms of different anodes, including Mg, Zn, Al, and Fe, vary with the environment's pH [46, 54]. At acidic pH levels, these metals dissolve due to the reduction in hydrogen ion concentration. In neutral conditions, oxygen reduction is a significant cathodic reaction that forms oxide and hydroxide ions. Dissolved metal ions react with oxide and hydroxide ions, forming the corresponding metal oxides and hydroxides, which passivate the metal surface. The protective nature of the passive layer varies depending on the nature of the metals, pH, and other environmental factors. The corrosion mechanisms of some common anodes, including Zn, Mg, Al, and Fe, are presented herein. A more detailed account of the inhibition mechanisms can be found elsewhere [46]. Among the different anode materials used in sustainable batteries, Zn has attracted particular attention owing to its favorable electrochemical properties and compatibility with aqueous electrolytes used in battery applications. Nevertheless, the corrosion behavior of Zn strongly depends on pH and the dissolved species of the electrolyte.

(i) Corrosion Behavior of Zn-Anode

Zn is a sacrificial anode in different systems as it readily oxidizes and forms Zn^{2+} ions. In acidic conditions, zinc dissolves by reducing H^+ ions, releasing hydrogen gas (H_2). In neutral environments, reduction of O_2 occurs as a major cathodic (reduction) reaction, forming $Zn(OH)_2$ that provides slight corrosion protection. Zn forms highly soluble $Zn(OH)_4^{2-}$ (zincate) ions in alkaline conditions. $Zn(OH)_4^{2-}$ ions accelerate the dissolution of the passive layer, thereby increasing the corrosion rate, particularly at elevated alkalinity. The behavior of Zn corrosion in different pH levels is as follows:

Corrosion of Zn in acidic environments The nature of Zn corrosion greatly depends upon the electrolytes' pH, as seen by the Pourbaix diagram of the Zn-H_2O system (Fig. 4a). Figure 4b shows that the formation of different corrosion products also depends on pH: Low pH favors the formation of Zn^{2+} ions, whereas high pH favors the formation of $Zn(OH)_4^{2-}$ ions. On the other hand, the formation of ZnO and $Zn(OH)_2$ predominantly occurs at intermediate pH levels. The dissolution of Zn at the anode liberates electrons, which are consumed at the cathode by species, such as H^+, H_2O, and O_2, leading to self-dissolution. In acidic conditions, the anodic dissolution, cathodic Zn deposition, and H_2 evolution reactions occur as follows [46]:

$$Zn \rightarrow Zn^{2+} + 2e^- \quad \text{(anodic dissolution)} \tag{1}$$

$$Zn^{2+} + 2e^- \rightarrow Zn_{(solid)} \quad \text{(cathodic deposition)} \tag{2}$$

$$2H^+ + 2e^- \rightarrow H_{2(gas)} \quad (H_2\text{evolution}) \tag{3}$$

In acidic conditions, Zn^{2+} ions form as the thermodynamically most stable species, and the corrosion rate is mainly governed by the hydrogen evolution reaction (HER) [55, 56]. However, at slightly higher acidic pH (3–5), the diffusion of H^+ ions (to the cathode) becomes slower, and the rate of Zn corrosion is mainly governed

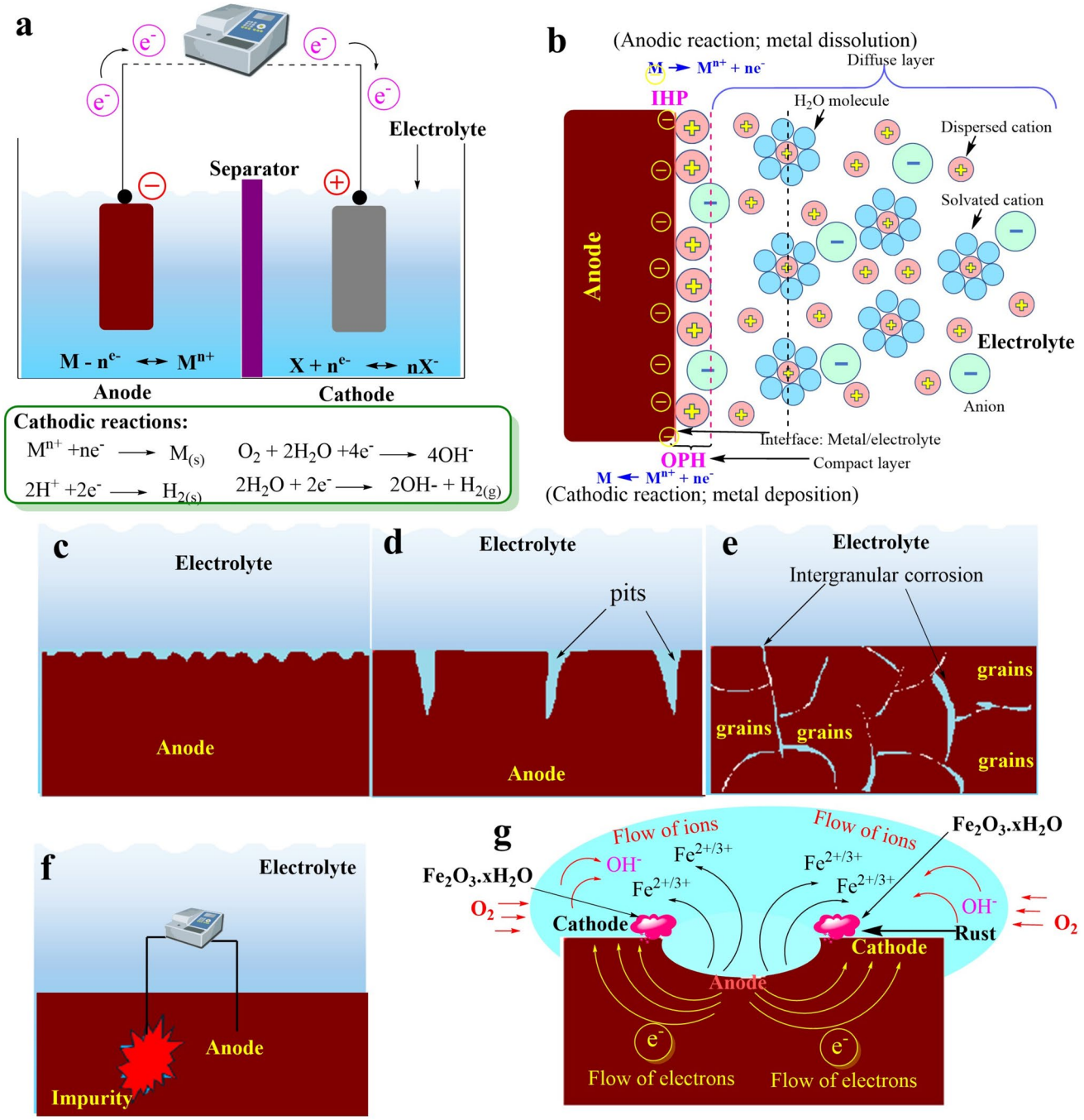

Fig. 3 Schematics showing **a** mechanisms of anodic and cathodic reactions in aqueous electrolytes, **b** formation of the electric double layer/interface between metal and electrolyte, **c** uniform (general) corrosion, **d** pitting corrosion, **e** intergranular corrosion, **f** galvanic corrosion, and **g** the formation of aeration concentration cells due to oxygen gradient

by H^+ ions diffusion or mixed kinetics [57, 58]. Figure 4c, d represents the mechanism of Zn corrosion in acidic environments.

Corrosion of Zn in neutral environments In neutral or mildly acidic electrolytes, the corrosion rate (C_R) determining process shifts from HER to oxygen reduction reaction (ORR). In these circumstances, the cathodic reactions can be illustrated as follows [46, 56]:

$$H_2O + 2e^- \rightarrow 2OH^- \quad \text{(deaerated environment)} \tag{4}$$

https://doi.org/10.1007/s40820-026-02178-9

$$O_2 + 2H_2O + 4e^- \rightarrow 4OH^- \quad \text{(Aerated environment)} \tag{5}$$

The ORR reaction kinetics are activation-controlled, and because of their very high irreversibility, they are independent of electrolyte pH. The presence of oxygen can significantly increase the C_R. In these conditions, the anodic dissolution reactions are relatively complex and involve many ways, including Eq. (1). The anodic responses can be expressed as follows [46, 56]:

$$Zn^{2+} + 2OH^- \rightarrow Zn(OH)_2 \tag{6}$$

$$Zn(OH)_2 \rightarrow ZnO + H_2O \tag{7}$$

$$Zn(OH)_2 + 2OH^- \rightarrow Zn(OH)_4^{2-} \tag{8}$$

Notably, corrosion products are relatively porous, allowing the diffusion or penetration of corrosive species, such as Cl^- and SO_4^{2-} ions. These ions may react with Zn^{2+} and other corrosion products to form corresponding Zn salts. For example, Cl^- ions can react with Zn^{2+} and $Zn(OH)_2$ to form corresponding hydroxide compounds, as expressed by the following equations [46, 59]:

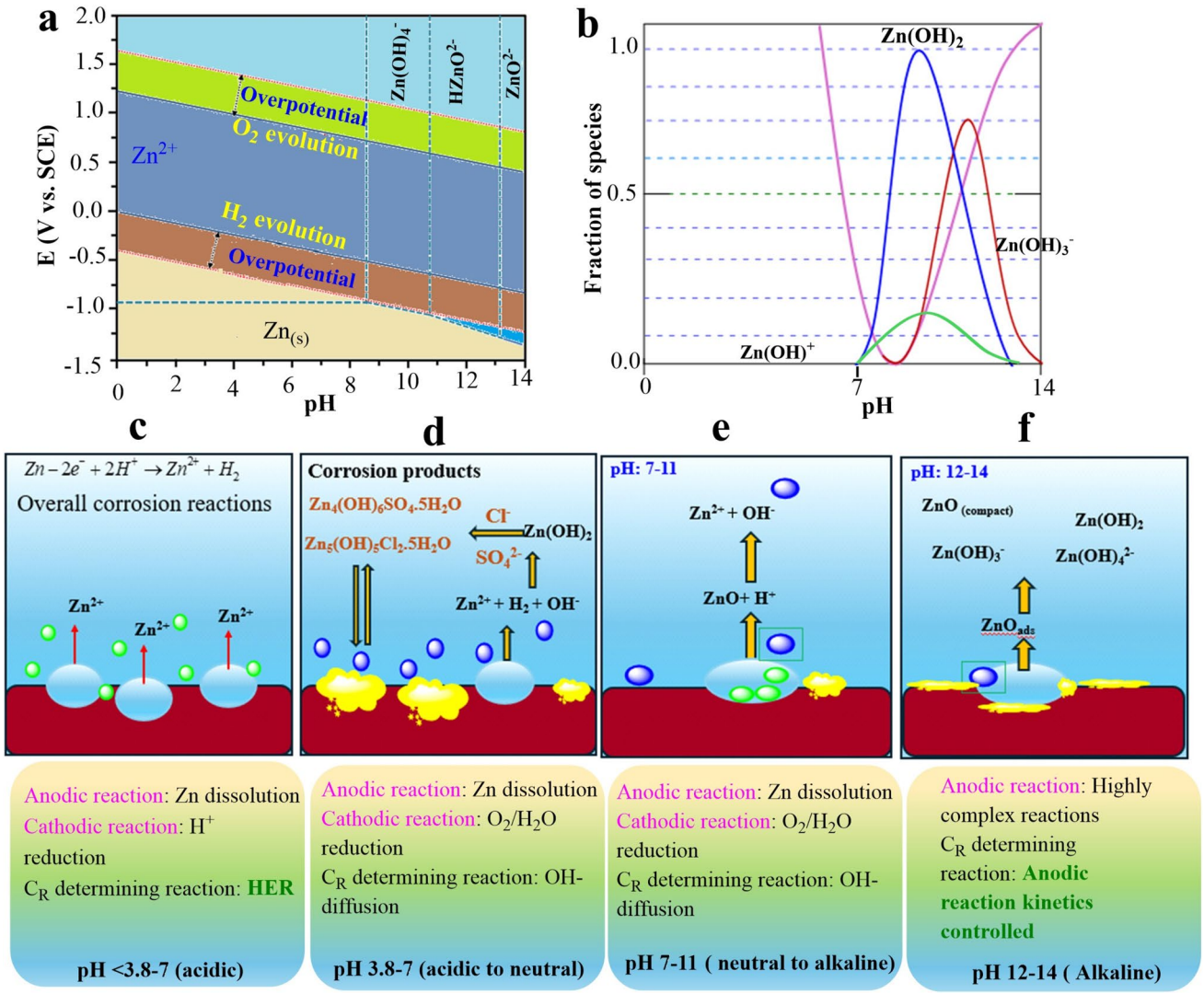

Fig. 4 Schematic illustrations of **a** Pourbaix diagram of Zn-H_2O system at RT, **b** relative fraction of different species at various pH, **c–g** the dissolution mechanisms of Zn, formation of different corrosion products at different pH, and protection mechanisms of corrosion products

$$5Zn^{2+} + 8OH^- + 2Cl^- + H_2O \rightarrow Zn_5(OH)_8Cl_2 \cdot H_2O \quad (9)$$

$$5Zn(OH)_2 + +2Cl^- + H_2O \rightarrow Zn_5(OH)_8Cl_2 \cdot H_2O + 2OH^- \quad (10)$$

Likewise, ClO_4^- and SO_4^{2-} ions can accelerate the Zn corrosion by following reactions [46, 59, 60]:

$$Zn + 2ClO_4^- \rightarrow Zn(ClO_4)_{2(aq)} + 2e^- \quad (11)$$

$$Zn(OH)_2 + 3Zn^{2+} + 4OH^- + SO_4^{2-} + 5H_2O \rightarrow Zn_4(OH)_6SO_4 \cdot 5H_2O \quad (12)$$

$Zn_4(OH)_6SO_4.5H_2O$ forms a more compact and protective layer than $Zn_4(OH)_8Cl.H_2O$, mainly due to the aggressiveness of Cl^- ions. The formation rate of ion pairs or complexes accelerates the Zn dissolution of these ions, following the following trend: $Cl^- > SO_4^{2-} > ClO_4^-$. The pH of Zn-based batteries typically ranges between 3 and 6 [46, 61].

Corrosion of Zn in alkaline environments In alkaline environments, the reduction of H_2O and O_2 (ORR) contributes as a significant cathodic reaction. In the pH range of 7 to 10, zinc dissolution occurs via two mechanisms.

$$Zn + H_2O \rightarrow ZnO + 2H^+ + 2e^- \quad (13)$$

$$Zn + H_2O + H^+ \rightarrow Zn(OH)^+ + 2H^+ + 2e^- \quad (14)$$

The passive film formed on the ZnO does not provide significant corrosion protection. This type of passive film is commonly called a pseudo-passive film. The formation of the pseudo-passive film is a net result of passive film destabilization by H^+ ions and its formation as the corrosion reactions progress. Notably, oxides and hydroxides form at high pH (11–13), and the kinetics of anodic reactions mainly govern the C_R. At pH 11, the insufficient supply of H^+ results in limited Zn hydrolysis, leading to small domains of passivity. At pH 12, a compact film of ZnO can be formed by the separate or combined actions of the adsorption and nucleation-growth models, which can be illustrated as follows [62, 63]:

$$Zn + OH^- \rightarrow ZnOH_{ads} + e^- \quad (15)$$

$$ZnOH_{ads} \rightarrow ZnO + H^+ + e^- \quad (16)$$

$$Zn + 2OH^- \rightarrow ZnO + H_2O + 2e^- \quad (17)$$

The compact ZnO film thus formed is referred to as a type III oxide. A type III oxide film is relatively thin but provides significant protection against further corrosion. $Zn(OH)_3^-$ forms on further increasing the alkalinity (pH: 13–14), as expressed below [46, 56]:

$$ZnOH_{ads} + OH^- \rightarrow Zn(OH)_2 + e^- \quad (18)$$

$$Zn(OH)_2 + OH^- \rightarrow Zn(OH)_3^- \quad (19)$$

As corrosion reactions progress, the formation of $Zn(OH)_3^-$ is hindered by local supersaturation, which restricts the transport of OH- ions at the metal-electrolyte interface, leading to the gradual deposition of $Zn(OH)_2$ on the surface. Simultaneously, the dissolution of $Zn(OH)_3^-$ and $Zn(OH)_4^{2-}$ also results in the building of ZnO, as per the following equations [46, 56]:

$$Zn(OH)_3^- + H^+ \rightarrow ZnO + 2H_2O \quad (20)$$

$$Zn(OH)_4^{2-} \rightarrow ZnO + H_2O + 2OH^- \quad (21)$$

Thus formed, the ZnO passive film is referred to as a type I oxide. In this process, the dissolution of $Zn(OH)_2$ is the rate-determining step. When the OH-concentration decreases, the dissolution of $Zn(OH)_2$ halts, and a well-defined, highly protective oxide film, known as a type II oxide, forms. Noticeably, type I and II oxides form relatively larger proportions; however, type III oxide plays a more significant role in transiting the Zn surface in the passive (oxide) state [63]. Typically, alkaline Zn and Zn-air batteries use highly concentrated KOH solutions with a pH above 13.

Cathodic reactions can be considered rate-determining steps in the corrosion of Zn anodes in batteries. In milder acidic conditions (pH 4–6), H^+ diffusion significantly affects the CR, whereas at pH 7–10, ORR becomes the main cathodic reaction. A higher pH favors the formation of corrosion-protective passive films. Numerous active species, including I_3^-, Br_2, and Br_3^-, can diffuse to the Zn anode, leading to chemical corrosion. Oxygen and hydrogen evolution are commonly experienced in Zn-I_2 cells, possibly due to interactions of iodine species with $Zn(OH)_2$ [64]. Self-discharge and chemical corrosion are influenced by the diffusion of active Br_2 and Br_3^- in Zn-Br_2 batteries. Localized corrosion, primarily pitting corrosion, is commonly encountered in Zn batteries due to the diffusion of halide ions through defective passive films. Sometimes, local

https://doi.org/10.1007/s40820-026-02178-9

acidification resulting from the hydrolysis of Zn and potential differences in pits and adjacent areas can form galvanic cells. Both localized processes increase the anodes' C_R. In practical Zn-based battery systems, these material degradation processes directly translate into reduced battery performance. The continuous, undesirable degradation and loss of Zn result in lower specific capacity and reduced active material utilization over repeated cycles. Moreover, H_2 evolution due to cathodic reduction accelerates electrolyte and electron consumption, promoting self-discharge and reducing coulombic efficiency. Localized corrosion and uneven metal dissolution or deposition can lead to dendrite growth and a rougher surface, which, in turn, shortens cycle life and increases polarization. The accumulation of corrosion products and ZnO on the electrode surface can adversely affect ion transport pathways, reduce rate capability, and increase impedance. Given these, effective corrosion mitigation is essential to achieve long-term cycling stability, a stable discharge voltage, and high reversibility in Zn-based battery systems. The corrosion on Zn is primarily governed by zincate formation and H_2 evolution in alkaline electrolytes. Al exhibits markedly different corrosion behavior due to its amphoteric nature and its ability to form highly stable, protective oxide films. Therefore, the mechanisms of Al corrosion have been analyzed and presented separately.

(ii) Corrosion Behavior of Al-Anode

Al-ion batteries, especially Al-air batteries, which use highly acidic or alkaline electrolytes, have recently shown great potential for battery applications. Being amphoteric, AL is highly sensitive to alkaline and acidic environments. The Pourbaix diagram of the Al-H_2O system indicates that Al is highly susceptible to corrosion due to the decomposition of water, as the stability domain of Al is significantly lower compared to that of H_2O. The dissolution of Al results in the formation of Al^{3+}, Al_2O_3, and AlO_2 depending on pH. Due to Al's high reactivity, a thin, compact oxide layer forms on the Al surface, which is highly soluble in acidic electrolytes. In acidic environments, the dissolution of the oxide layer involves a field-assisted or chemical process as expressed below [46, 65, 66]:

$$Al_2O_3 + 6H^+ \rightarrow 2Al^{3+} + 3H_2O \quad (22)$$

$$Al_{(ox)} \rightarrow 2Al^{3+}_{aq} + Al^{3-}_{Al(ox)} \quad (23)$$

In these equations, $Al_{(ox)}$, Al_{aq}^{3+}, and $Al_{(ox)}^{3-}$ represent Al atoms in oxide film, Al^{3+} ions in aqueous solution, and Al vacancy in oxide film, respectively. The H^+ ions present in the electrolyte can move to the oxide film and form H_2O by reacting with O^{2-}. Meanwhile, O^{2-} species can be eliminated, and Al^{3+} ions can enter the lattice to form Al_2O_3. The migration of Al^{3+} to Al vacancies, accompanied by the evolution of H_2 at the Al/Al_2O_3 interface, results in Al surface pitting corrosion. The aggressive H^+ ions freely attack the bare Al surface with a rapid increase in corrosion rate, once the surface oxide film is completely removed, as expressed as follows:

$$Al + 3H^+ \rightarrow Al^{3+} + 3/2H_2 \quad (24)$$

Aggressive anions, including SO_4^{2-}, Cl^-, and NO_3^-, complicate the corrosion process. Because of their great diffusibility and aggressiveness, the Cl^- ions produce more significant effects than other anions. Cl^- ions participate in Al corrosion and the oxide layer dissolution as follows [66]:

$$Al + nCl^- \rightarrow AlCl^{(n-3)-} + 3e^- \quad (25)$$

$$Al^{3+}(Al_2O_3) + 4Cl^- \rightarrow AlCl_4^- \quad (26)$$

Cl^- ions preferentially adsorb on the Al surface by replacing the pre-adsorbed H_2O molecules, favoring the transfer of Al from metal to solution phase. The mechanism of Al corrosion in acidic electrolytes containing SO_4^{2-} and NO_3^- ions is significantly slower, which may be attributed to their lesser aggressiveness compared to Cl^- ions. Some studies suggest that the presence of SO_4^{2-} ions decreases the aggressiveness of Cl^- ions by preferential adsorption of less aggressive SO_4^{2-} ions [67, 68]. Another opinion proposes that SO_4^{2-} ions form surface protective $Al_2(SO_4)_3.18H_2O$ and $Al(OH)SO_4^-$based passive films, which protect against corrosive dissolution [69]. NO_3^- ions increase the stability of the passive film, decreasing the C_R. Nevertheless, several species such as NO, N_2, $Al(NO_3)_3$, NO_2^-, and NH_3 form in the presence of NO_3^- ions, making the dissolution mechanism complex, unclear, and unestablished [70–72]. In some studies, the authors claimed that these species can react with Al/Al^{3+} to form complexes that can accelerate the C_R [73]. These discussions revealed that the dissolution of Al in acidic environments depends more on the nature and behavior of anions than on the pH of electrolytes.

The oxide film is highly stable and insoluble, according to the mechanism of Al dissolution in neutral electrolytes. Coronation starts with the hydrolysis of the Al–O–Al bond of Al_2O_3, which forms the corresponding Al–OH species. As hydrolysis continues, the surface oxide film converts to a highly porous, poorly crystallized pseudo-boehmite (i.e., AlOOH) film, allowing water molecules to diffuse to the Al-AlOOH interface. Obviously, at this stage, C_R is controlled by hydrolysis. Corrosion begins immediately when H_2O molecules meet the Al surface. The Al^{3+} ions so formed react with OH^- ions of water, as presented below [46, 74]:

$$Al^{3+} + OH^- \rightarrow Al(OH)^{2+} \quad (27)$$

$$Al^{3+} + 2OH^- \rightarrow Al(OH)_2^+ \quad (28)$$

$$Al^{3+} + 3OH^- \rightarrow Al(OH)_3 \quad (29)$$

The growth and nucleation of Al hydroxide govern the C_R at this stage. $Al(OH)^{2+}$ and $Al(OH)_2{}^+$ species diffuse into the solution, and H_2O molecules diffuse to the interface of Al/Al_2O_3. Over time, the oxide film thickness and its passivating behavior increase, reducing the C_R. Therefore, the transport of these species determines the C_R. The nucleation and growth of H_2 gas bubbles at the Al/Al_2O_3 interface may adversely affect surface passivation, leading to pitting corrosion. In mild alkaline solutions, the corrosion mechanism is like that in neutral electrolytes, forming numerous species, including $Al(OH)_3$, Al_2O_3, and AlOOH. OH- ions of water may diffuse to Al/Al_2O_3 and disrupt the oxide film stability as follows:

$$Al(OH)_3 + OH^- \rightarrow Al(OH)_4^- \quad (30)$$

At this stage, diffusion of $Al(OH)_4{}^-$ and OH^- to or from the Al_2O_3/electrolyte interface can be considered the rate-determining step. In alkaline electrolytes, the Al^{3+} ions are thermodynamically unstable, which renders their direct ejection from the oxide films. Nevertheless, the dissolution of Al_2O_3 films proceeds as per the following equation:

$$Al(OH)_3 + OH^- + H_2O \rightarrow Al(OH)_4^- \quad (31)$$

The oxide film is completely dissolved in fundamental (alkaline) solution, resulting in direct attack of the Al surface by OH^- ions, as expressed below:

$$Al + 4OH^- \rightarrow Al(OH)_4^- \quad (32)$$

Moreover, the diffusion of $Al(OH)_4{}^-$ and OH^- does not significantly influence the C_R in highly alkaline solutions. Moreover, the presence of alloying metal impurities leads to the formation of galvanic cells and subsequent galvanic corrosion in Al batteries. Mg demonstrates even greater dissolution complexity and chemical reactivity than Zn and Al. Mg-based systems are particularly challenging in aqueous batteries, as they are prone to substantial hydrogen evolution and are subject to multiple competing models.

(iii) Corrosion Behavior of Mg-Anode

The Mg anode exhibits higher self-corrosion than Zn and Al due to its high reactivity. Due to its high reactivity, Mg in intermetallic alloys such as Mg_2Si and Al_3Fe acts as the anode, with the remaining alloying elements serving as the cathodes. Mg-air and Mg-MnO_2 are typical examples of Mg-based aqueous batteries. Rechargeable Mg-air batteries face significant challenges due to their poor high-rate stability and low energy conversion efficiency. The Pourbaix diagram indicates that Mg lacks a stable domain in aqueous electrolytes because its equilibrium potential is lower than that for H_2 evolution. The behavior of Mg corrosion is more complicated than that of Zn and Al. Several hypothetical mechanisms, including the univalent film-based model, the Mg-hydride intermediate model, the Mg-based model, and the metal spalling model, have been proposed to explain the dissolution of the Mg anode in Mg-based aqueous batteries. These models have their own benefits and drawbacks. The Mg-hydride intermediate model suggests that on the Mg surface, MgH_2 exists and plays a significant role in corrosive dissolution [75, 76]. Firstly, Mg is reduced to form MgH_2, followed by its oxidation in neutral or alkaline solution to form $Mg(OH)_2$ or Mg^{2+} ions in acidic solution, as expressed follows:

$$Mg + 2H^+ + 2e^- \rightarrow MgH_2 \quad (33)$$

$$MgH_2 + 2H_2O \rightarrow Mg(OH)_2 + 2H_2 \quad (34)$$

$$MgH_2 + 2H^+ \rightarrow Mg^{2+} + 2H_2 \quad (35)$$

The unprotected Mg can also be dissolved directly to form Mg^{2+} ions, as shown below [77]:

$$Mg \rightarrow Mg^{2+} + 2e^- \quad (36)$$

https://doi.org/10.1007/s40820-026-02178-9

The univalent model proposed that Mg dissolution initiates with the formation of univalent Mg (Mg^+), as expressed below:

$$Mg \rightarrow Mg^+ + e^- \quad (37)$$

The univalent Mg^+ ions are volatile and readily oxidized to Mg^{2+} as per the following mechanisms:

$$2Mg^+ + 2H^+ \rightarrow 2Mg^{2+} + 2H_2 \quad (38)$$

$$2Mg^+ + 2H_2O \rightarrow 2Mg^{2+} + 2OH^- + H_2 \quad (39)$$

These dissolution processes have been extensively studied in acidic electrolytes, but the mechanisms of dissolution in neutral and alkaline electrolytes remain unclear. The film-based model proposes that, due to Mg's high reactivity, it readily forms $Mg(OH)_2$ and MgO passive films, even in cathodic polarization zones. The passive films break once the anodic polarization potential exceeds the breakdown potential, leading to Mg dissolution [46, 78]. The uneven dissolution was attributed to a spalling mechanism, in which Mg dissolves as flakes or small particles, leading to H_2 evolution without current flow [46, 79]. The recent findings suggest that insoluble Mg and Mg^{2+} ions do not participate in the dissolution process. Another model suggests that in the presence of aggressive ions, Mg dissolution starts by breaking down the MgO film at reactive sites. This ultimately results in the formation of $Mg(OH)_2$, increasing Mg corrosion and H_2 evolution. This process occurs at the MgO/$Mg(OH)_2$ interface, where Mg^{2+} ions can diffuse in the electrolyte or precipitate on the surface as $Mg(OH)_2$ [80, 81]. In neutral electrolytes, the overall corrosion reactions can be presented as follows:

$$Mg + 2H_2O \rightarrow MgO + 2OH^- + H_2 \quad (40)$$

Mg-air and Mg-MnO_2 batteries primarily use NaCl-based aqueous electrolytes, and the corrosion mechanism of the Mg anode can be described by the equation above. At high pH (above 10.5), the $Mg(OH)_2$ film provides anticorrosion protection through passivation. The MgO and $Mg(OH)_2$ films are volatile and soluble in acidic electrolytes, accelerating the C_R, as follows [82, 83]:

$$MgO + 2H^+ \rightarrow Mg^{2+} + H_2O \quad (41)$$

$$Mg + 2H^+ \rightarrow Mg^{2+} + H_2 \quad (42)$$

In Mg-based alloys, Mg dissolution follows trends like those of pure Mg, with H_2 evolution as the dominant cathodic reaction. The presence of alloying metal impurities leads to the setting of galvanic cells and subsequent galvanic corrosion in Mg batteries. The dissolution mechanism of the Fe anode and other metal anodes can be found elsewhere [45, 46, 84]. Although Zn, Mg, and Al anodes exhibit different electrochemical behavior, their corrosion mechanisms share a common fundamental: anodic metallic dissolution (actual electrode loss) and cathodic hydrogen evolution reaction (HER) or oxygen reduction reaction (ORR). In these systems, corrosion rates and mechanisms are strongly influenced by pH-dependent passivation and the stability of passive (oxide or hydroxide) films. Nevertheless, the significant differences originate from the properties of oxide layers and their intrinsic thermodynamic stability. Obviously, Zn forms amphoteric corrosion products, such as zincate, in alkaline electrolytes and exhibits relatively moderate self-corrosion. In acidic and neutral environments, corrosion is mainly controlled by the reduction of protons to form hydrogen gas and by the decrease in oxygen. In contrast, Al forms a highly stable, compact, and uniform oxide film under neutral conditions, resulting in relatively superior passivation. However, due to the amphoteric nature of Al-based passive films, they are susceptible to strong acidic or alkaline conditions and become highly unstable under such conditions.

Mg acquires a more negative equilibrium potential and is electrochemically more reactive. Mg lacks a wide stability domain in aqueous electrolytes and undergoes pronounced self-corrosion, leading to extensive H_2 evolution. The uneven accumulation of corrosion products results in a rough Zn-based surface, leading to halide-induced dendrite growth and localized pitting corrosion. Likewise, chloride ingress also breaks the passive layers on the Al surface, while in Mg, galvanic coupling with intermetallic phases and passive film instability govern the passive film stability. These discussions show that, while corrosion mechanisms across different electrolyte systems and electrodes can be described by a unified mechanism, their severity, major degradation pathways, and passivation stability differ remarkably, necessitating material-specific corrosion protection strategies. The development, breaking, and regeneration of oxide- or hydroxide-based passive films play a significant role in controlling the kinetics of anodic dissolution reactions. The stability of these oxide or hydroxide films largely depends on transport phenomena, ionic species, pH,

and applied polarization potential. Moreover, in Zn, Al, and Mg, localized (pitting or intergranular) corrosion occurs by the ingress or diffusion of corrosive species through surface defects, galvanic coupling among microstructural heterogeneities, and concentration gradients. As a result, anode corrosion in battery systems can be described as the coupling of different phenomena, including redox (electrochemical) reactions, transport processes, and passivation, which are governed by thermodynamic stability, mass transport, and corrosion kinetics.

In battery systems, in addition to intrinsic material and electrolyte properties, the degradation mechanisms and corrosion kinetics of anodes are greatly governed by operating conditions. By increasing the diffusion coefficients and charge transfer kinetics, temperature significantly increases corrosion and dissolution rates [85, 86]. Elevated temperatures adversely affect the stability of protective films, promoting the risks of localized corrosion and hydrogen evolution [87]. Similarly, fast charging rates and relatively high current density promote dendritic growth, leading to localized pitting, anodic polarization, and increased overpotential [88, 89]. High depth-of-discharge and repeated cycling conditions can induce mechanical stress on passive films, increasing the risk of cracking and exposing a fresh anodic surface to corrosive electrolyte [88, 89]. In seawater and flow-based battery systems, the hydrodynamic and electrolyte velocity conditions affect the mass transport of corrosive species (e.g., SO_4^{2-}, Cl^-), thereby influencing concentration cell formation and localized corrosion [90, 91]. Moreover, pressure and state-of-charge fluctuations and oxygen concentration gradients may promote galvanic coupling and adversely affect interfacial stability [92, 93]. Thus, in practical battery systems, corrosion behavior not only depends on the nature and properties of the anodes and the electrolyte composition but is also coupled with real operating parameters.

Under extreme conditions, e.g., elevated temperature and high voltage, metal-ion corrosion in aqueous electrolytes is significantly intensified, significantly limiting the practical operating window. The thermodynamic driving force for anodic dissolution increases at relatively high anodic potential (E_{anodic}), leading not only to accelerated oxidation and metal dissolution but also to destabilization of protective passive films [94]. Likewise, increased voltage can trigger electrolyte oxygen evolution reaction (OER), electrolyte decomposition, and degradative side reactions [95, 96]. These side reactions also generate several active species, which diminish the protective properties of oxide or hydroxide passive films. In Al-, Mg-, and Zn-based battery systems, the stability domains defined by the Pourbaix diagram may shift into instability domains due to local potential shifts at high polarization, accelerating the risks of pitting corrosion or active metal loss [97]. At the same time, an increase in temperature enhances charge transfer kinetics at the metal-electrolyte interface, ionic mobility, and the diffusion coefficient, thereby increasing HER and i_{corr} [98, 99]. An increase in temperature is also consistent with the high solubility of corrosion products, diminishing the integrity of oxide or hydroxide passive films and intensifying the risk of localized corrosion due to faster mass transport of aggressive anions such as Cl^- or SO_4^{2-}. Therefore, extreme conditions (elevated temperature and high voltage) can bring corrosion-mediated adverse effects, including capacity fading, dendrite formation and growth, impedance growth, and gas accumulation.

In practical battery systems, corrosion does not occur under static electrolyte conditions; instead, it appears in dynamically evolving chemical environments [100, 101]. During the cycling process, due to concentration polarization, oxygen reduction, metal-ion hydrolysis (solvation), and hydrogen evolution, the local pH can fluctuate. At the same time, several anions, including NO_3^-, Cl^-, SO_4^{2-}, and other active species, may coexist with varying concentrations. Under such complex-electrolyte conditions, corrosion mechanisms compete and may transform in response to kinetic accessibility and thermodynamic stability [102, 103]. Thermodynamically, using the Pourbaix diagram, the dominant corrosion mechanism can be rationalized, providing solid insights into the domains of metal, oxide, and soluble species as a function of potential and pH [104]. Nevertheless, in practical systems, corrosion pathways are often controlled by kinetic parameters such as oxygen transport, diffusion of OH^- or H^+, kinetics of passive film dissolution, adsorption strength of aggressive anions available in the electrolyte, and charge transfer resistance at the interface [105, 106]. For example, in zinc-based systems, corrosion or dissolution is mainly controlled by hydrogen evolution at low pH, whereas at neutral pH, dissolution is primarily controlled by the oxygen reduction reaction [107]. The presence of Cl^- at high concentrations induces a kinetically favored localized pitting corrosion, driven by autocatalytic local acidification and the breakdown of protective (passive) films. Conversely, sulfate

https://doi.org/10.1007/s40820-026-02178-9

ions may accelerate the formation of protective sulfate-containing surface films, shifting the corrosion mechanism toward uniform behavior. A similar competition can also be observed in Mg- and Al-based battery systems, where aggressive anion adsorption, oxide stability, and hydrolysis (solvation) reactions collectively determine whether uniform or localized dissolution predominates or passivation occurs. Therefore, in sustainable batteries, corrosion mechanisms depend on thermodynamic and kinetic factors.

The qualitative monitoring of the corrosion behavior of anode materials is of great practical importance, in addition to mechanistic knowledge and the factors that affect it, particularly in extensively employed Li-ion battery (LIB) systems [108, 109]. In LIB systems, corrosion mainly affects Cu and Al current collectors under elevated temperatures, over-discharge, and high-voltage conditions [110]. Therefore, electrochemical techniques such as electrochemical impedance spectroscope (EIS), linear polarization resistance (LPR), and potentiodynamic polarization (PDP) have been widely used to evaluate functional qualitative parameters such as R_{ct} (charge transfer resistance), R_p (polarization resistance), E_{corr} (corrosion potential), and i_{corr} (corrosion current density), to provide qualitative insight about passive films stability and kinetics of corrosion reactions [111–113]. Moreover, weight -loss and hydrogen evolution analyses are also employed to determine corrosion rates. The literature investigation also shows that several advanced surface characterization techniques, including SEM (scanning electron microscope), EDS (energy-dispersive X-ray spectroscopy), XPS (X-ray photoelectron spectroscopy), and ICP-MS (inductively coupled plasma mass spectrometry), have been used to detect trace metal dissolution and surface degradation [111]. Nowadays, in situ and operando diagnostic approaches have also emerged as a potential tool for studying interfacial material degradation via electrochemical mechanisms in realistic environments [114–116].

Corrosion behavior of electrodes in battery systems has been extensively studied using electrochemical techniques. In most of these investigations, electrochemical inhibition efficiencies are derived under simplified laboratory conditions, especially for short-duration experiments. Several electrochemical indices, such as R_p, R_{ct}, and i_{corr}, while providing valuable insights into mechanisms, do not fully capture long-term dissolution under practical battery cycling conditions, which are generally characterized by temperature fluctuations, mechanical stress, repeated charge–discharge cycles, and changing electrolyte composition. Moreover, testing protocols, such as applied current density, exposure times, electrolyte composition (concentration), and the units used for reporting, vary widely across studies. The inconsistencies in these protocols and outcomes make direct comparison difficult, leading to inconsistent conclusions and challenging the assessment of the best-performing materials. The founding of unified benchmarking standards is highly vital for the next-generation sustainable battery systems to establish practice performance thresholds including: (i) sustained Coulombic efficiency of > 99%; (ii) capacity retention of > 80%-90% after extended cycling (e.g., over 1000–5000 cycles varying upon system); (iii) controlled H_2 evolution rates; and (iv) stable impedance growth below defined limits over prolonged operations. To accelerate technology translation and enhance compatibility, long-term corrosion testing protocols are essential, especially in realistic operating battery conditions. The integrated testing frameworks will enable reproducibility, benchmarking, and the industrial implementation of corrosion mitigation approaches in sustainable battery systems.

The pH of electrolytes significantly impacts corrosion pathways, corrosion behavior, and the stability of passive films. Several anions, such as Cl^-, Br^-, and SO_4^{2-} ions, enhance C_R, whereas certain anions, especially NO_3^- and CrO_4^{2-}, passivate the metal surface and decrease C_R [117–119]. Generally, an increase in temperature results in a rise in C_R, and similar trends are observed with increasing current density (i_{corr}). Properties of anodic metals, such as particle size, grain properties, distribution, and surface area, also affect the corrosion resistance behavior of anodes [46, 120]. The presence of elemental impurities may accelerate or decrease C_R. The presence of contaminants, especially anions, in electrolytes may positively or negatively affect the C_R of anodic materials. In different battery systems, the degree of electrode corrosion is closely associated with the performance decay trends observed during cycling. The corrosion current density (i_{corr}) derived through potentiodynamic polarization can be correlated with the capacity retention and self-discharge rates. Generally, an increased i_{corr} value is associated with reduced capacity retention and an increased self-discharge rate. Likewise, the formation of corrosion products and the development of passive films are associated with increased impedance values in EIS studies and larger voltage hysteresis during charge–discharge

processes. These points indicate that monitoring i_{corr}, R_{ct}, R_p, R_f, E_{corr}, and other parameters provides indirect but reliable indicators of battery porosity, health, and performance. In battery systems, the corrosion behavior of electrodes is strongly influenced by several interrelated physicochemical parameters, including temperature, pH, electrolyte composition, the nature of aggressive ions, and the applied potential ($E_{applied}$). Each of these parameters can alter corrosion mechanisms, H_2 evolution kinetics, mass transport properties, and the stability of passive films. Table 2 summarizes the physicochemical parameters that induce primary corrosion.

1.3 Corrosion Could Be a Barrier and Stealing Problems in Sustainable Batteries

Corrosion poses a multifaceted barrier to the future of the battery industry, particularly for aqueous electrolyte-based batteries (Fig. 5) [49]. Corrosion adversely affects both the external casing and the internal electrochemical interfaces of batteries, reducing their lifespan, safety, and performance. Corrosion impedes the electrical conductivity between the battery and the device, leading to several severe issues, such as power loss or slow charging [121]. This results in sulfation and undercharging overtime. Once corrosion is initiated, it can spread to other components of the battery, causing further corrosion and damage. The corrosion of the battery terminals can also adversely affect the lifespan and performance. Overheating spots developed by corrosion may lead to parasitic shorts or drains. Qin et al. observed that corrosion from hydrothermal salt spray leads to a 76% decrease in the elastic modulus and induces swelling due to NaCl infiltration, resulting not only in reduced mechanical strength but also compromised integrity and safety risks, including thermal runaways and short circuits [122]. The challenges are particularly encountered in environments of high humidity. Corrosion-mediated failures affect the energy storage systems in electric marine vehicles (EMVs), coastal grids, and offshore installations. Du and coworkers demonstrated that galvanic and anodic corrosion, as well as electrolyte decomposition, degrade current collectors and electrodes, leading to capacity fading, gas evolution, and increased impedance [123]. Cu and Al collectors in Li-ion batteries experience galvanic and pitting corrosion, especially in humid environments, at elevated temperatures, and under elevated voltage.

In aqueous electrolyte-based batteries, Zn, Fe, Al, and Mg anodes readily corrode, evolve H_2 gas, and form oxide (passive) films in the presence of O_2 and H_2O, thereby impeding charge transfer. Recent reports indicate that safe, sustainable, and recyclable battery systems rely heavily on the recovery of metals such as Co, Mn, Ni, Al, Mg, and Li [124–126]. However, corrosion degradation and the mixing of corrosion products, mainly oxides and hydroxides, reduce the purity of recovered metals and their recovery efficiency. Moreover, corrosion-mediated

Table 2 A summary of physicochemical parameters mediated corrosion phenomena and their mechanistic aspects

S/N	Physicochemical parameter	Corrosion phenomenon	Mechanism(s)
1	Low pH (acidic condition)	Uniform corrosion; enhanced HER	Destabilization of passive films; accelerated H^+ reduction
2	Neutral pH	ORR as a major cathodic reaction; porous oxide films	Diffusing controlled process; oxides or hydroxides formation
3	High pH (alkaline condition)	Zn, Al, and Mg form zincate, amphoteric Al_2O_3, and $Mg(OH)_2$, respectively	Passive film dissolution; anodic activation at very high pH
4	Aggressive ions (e.g., Cl-)	Localized attacks, pitting corrosion	Local acidization and breakdown of passive (oxide) films
5	Relatively less aggressive ions (e.g., SO_4^{2-} and NO_3^-)	Reduced localized pitting; improved passivation	Form relatively compact sulfate/nitrate-based films
6	High voltage	Localized corrosion, OER activation, and accelerated breaking of passive films	Electrolyte decomposition and shift stability domains in the Pourbaix diagram
7	Elevated temperature	Passive films weakening; increased H_2 evolution; increases icorr and	Enhanced charge transfer kinetics; enhanced diffusion
8	Presence of oxygen	Aeration (concentration) cells; enhanced ORR-mediated corrosion	Concentration gradient development; cathodic activation
9	Accelerated current density	Localized corrosion; Dendrite growth	Polarization-induced instability; nonuniform ion flux

https://doi.org/10.1007/s40820-026-02178-9

contamination can adversely affect the recycling process. The corroded and damaged casing, as well as electrode residue, may increase safety risks, especially in aged batteries, which require strict design and recycling standards.

2 Electrochemical Corrosion Problems in AESs: Mechanisms, Consequences, and Mitigation

To thoroughly understand the corrosion mechanisms in battery systems, it is crucial first to examine the basic electrochemical reactions governing metallic dissolution and passivation in aqueous environments. Although the mechanism of corrosion varies depending on the nature of the metal and the electrolyte, it is generally governed by interfacial redox (electrochemical) reactions, the formation of passive (oxide) films, and mass transport processes. In this section, the corrosion behavior and mechanisms of representative anode materials, such as Zn, Mg, and Al, are discussed to highlight similarities and differences. In addition to gaining insights into corrosion mechanisms in battery systems, developing effective corrosion protection strategies is vital for enhancing the electrochemical stability and service life of next-generation sustainable batteries. In these systems, the corrosion protection strategies can be classified

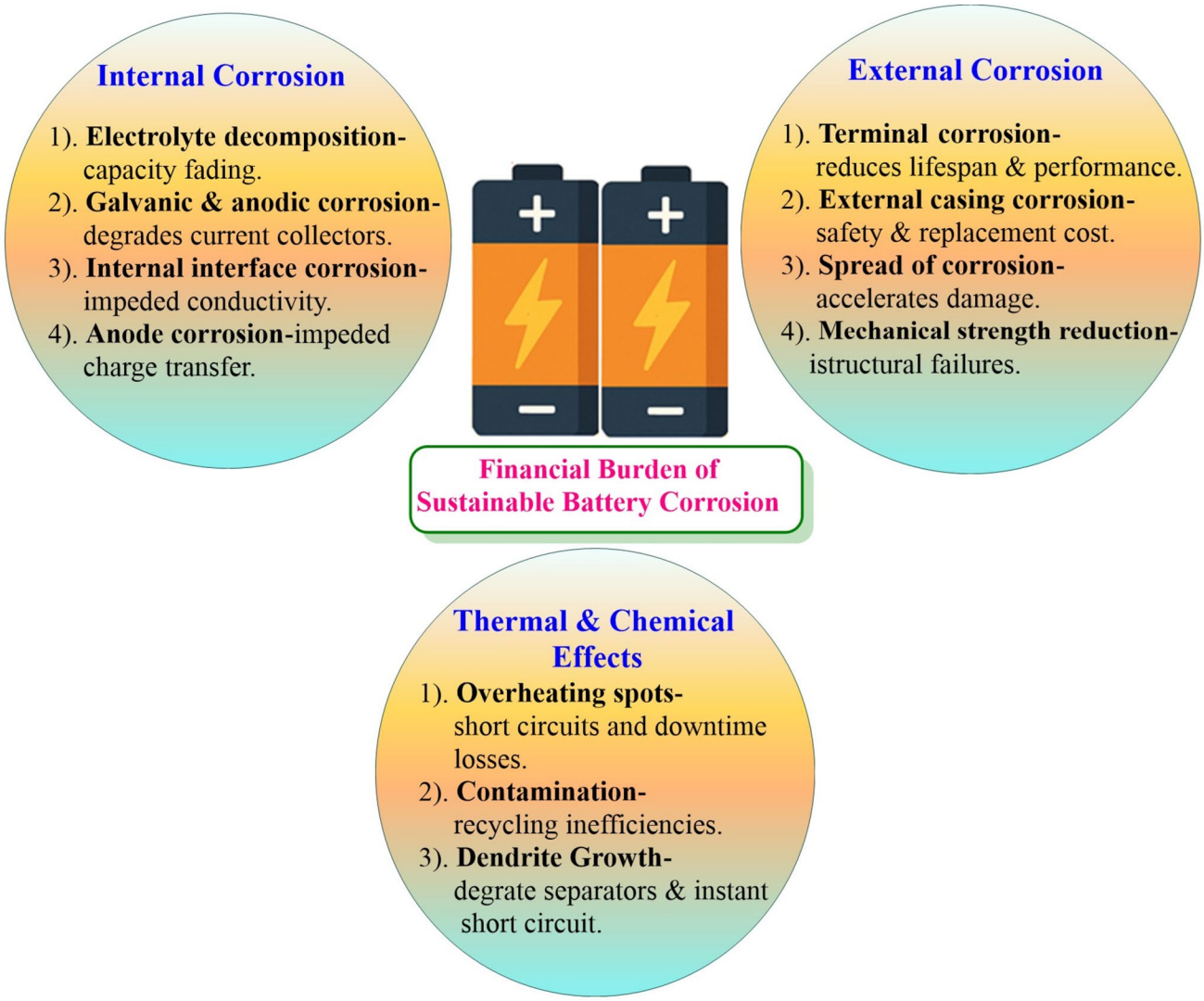

Fig. 5 Schematic diagram showing corrosion-related multifaceted barrier to the future of the battery industry, particularly for aqueous electrolyte-based batteries

into three broad categories: (i) strategies related to intrinsic material designs that include microstructural optimization and alloying; (ii) strategies related to surface engineering, such as passivation, coatings, and artificial interphases [127]; and (iii) strategies related to electrolyte modification through the incorporation of solvation-controlling species, corrosion inhibitors, and functional additives. The objectives of these strategies include suppressing anodic electrode dissolution, cathodic H_2 evolution, stabilizing passive films, reducing dendrite growth, and homogenizing metal deposition. These protection strategies, along with representative mechanisms, are systematically discussed in the following sections. In battery systems, corrosion protection strategies depend heavily on the form of corrosion.

The use of gel electrolytes has emerged as a practical approach to prevent interfacial corrosion in aqueous metal-ion batteries, particularly in Al-, Mg-, and Zn-based systems [128–131]. Unlike conventional electrolytes, gel-based systems are composed of confined water molecules within polymer networks, thereby reducing undesirable HER and water activities [128, 129, 132]. Moreover, the polymer matrix also restricts the ingress of aggressive anions, including sulfate and chloride, present in the electrolyte, thereby minimizing the risks of concentration-gradient-mediated galvanic effects and localized pitting corrosion [133–135]. Additionally, these electrolytes can accelerate the formation of relatively more uniform and stable solid-electrolyte interphases, which can serve as protective films, thereby reducing current density and improving the kinetics of interfacial charge transfer [136, 137]. Being mechanically robust, gel electrolytes also suppress dendrite propagation by regulating ion flux at the electrode surface. Therefore, gel-based electrolyte systems offer several benefits for batteries, including lower HER, reduced metal dissolution, improved Coulombic efficiency, enhanced safety, and long-term cycling stability [138, 139]. Owing to these properties, i.e., interfacial protection and electrolyte stabilization, the use of gel-based electrolytes in next-generation aqueous sustainable batteries is gaining particular attention.

In addition to gel and specific additive electrolyte systems, the balanced design of corrosion-resistant electrolytes also requires systematic consideration of physicochemical parameters under both alkaline and acidic conditions. Buffering capacity and pH control are highly critical parameters, as the corrosion rate depends strongly on hydroxide concentration and proton availability [140]. Obviously, the stable pH domains reduce the possibilities of passive film breakdown and retards excessive H_2 evolution by reducing HER [141, 142]. Solvation structure and water activity are other important parameters that play a central role in the design of corrosion-resistant electrolytes [143]. Generally, free water molecules promote anodic dissolution and HER. The reactivity of water and its adverse consequences can be minimized using water-in-salt systems, high-concentration electrolytes, the incorporation of an external additive, or gel electrolytes [144–146]. These species form intermolecular hydrogen bonds with free water molecules, thereby reducing their activity and consequences. The selection of anions and their control of aggressiveness could be other practical approaches to designing corrosion-resistant electrolytes. For example, Cl^- ions promote localized corrosion by dissolving or diffusing through the surface oxide films, leading to pitting corrosion, whereas NO_3^- or SO_4^{2-} ions promote the formation of protective passive films [147, 148]. To avoid excessive side reactions and undesirable corrosion, the electrochemical stability window (ESW) and redox compatibility with electrode materials must be appropriately ensured. Excessive dendrite growth and polarization can be avoided by optimizing transport homogeneity and ionic conductivity [149, 150]. Moreover, SEI-forming ability and interfacial compatibility are crucial for stabilizing artificial interphases or oxides during cycling. Screening these parameters can provide a systematic framework for designing and developing corrosion-resistant electrolytes tailored to alkaline or acidic metal-ion batteries.

Table 3 summarizes the significant forms of electrochemical corrosion in aqueous electrolyte-based battery systems, along with their corresponding mechanisms, affected components, significant consequences, and primary prevention strategies. The corrosion in these systems manifests in several ways, including uniform, pitting, galvanic, and intergranular corrosion, as well as hydrogen- and dendrite-mediated corrosion and passive film instability. The different corrosion forms share the common anodic dissolution and cathodic HER or ORR reactions, but they differ in severity, effect on electrochemical performance, and localized behavior. The consequences range from gradual, slow material and capacity loss to increased impedance, polarization, and the risk of short circuits. Effective corrosion mitigation strategies include alloy design, microstructure control, grain refinement, corrosion inhibitors, surface engineering, electrolyte regulation, and interfacial stabilization.

https://doi.org/10.1007/s40820-026-02178-9

2.1 Electrochemical Corrosion and Corrosion Inhibition of Sustainable Zinc-based Batteries

Zn-based anodic materials have long been recognized for primary (non-rechargeable) as well as secondary (rechargeable) batteries owing to their cost-effectivity, high theoretical capacity (820 Ah kg^{-1}), and electrochemical reversibility [151–154]. Nevertheless, their practical applications are significantly hindered by their susceptibility to corrosion in alkaline electrolytes, particularly for Zn-MnO_2 and Zn-air batteries [155, 156]. Mercury amalgamation was widely employed in conventional batteries to prevent or minimize undesirable anodic corrosion (dissolution) by passivating the anode surface [84]. The growing interest in sustainable development in the early 1990s, following the establishment of green chemistry principles, led to efforts to mitigate battery corrosion in the search for Mercury-Free strategies. These strategies include alloy-based modifications and the use of external additives, commonly referred to as corrosion inhibitors. Organic compounds, primarily heterocycles, featuring various heteroatoms and polar functional groups, serve as effective corrosion inhibitors for anodic dissolution [157, 158]. These electron-rich sites serve as adsorption centers during their coordination with the anode (Zn) surface. For example, Nartey et al. screened the inhibition performance of a series of organic inhibitors for the dissolution of Zn in KOH solution [159]. The outcomes of different analyses showed that they strongly bind to the metallic surface and form protective hydrophobic films via π-orbital or coordination bonds. The presence of corrosion inhibitors significantly improves the charge–discharge stability and minimizes the H_2 evolution. These effects typically improve capacity retention, Coulombic efficiency, cycle life, and reduce polarization under practical operating conditions. A year later, Kannan and coworkers adopted an alloying approach, integrating trace amounts of Mg, Pb, and Al into high-purity Zn to improve battery performance and corrosion resistance [160]. The alloying elements not only improve battery performance but also replace traditional inorganic additives, such as CaO, sodium citrate, and sodium stannate. The authors observed that cathodic H_2 evolution and anodic dissolution were significantly retarded by alloying, attaining anodic inhibition efficiency of up to 99%. The literature study reveals that in the early 2000s, the use of protective thin films and polymeric surfactants began to protect against anodic dissolution [161]. They synergistically improve the surface morphology, retard H_2 evolution, and anodic dissolution.

Zhu et al. proposed a Nb-based surface modification approach in which $Pb(NO_3)_3$ produces a protective Nb-rich surface oxide (passive) film on the Zn surface for adequate protection [162]. The Nb-rich surface oxide films provide uniform corrosion protection, minimize corrosion rate (C_R), reduce current density (i_{corr}), and increase charge transfer resistance (R_{ct}). Significant progress in the use of organic and surfactant-type corrosion inhibitors to protect Zn anode dissolution was made between 2009 and 2015. These species, such as amidopoly ethylamines, develop a corrosion-protective hydrophobic layer, thereby inhibiting both anodic and cathodic reactions [163]. Mainly, they serve as mixed-type corrosion inhibitors, meaning that they retard both anodic Zn dissolution and cathodic H_2 evolution without significantly shifting the corrosion potential (E_{corr}) (by more than 85 mV). Their adsorption mostly obeyed the Langmuir isotherm model. Polyethylene glycol (PEG), DTAB, Tween-20, Polyoxyethylene (40) nonylphenyl ether (PNE), and hydroxyethyl cellulose (HEC) are employed as effective and eco-friendly substitutes to mitigate Zn anode corrosion [157, 164–167]. They exhibit 80–98% anodic dissolution inhibition efficiencies, depending on the nature of the electrolytes. Recent advancements in green chemistry and sustainable development necessitate the use of green, especially bio-based polymers, such as PEG and HEC, for anticorrosion applications in batteries. They are highly flexible, hydrophilic, cost-effective, and compatible, with remarkable film-forming and ionic conductivity properties.

The idea of using bio-based additives was further explored by Yang et al. [168]. They observed that CMC (carboxymethyl cellulose) passivates the Zn surface and retards dendrite growth in 6 M KOH. CMC forms a non-porous, uniform hydrophilic-hydrophobic interface layer that prevents the diffusion of corrosion species, reduces C_R and i_{corr}, and enhances R_{ct}. The formation of protective hydrophobic films of 2-octanone ethylene diamine (OED) via coordination bonding was studied in a separate study [169]. The results showed that a 4 wt% loading of OED manifested more than 95% efficiency. OED minimized the risks of pitting corrosion by providing a uniform layer. The H_2 evolution, i.e., cathodic reactions, was significantly reduced, as OED primarily serves as a cathodic-type inhibitor. The polymer-based inhibitors mostly form a uniform and compact monolayer, as indicated by the Langmuir isotherm [170, 171].

Table 3 A summary of significant forms of electrochemical corrosion, mechanisms, affected components, significant consequences, and primary prevention strategies in aqueous electrolyte-based battery systems

S/N	Form of corrosion	Major degradation mechanism(s)	Major consequences	Components undergo degradation	Main mitigation strategies
1	General (uniform) corrosion	Uniform anode dissolution through ORR or HER	Gradual loss of electrodes, increased icorr, and reduced specific capacity	Anodes (Mg, Al, and Zn) and current collectors	Alloying, protective coatings, electrolyte modification, and inhibitors
2	Pitting	Breakdown of passive film, halide-induced degradation	Risks of short-circuits, rapid localized attacks, and dendrite growth	Al and Zn anodes in chloride-based electrolytes	Surface coatings, anion regulation (e.g., sulfate can be preferred over Cl^-), and inhibitors
3	Intergranular corrosion	Preferential corrosion along with grain boundaries	Performance loss, mechanical strength loss, and crack development	Polycrystalline Mg, Al, and Zn anodes	Alloy design, passivation stabilization, and grain refinement
4	Galvanic corrosion	Intermetallic phases or dissimilar metal coupling	Localized corrosion and reduced cycle life	Current collectors (Cu/Al) and alloyed anodes	Impurity removal, surface homogenization, and control of microstructure
5	Instability of passive films	pH-dependent dissolution of passive films	Capacity fading due to increased polarization and impedance	Dissolve oxides and hydroxides, i.e., ZnO, Al_2O_3, and $Mg(OH)_2$ films	Electrolyte buffering, pH control, and solvation control
6	H_2 evolution catalyzed corrosion	HER-mediated anodic corrosion	Reduced Coulombic efficiency, self-discharge, and gas accumulation	Mg and Zn in H_2O-based electrolytes	Reduction of H_2O activity, cathodic protection, and electrolyte control
7	Dendrite-mediated corrosion	Localized corrosion due to uneven deposition	Capacity fading and risks of short circuits	Rechargeable Mg and Zn anodes	Surface modification and tip-blocking

https://doi.org/10.1007/s40820-026-02178-9

The inhibitor films provide 90%–96.8% anodic dissolution inhibition efficiency. The use of surfactants and polymers can be considered as Hg-free, next-generation, amphiphilic, sustainable alternatives for corrosion protection in battery systems.

The literature survey reveals that several corrosion inhibitors have been developed and employed in battery systems. Their modes of action can be rationalized within a combined mechanistic classification framework. The different inhibitors described in the present section can be divided into three classes: (i) adsorption and film-forming surfactants and polymers, including DTAB, PEG, Tween-20, HEC, CMC and PNE, which produce corrosion-protective physical barrier the interface and retard anodic Zn corrosion and cathodic H_2 evolution; (ii) chelating and multidentate heterocycles, including benzotriazole and imidazole derivatives, BHB, nitrilotriacetic acid (NTA) and gluconate-based complexes, which coordinate with metallic and ionic Zn sites and form highly protective chelated protective films through chemisorption mechanism; and (iii) inorganic or ionic modifiers, including Sc^{3+} cations, Nb-based treatments, oxygen scavengers (AQS) and sulfate salts, which control interfacial charge distribution, nucleation behavior and composition of passive films [172, 173].

Their molecular and structural properties primarily determine their effectiveness as protectants. Corrosion inhibitors containing electron-rich polar functional groups of heteroatoms (N, S, O), π-conjugated systems in the form of aromatic rings or side chains, and multiple adsorption sites with the potential for chelation significantly enhance adsorption effectiveness through chemisorption on the ionic or metallic Zn surface. The adsorption of corrosion inhibitors and the formation of hydrophobic protective films are consistent with improved coulombic efficiency, increased R_{ct} (or R_p), and decreased icorr. In polymer- and surfactant-based corrosion inhibitors, the balance between hydrophilic segments (headgroups) and hydrophobic segments (alkyl chains) determines wettability, ion transport, and the compactness of protective films, and directly affects dendrite formation and H_2 evolution. Generally, hybrid formulations having polymers (or organic) components mixed with inorganic ions provide synergistic protection by suppressing both anodic and cathodic reactions.

A noticeable transition occurred between 2009 and 2018, as $ZnSO_4$-based systems replaced alkaline batteries, enabling rechargeable Zn-ion batteries with enhanced reversibility, safety, and stability. Sun et al. manifested that sodium anthraquinone-2-sulfonate (AQS) behaved as a self-oxidizing oxygen scavenger [174]. AQS achieves a coulombic efficiency of over 99% and cycling stability of more than 2500 h. Through the deoxygenation mode, AQS also retards dendrite growth, surface precipitation, C_R, and i_{corr}, enabling long-lasting cycling. Gelman and coworkers demonstrated that the PEG-Zn hybrid systems form a significantly denser, more uniform protective film [175]. Hybrid systems not only improve corrosion resistance but also enhance battery performance and lifespan [175, 176]. The use of hybrid systems (organic/polymers and inorganic additives) has also been explored elsewhere [177–179]. The presence of Pb^{2+} and Mg^{2+} ions improves the inhibition performance of pyrazole and gelatine, respectively. In Zn-air and Zn-alkaline systems, amphiphilic inhibitors address long-standing problems by suppressing H_2 evolution, dendrite growth, and ZnO passivation. Many surfactants, including SDS, Tween-20, and SDBS, have shown noticeable improvements in the discharge performance and electrochemical stability of the anode materials [180–182]. These surfactants served as interfacial regulators, diminishing electrode polarization, improving ion transport, and stabilizing the anodes.

Li et al. proposed using a more complex amphiphilic PEI (polyethylenimine) inhibitor for dendritic suppression and corrosion protection [184]. A relatively noticeable transformation was the use of coordination-complex-based corrosion inhibitors in battery systems. The counterions of these complexes not only regulate the nucleation but also stabilize the redox reactions. We et al. studied the corrosive dissolution of Zn foils in an alkaline solution of ZnO with and without Zn acetate (ZA) and Zn gluconate (ZG) [183]. The Nyquist and Bode plots for Zn corrosion in 6M KOH with and without ZA and ZG are shown in Fig. 6. The careful inspection reveals that, initially, inhibitors exhibit incomplete adsorption; however, after 24 h of immersion, a complete adsorption film can be inferred from the development of a well-defined capacitive semicircle in Nyquist plots. ZG produced the largest diameter with the highest phase angle (~37°) among the studied systems, indicating the best resistance, most effective adsorption, and thickest inhibitive films. The nucleation of Zn^{2+} ions in an alkaline solution containing ZA and ZG, which proceeds mainly via 3D diffusion, is schematically measured through chronoamperometry (CA) and chronopotentiometry (CP) and is shown in Fig. 7a, b. Figure 7c shows that acetate ions bind effectively to the 002

Zn surface by replacing the pre-adsorbed H_2O molecules, thereby reinforcing the deposition and desolvation of Zn^{2+} ions. The adsorption and formation of protective film by gluconate and acetate ions are illustrated in Fig. 7d. They form a uniform, non-porous protective film that prevents the diffusion of corrosive species.

Recently, advanced molecules for mitigating anodic dissolution, including polyols, ionic liquids (ILs), and metal–organic frameworks (MOFs), have emerged as practical and multifunctional alternatives [64, 173, 185, 186]. MOFs provide anticorrosion protection and enhance battery performance, achieving more than 85% capacity retention and 99.6% Coulombic efficiency even after over 6000 cycles. ILs form a corrosion-protective hydrophilic film, providing more than 91.3% efficiency at concentrations as low as 2.5 mM. MOFs and ILs retards the dendrite growth, minimize sulfate precipitation, and homogenize the metallic surface. The use of ion-assisted and functionalized electrolytes can be considered another notable transformation in protecting battery anodes through solvation, film formation, and ion-surface interactions. Kim and coworkers proposed that Sc^{3+} cations force uniform Zn deposition, which retard dendrite growth [187]. The Sc^{3+} cations' "tip-blocking" mode of action was associated with a coulombic efficiency exceeding 99% over 100 cycles. The polyhydroxylated sugars (polyols), such as trehalose, develop an H-bonding network and minimize the presence of free water molecules [188]. The coordination of trehalose with Zn^{2+} and the subsequent hydrogen-bonding networks decreased cathodic H_2 evolution and anodic Zn dissolution, thereby promoting Zn deposition. The organic and ionic components regulate the deposition and solvation kinetics.

Nowadays, artificial intelligence (AI) assisted screening has emerged as one of the most potent and effective tools in electrolyte optimization and materials discovery in energy storage systems [189, 190]. High-throughput

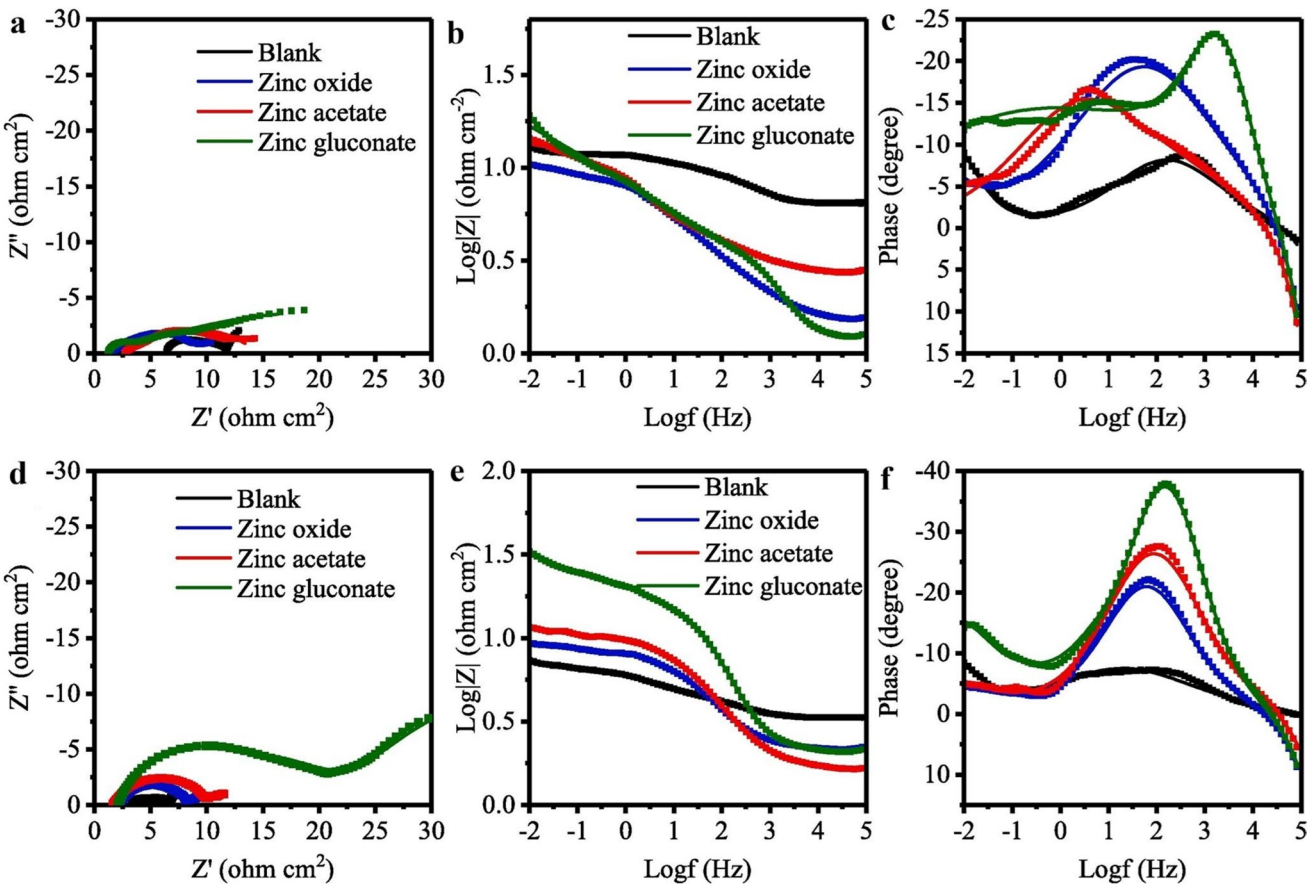

Fig. 6 Fitted findings and EIS test curves for the zinc anode following immersion in four electrolytes for **a–c** 0.5 h and **d–f** 24 h [183]. (Reproduced with permission. © 2024 Elsevier)

https://doi.org/10.1007/s40820-026-02178-9

computational screening using machine learning (ML) and data-driven modeling approaches enables the assessment of several vital parameters, including binding affinity, electrochemical stability window (ESW), solvation structure, hydrogen evolution activity, and adsorption energy [191–195]. Nowadays, ML-driven studies on proton-conducting electrolysis and H_2 evolution electrocatalysts have shown that data-driven strategies can effectively tailor or fabricate active-site distributions, electronic structures, and overall surface chemistry to improve interfacial stability and reduce HER kinetics [196, 197]. Such approaches provide useful insight for designing effective corrosion-resistant electrolytes for aqueous battery systems. AI models can also be used to correlate molecular descriptors such as energies of frontier molecular orbitals, i.e., energy of highest occupied molecular orbital (E_{HOMO}), energy of lowest unoccupied molecular orbital (E_{LUMO}), their difference ΔE ($E_{LUMO} - E_{HOMO}$), electronegativity (χ), dipole moment (μ), and hydrogen-bonding potential, to design corrosion-resistant electrolytes. These computed parameters can be correlated to experimentally derived parameters such as inhibition efficiency (%IE), R_{ct}, R_p, or i_{corr}. Fortunately, computational approaches enable the identification of effective electrolyte additives and corrosion inhibitors without the tedious synthesis and experimental trials [198–200].

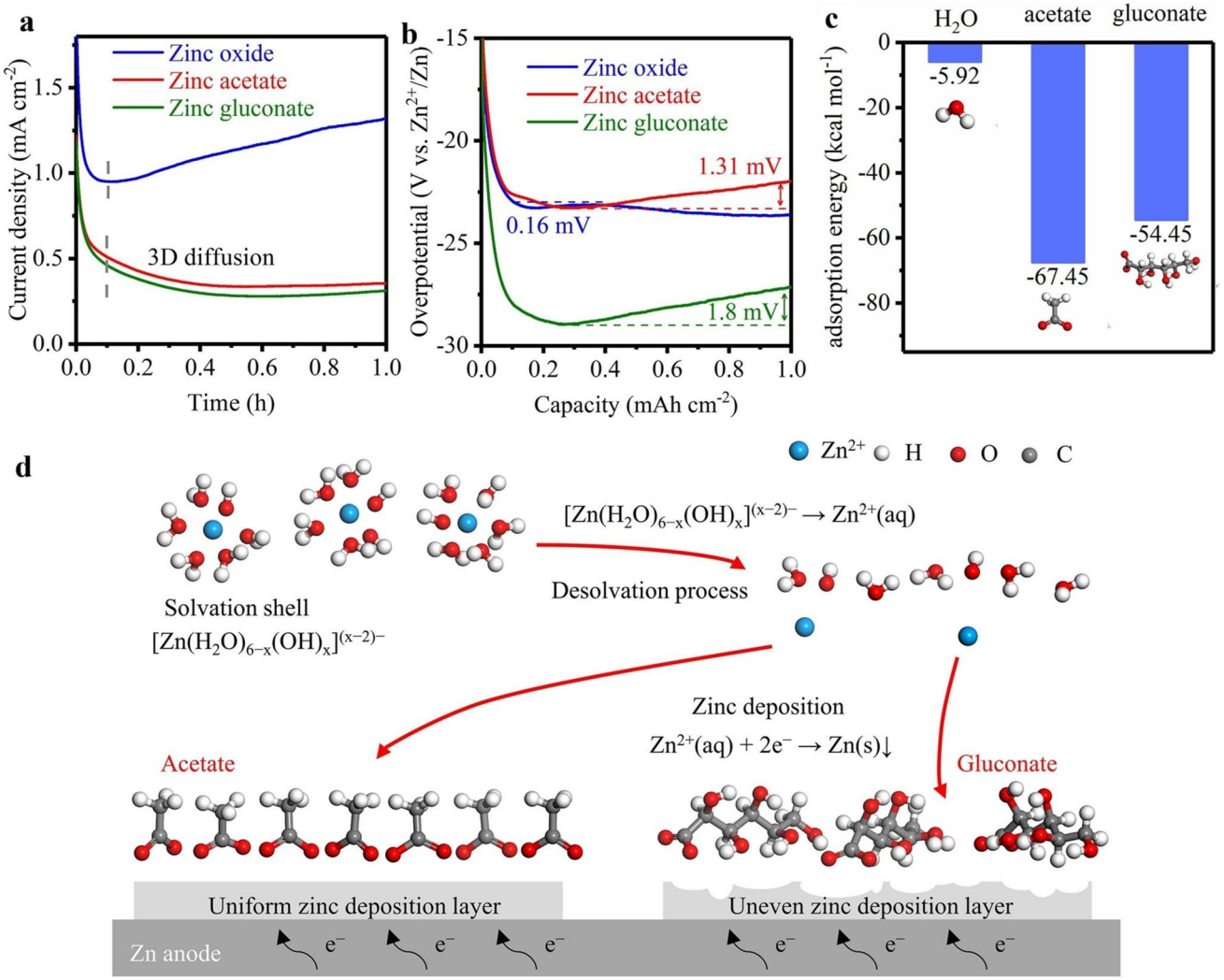

Fig. 7 **a** Zn anode CA and **b** CP measured in various electrolytes. **c** The energy of adsorption of gluconate, acetate, and H_2O on the Zn (0 0 2) plane. **d** Additives and the zinc deposition process schematics [183] (Reproduced with permission. © 2024 Elsevier)

For example, DFT-derived parameters combined with ML algorithms can be used to predict the adsorption nature and effectiveness of corrosion inhibitors on electrode (Mg, Al, Zn, etc.) surfaces. In contrast, molecular dynamics (MD) and Monte Carlo (MC) simulations can be used to study water activity and solvation structure in gel-based or concentrated electrolyte systems [198–200]. AI can also be used to gain helpful insight about the selection of optimized anions by predicting pitting susceptibility and oxide film stability under different operating conditions, such as varying voltage, temperature, and pH [201, 202]. Moreover, predictive models developed using electrochemical datasets may help define safe and effective operational windows under extreme conditions, i.e., high temperature and voltage, by linking corrosion kinetics to electrolyte composition. Given this, combining electrochemical outcomes and mechanistic modeling and AI-driven strategies offers a promising pathway toward designing and developing corrosion-resistant electrolytes and corrosion inhibitors for the next-generation sustainable batteries.

Inorganic and anionic modifications further expanded the design of corrosion-resistant electrolytes. Lin et al. observed that the presence of SPS (anionic sodium 3,30-dithiodipropane sulfonate) in corrosive alkaline solution forced horizontal Zn growth through the selective adsorption of sulfonate groups available at the high-energy sites, favoring the development of corrosion resistance orientation [203]. This type of orientation enabled dendrite-free cycling for over 4400 h, with a coulombic efficiency exceeding 99.7%. Likewise, Na_2SO_4 facilitates the formation of passive films over the Zn surface, minimizing C_R, H_2 evolution, and i_{corr} [204]. Currently, considerable attention is being paid to the development and application of multidentate heterocyclic and chelating inhibitors for zinc stabilization in aqueous battery systems. NTA (nitrilotriacetic acid) serves as a multidentate additive that coordinates Zn^{2+} and develops chelating films (NTA-Zn^{2+}), reducing $Zn(OH)_2$ formation and cathodic H_2 evolution [205]. 0.15 wt% NTA reduced i_{corr} by more than 90% and achieved a coulombic efficiency of 99.4% after 800 cycles. NTA also promotes uniform Zn deposition and Zn^{2+} desolvation. Similarly, BHB (6-bromo-1H-benzimidazole) coordinates to the Zn surface via its Br and N atoms, promoting effective film formation and retarding H_2 evolution and dendrite growth [206]. A coulombic efficiency of 99.24% was observed after 1150 h in the presence of 0.25 mM. BHB greatly enhanced corrosion resistance. The Nyquist and Bode plots, which reveal a significant increase in corrosion resistance, are shown in Fig. 8a, b.

The Nyquist curves were suitably fitted in equivalent circuits to get the desired EIS parameters (Fig. 8c, d). The increase in R_{ct} and impedance values indicated adsorption and the formation of a protective BHB film. The adsorption was also supported by high film resistance (R_f) and lower double-layer capacitance (C_{dl}). The adsorption of BHB followed the Langmuir isotherm (Fig. 8e), suggesting that it forms a chemisorbed monolayer. Potentiodynamic polarization (PDP) curves in the presence of BHB showed a slight decrease in H_2 evolution and i_{corr}, with a protection efficiency of approximately 99% (Fig. 8f, g). Computational studies support the interactions between the Zn surface and BHB. The differential charge density map reveals electron accumulation around Br and N and depletion on Zn sites, thereby establishing coordination and charge transfer processes. MD simulation analyses showed that BHB forms a robust monolayer through parallel adsorption, resulting in a compact hydrophobic layer that prevents the diffusion of corrosive species, including water (Fig. 9a-e). Figure 9f, g shows the Zn growth behavior with and without BHB. The uniform, smooth, and dendrite-free Zn growth was clearly revealed in the presence of BHB, indicating homogenous nucleation and prolonged surface stability.

Nearly complete corrosion protection was observed using a dual-layer surfactant system (OP-10P) for the Zn-air battery [207]. DD (1,10-decanedithiol) coordinates with Zn^{2+} and forms an outer, protective, hydrophobic layer that reduces self-discharge and enhances conductivity during cycling. The electronic properties of OP-10P and DD were investigated using DFT. FMOs and their respective energies and energy gaps are illustrated in Fig. 10. DD has a higher E_{HOMO} value, favoring more donation or coordination, whereas OP-10P is more susceptible to better acceptance due to a lower E_{LUMO} value. The relatively low ΔE values for OP-10P and DD indicate that they chemisorb to the metal surface, forming uniform, compact corrosion-protective films. Likewise, the N-atom of Pyr (pyrazine), Pym (pyrimidine), and Pyd (pyridazine) coordinates with the Zn surface and forms corrosion-protective, hydrophobic films [208]. The DFT study revealed that pyrimidine with N atoms at 1st and 3rd (meta-) position, favored parallel adsorption, balancing and controlling the coordination and desolvation kinetics.

https://doi.org/10.1007/s40820-026-02178-9

The use of bio-based inhibitors has been identified as a promising new avenue for sustainable anode stabilization and corrosion protection. Ren et al. reported that fucoidan (FCD), a natural polysaccharide, forms an 8 nm covalently bonded film on a metallic substrate by coordinating through its oxygen atoms [155]. The covalently monolayer film so formed reduced the H_2 evolution and retard the corrosion without affecting the Zn^{2+} transport, providing up to 2700 h cycling. The bio-based chelating FCD revealed a coulombic efficiency of 99.5% after 300 cycles. Likewise, protonated triglycine (ggg), a zwitterion, interacts with the Zn surface through $–NH_3$ and $–COO^-$ and reduced water activities and H_2 evolution [209]. The use of biocompatible compounds in Zn anode corrosion protection has also been explored in other reports [210, 211]. Organophosphonates, polyols, and metal–organic complexes have been established as effective multifunctional additives for Zn-based aqueous batteries [212–214]. They provide anticorrosion protection by adsorbing at the interface of the Zn surface and aqueous electrolytes. They reduce the C_R, i_{corr}, and H_2 evolution and enhance R_{ct} for Zn corrosion in such electrolytes. They also improve the battery performance, including coulombic efficiency over 99%.

The use of complexing and film-forming additives for enhanced stability and corrosion protection has been further advanced in recent studies. Sn and coworkers developed dopamine-derivatized polypyrrole (DA-PPy) for H_2 evolution reduction and corrosion protection [215]. DA-PPy, with its numerous coordination sites, effectively binds to the surface, retarding corrosion without affecting Zn^{2+} transport. Zn-pyrrolidone carboxylate (Zn-PCA) stabilizes cathodic and anodic processes in Zn-I_2 batteries [216]. Polyiodide adsorbs and reduces dendrite growth and corrosion, with 87% capacity retention after 30,000 cycles. PCA- anions mainly coordinated with I_2. Imidazo[1,2-b]pyridazine (IP) provides dual functionalities, i.e., anchoring and shielding effects [217]. The coordination and chemisorption of IP via N atoms displace pre-adsorbed water molecules. This results in dendrite-free deposition and stable cycling over 2200 h with a very high coulombic efficiency of 98.7%.

Ma et al. elucidated sodium gluconate (SG) as a cost-effective and multifunctional filming corrosion inhibitor

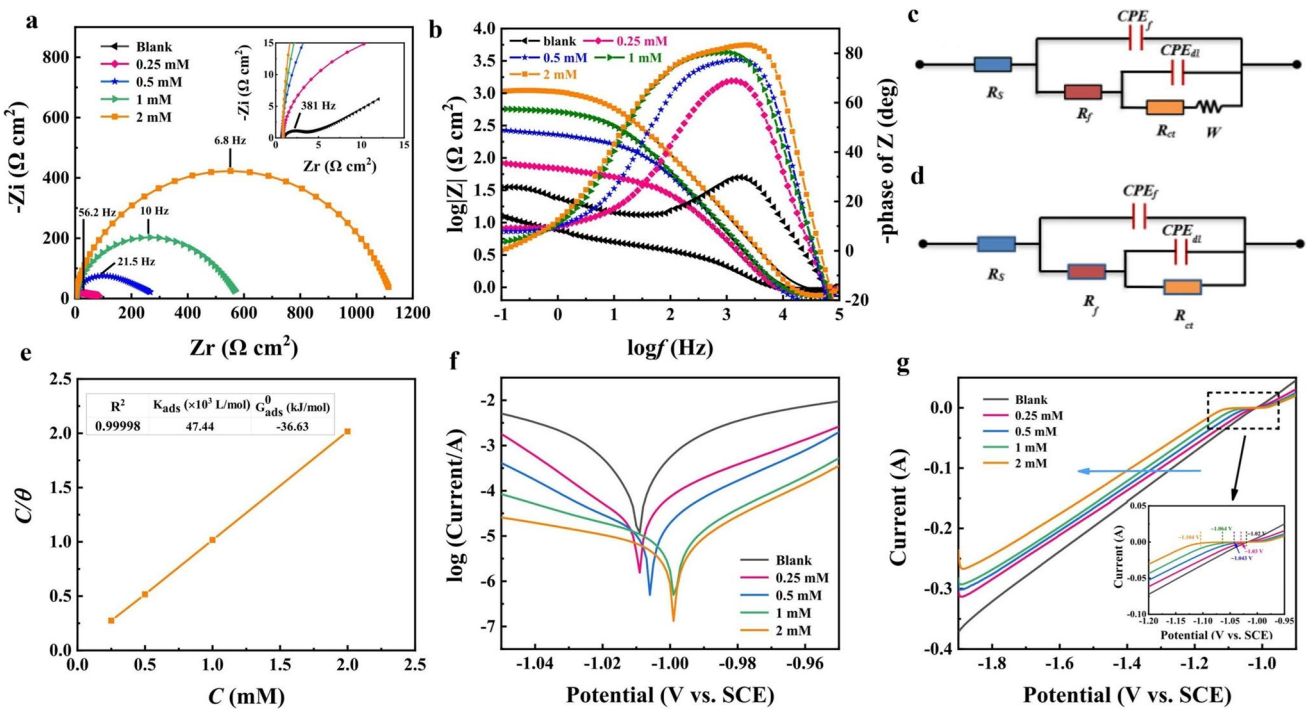

Fig. 8 The zinc electrode was submerged in a 2 M $ZnSO_4$ solution, with and without BHB. **a** Nyquist graph, **b** Bode plots, **c**, **d** equivalent circuits, **e** Langmuir isotherm adsorption curves, **f** linear polarization curves, and **g** LSV curves [206] (Reproduced with permission. © 2023 Elsevier)

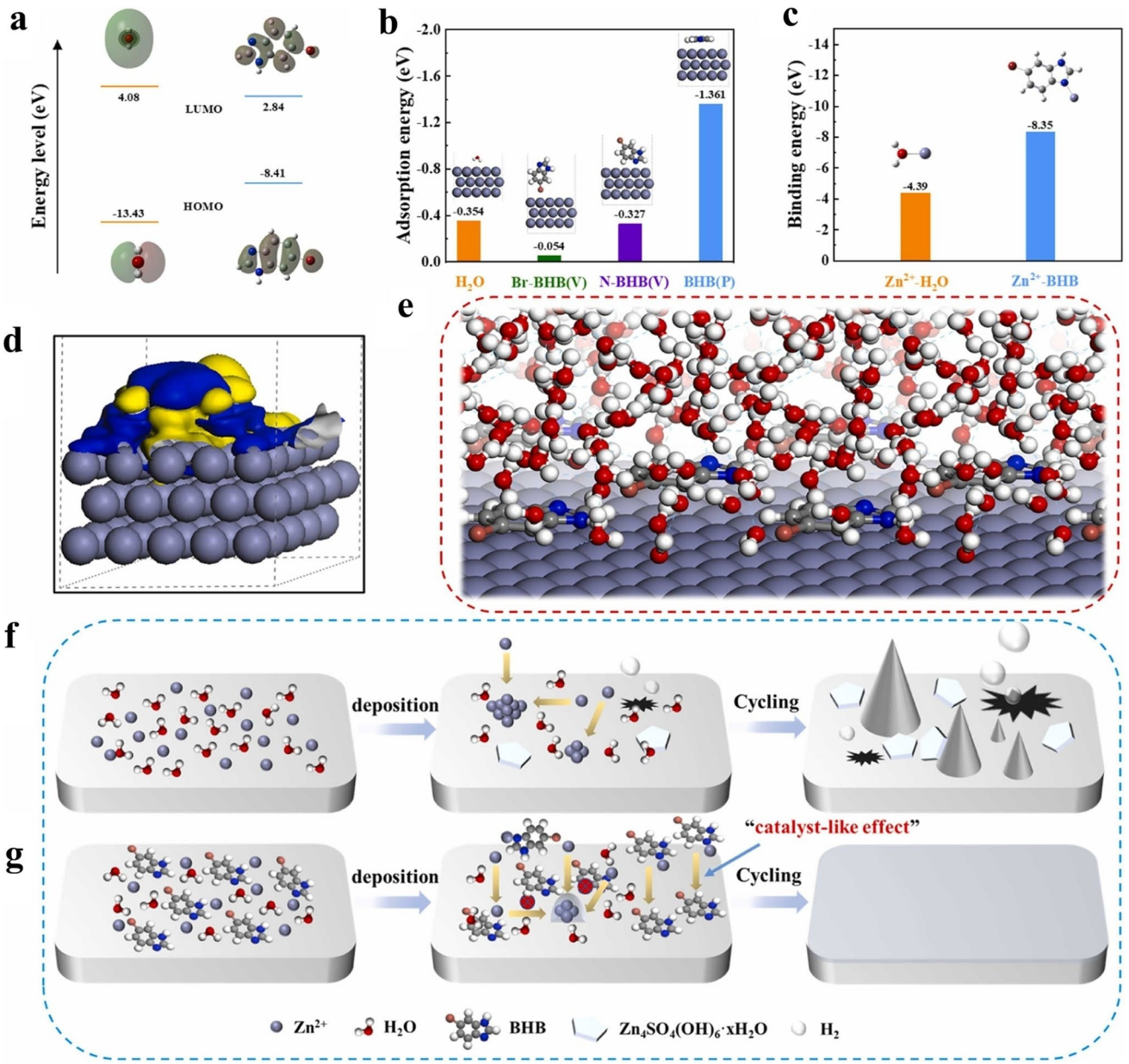

Fig. 9 **a** HOMO and LUMO for molecules of BHB and water. **b** Water and BHB adsorption energy on the zinc surface. **c** Zn^{2+}-H_2O and Zn^{2+}-BHB complex binding energies. **d** Map of differential charge density, where blue indicates decreasing charge density, and yellow indicates rising charge density. **e** MD simulation snapshot. The schematic diagrams of Zn deposition behavior for $ZnSO_4$ and $ZnSO_4$ + BHB electrolytes are shown in **f** and **g**, respectively [206] (Reproduced with permission. © 2023 Elsevier)

for Zn corrosion [218]. Gluconate anions form a chelating complex that prevents the attack by corrosive species, including SO_4^{2-} ions. In the presence of these anions, the solvated Zn^{2+} converts into $[Zn(gluconate)(H_2O)_5]^+$, which reduced C_R and H_2 evolution. The working mechanism of SG is illustrated in three steps in Fig. 11. The adsorption of gluconate ions produces corrosion-preventive films that avoid direct water contact and attack. GS guided uniform Zn plating via electrostatic shielding of Na^+ and SO_4^{2-} ions at the interface. The replacement of H_2O molecules by gluconate ions results in the formation of new solution shells; $Zn(gluconate)(H_2O)_5]^+$. These result in reduced byproduct

https://doi.org/10.1007/s40820-026-02178-9

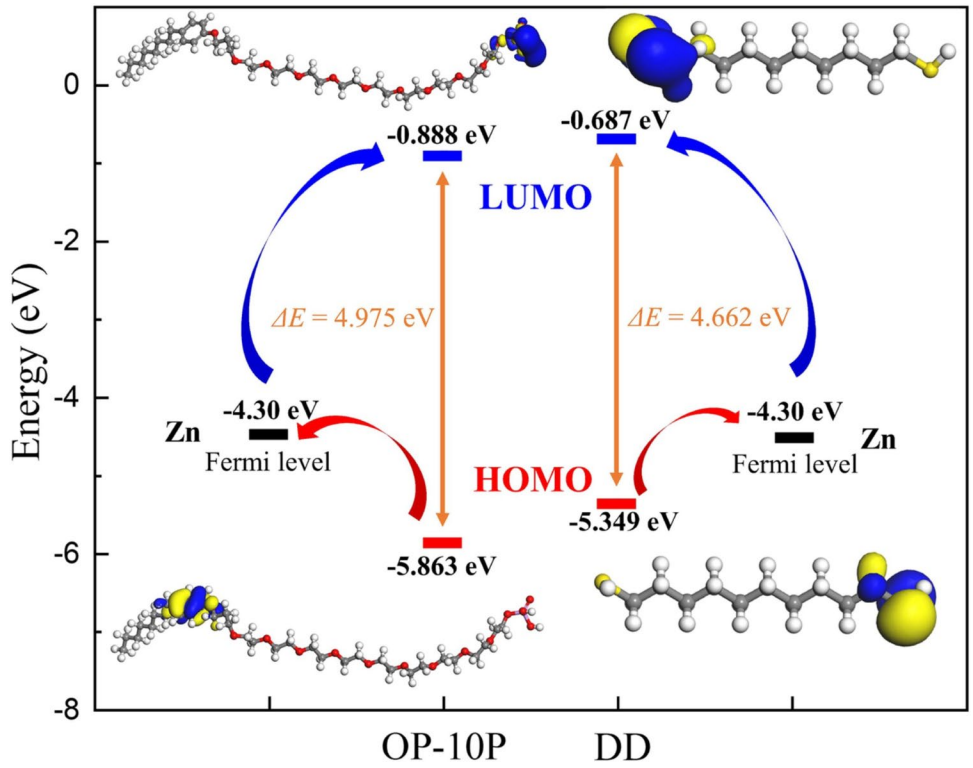

Fig. 10 Schematic presentation of the EHOMO, ELUMO, and ΔE for OP-10P and DD are among the pertinent parameters that are computed in quantum chemistry [207] (Reproduced with permission. © 2024 Elsevier)

production, dendrite growth, C_R, and improved uniformity in Zn deposition. MD simulations and DFT analyses revealed that SG replaced H_2O molecules in the solvation shells, enabling the formation of stable complexes and preventing corrosion (Fig. 12). The $E_{binding}$ for gluconate and Zn^{2+} was much greater than that of the water and Zn^{2+} system. The adsorption of SG follows a chemisorption mechanism retarding corrosion. Moreover, Na^+ ions enhance Zn^{2+} nucleation through electrostatic field modulation and preferential adsorption, thereby reducing dendrite growth.

The use of advanced molecules such as urotropine (URT) and 2-amino-6-trifluoromethoxybenzothiazole (TBA) in stabilization and corrosion protection of Zn anodes gained significant advancement [219, 220]. Le et al. demonstrated that TBA manifests remarkable capability by developing a zincophilic-hydrophilic interface coordinating with a benzothiazole anchor moiety and a terminal trifluoromethoxy group [219]. These result in steric shielding and selective chemisorption at the Zn-electrolyte interface. The electrochemical behavior of the Zn surface in 2 M $ZnSO_4$ solution with and without TBA is shown in Fig. 13. The larger diameter of the Nyquist plot semicircle in the presence of TBA suggests an increase in R_{ct} due to surface passivation (Fig. 13a). The Bode plots exhibit broadening of the phase angle and an increase in the impedance modulus, indicating enhanced capacitive properties and the formation of protective films at the Zn-$ZnSO_4$ electrolyte interface (Fig. 13b). The equivalent circuits used for fitting the EIS graphs are shown in Fig. 13c. TBA becomes effective by adsorbing onto the metallic surface, following the Langmuir isotherm model (Fig. 13d). PDP analyses showed that TBA decreased C_R and i_{corr} without a significant shift in E_{corr}, indicating that TBA is a mixed-type inhibitor (Fig. 13e). Lastly, LSV curves showed that the H_2 evolution potential shifted slightly to more negative values, suggesting reduced H_2O decomposition and H_2 evolution. The increased R_{ct}, decreased C_R, and i_{corr} values suggest that TBA becomes effective by blocking the surface-active sites through chemisorption.

Recently, the use of anticorrosive coatings to enhance corrosion resistance, electrochemical stability, durability, and rechargeability of the Zn anodes is gaining particular attention in battery technology [237]. Metal oxide-based

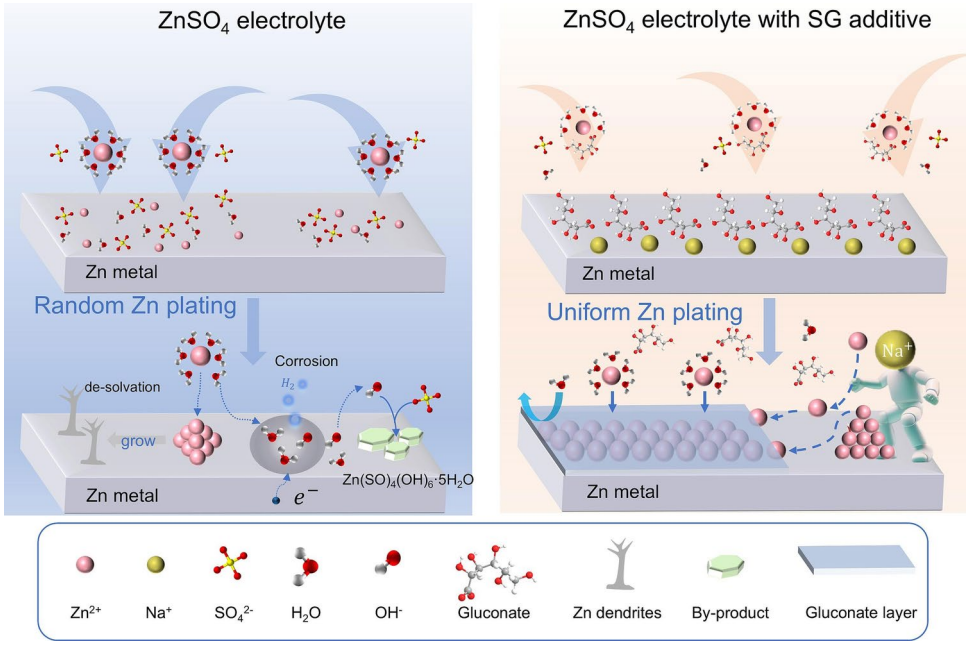

Fig. 11 Diagrammatic representation of SG and the related mechanisms of action [218] (Reproduced with permission. © 2024 Elsevier)

anticorrosive coatings, including TiO_2, Al_2O_3, CeO_2, and ZrO_2, have manifested remarkable performance in reducing C_R, i_{corr}, corrosion, and H_2 evolution while unchanging the electrochemical nature and stability of batteries. These metal oxides form stable and inherent films that separate the metallic substrates from corrosive environments. Al_2O_3 coatings (1.5 wt%) of Zn surface prepared by ALD and sol–gel approaches reduced i_{corr} by almost 79% and enhanced the capacity retention to 85–89.4% [221, 222]. The literature study reveals that Al_2O_3 coatings have been widely used due to their strong adhesion, barrier properties, inertness, and ability to block electron transfer. Al_2O_3 promotes the uniform deposition of Zn^{2+}, minimizes H_2 evolution (HER), and corrosion rate. Titanium dioxide (TiO_2)- based coatings have also been used to protect Zn anodes. Zhao et al. observed that TiO_2 minimized the formation of $Zn(OH)_2$, along with reducing the HER and C_R [223]. The TiO_2-coated Zn anode showed nearly 85% capacity retention after 1000 cycles. TiO_2 coatings also provide the blocking effects for O_2 and H_2O diffusion, minimizing the risks of localized corrosion [224]. Silica (SiO_2) based coatings are generally achieved by chemical solution and chemical vapor deposition (CSD and CVD) techniques.

Zn_2SiO_4 (zinc silicate) or SiO_2 coatings provide insulating properties while maintaining the electrochemical stability [225]. The highly adherent and compact layers of these coatings reduced HER, C_R, and i_{corr}. SiO_2 coatings also provide chemical barriers by limiting the gas evolution and hydroxide (OH^-) adsorption. The use of ZrO_2 coatings for Zn anode protection is highly rated, as they improve electrochemical stability and mechanical integrity. Lian and coworkers showed that ZrO_2 coatings stabilized the Zn-MnO_2 cells [226]. The adherent ZrO_2 layer promotes uniform nucleation of Zn^{2+} and acts as a physical barrier, preventing direct contact with the electrolyte. ZrO_2 coatings also reduced ZnO densification, thereby improving the corrosion rate and coulombic efficiency to 99.35% after more than 3800 h. The development of CeO_2 coatings for Zn anode protection can be considered one of the most advanced coating approaches, as Zn deposition along the (002) crystal planes reduces HER and dendrite growth [227]. CeO_2 coatings also reduced the contact angle (Fig. 14a, b). XRD analysis reveals the formation of effective and adherent coatings (Fig. 14c). The SEM images of bare and CeO_2-coated samples with and without immersion are shown in Fig. 14d–g. The PDP study revealed that the anodic and cathodic curves were significantly affected, and i_{corr} decreased notably with CeO_2 coatings (Fig. 14h). The CeO_2-coated anode shows 98.5% capacity retention after 4000 cycles. Overall, the CeO_2 coatings improve kinetic stability, retard side reaction and formation

https://doi.org/10.1007/s40820-026-02178-9

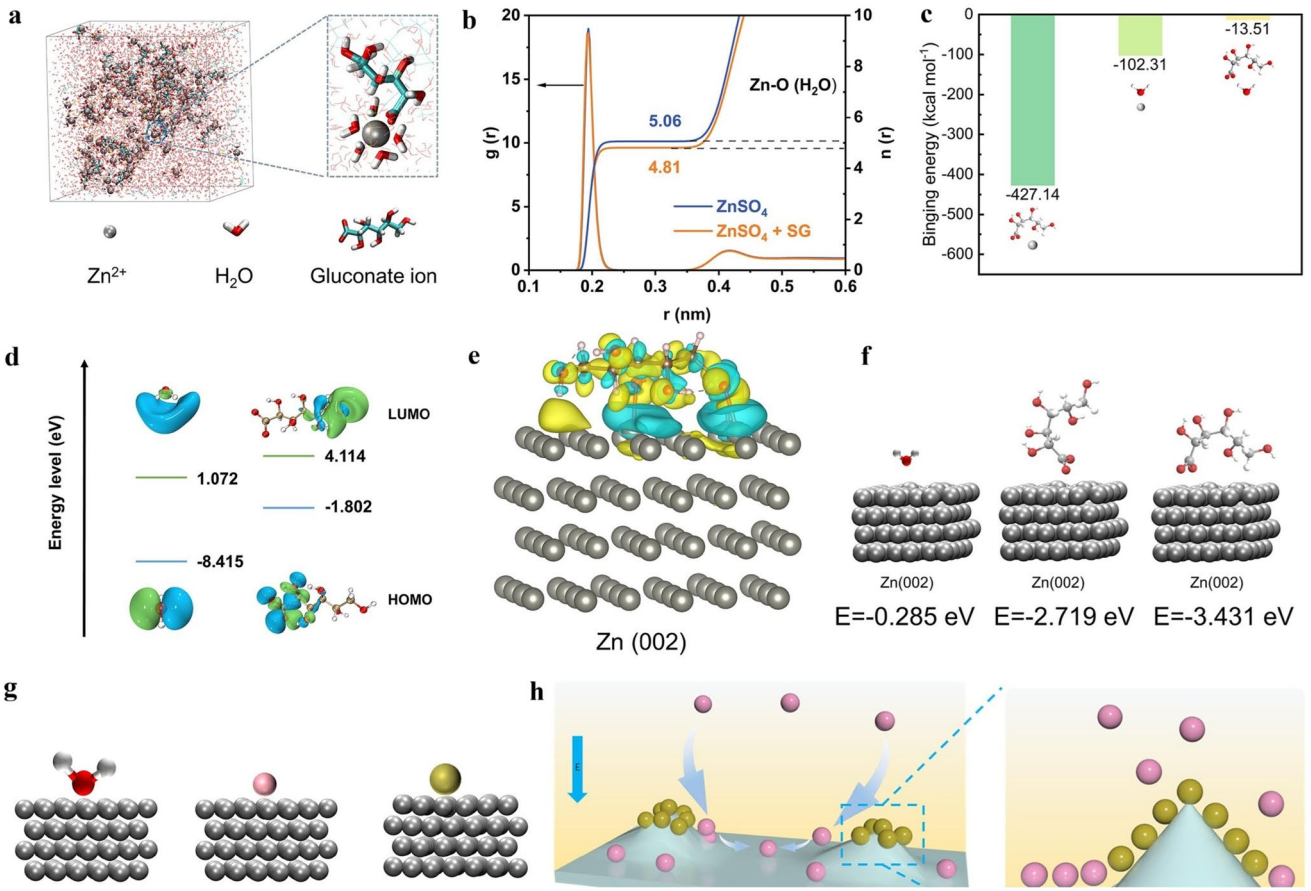

Fig. 12 **a** A partial magnified image depicting the Zn^{2+} solvation structure and a 3D photo of the $ZnSO_4$-SG system derived from MD simulations. **b** RDFs for Zn–O (H_2O) obtained from MD simulations of $ZnSO_4$-SG electrolyte. **c** Zn^{2+} binding energy with gluconate and H_2O molecules as determined by DFT. **d** LUMO and HOMO levels of gluconate and the H_2O molecule. **e** 3D isosurface diagrams showing the adsorption energy and charge density differential of SG (parallel) on Zn foil. **f** Comparison of gluconate and H_2O absorption energies on the Zn (002) crystal plane. **g** H_2O, Zn^{2+}, and Na^+ adsorption energies on the Zn (101) crystal plane. **h** Schematic illustration of how Na^+ suppresses Zn dendrites by electrostatic shielding [218] (Reproduced with permission. © 2024 Elsevier)

of byproducts, and promote uniform Zn growth. Similar observations have also been reported in the literature for $ZnNb_2O_6$ (zinc niobate) and $Al_2Si_2O_5(OH)_4$ (kaolin)-based coatings [228, 229].

Organic and polymer coatings provide both physical and flexible barriers that protect Zn anodes from H_2 evolution and corrosion, while retaining their excellent mechanical integrity and electrical conductivity. Jo et al. observed that PANI coatings prevent direct contact between the aqueous electrolyte and Zn particles [230]. The PANI coatings reduced the HER and self-discharge potential, maintaining a capacity retention of 97.8% after 24 h. The coatings demonstrated an effectiveness of 85% in providing corrosion protection. A similar observation was reported in another study involving PVDF-based coatings containing TiO_2 [230]. The hybrid coatings enhance chemical shielding and electrochemical stability. Carbon-based coatings offer multifaceted benefits, including reduced HER, C_R, and i_{corr}, uniform Zn deposition, and improved mechanical integrity and electrical conductivity. In the Zn@C shell structure, the carbon shell protects Zn from corrosion in alkaline solution and retards the ZnO leaching [231]. Nearly 99% capacity retention was derived after 400 cycles for the Zn@C shell structure. A Zn surface coated with surface-modified CNT (sCNT) blended with Zn_2SiO_4 exhibits excellent corrosion resistance properties [232]. The sCNT coatings offer dendrite-free cycling with a coulombic efficiency of nearly 99.5%. Cellulose nanofiber (CNF) and graphene acid (GA)- based

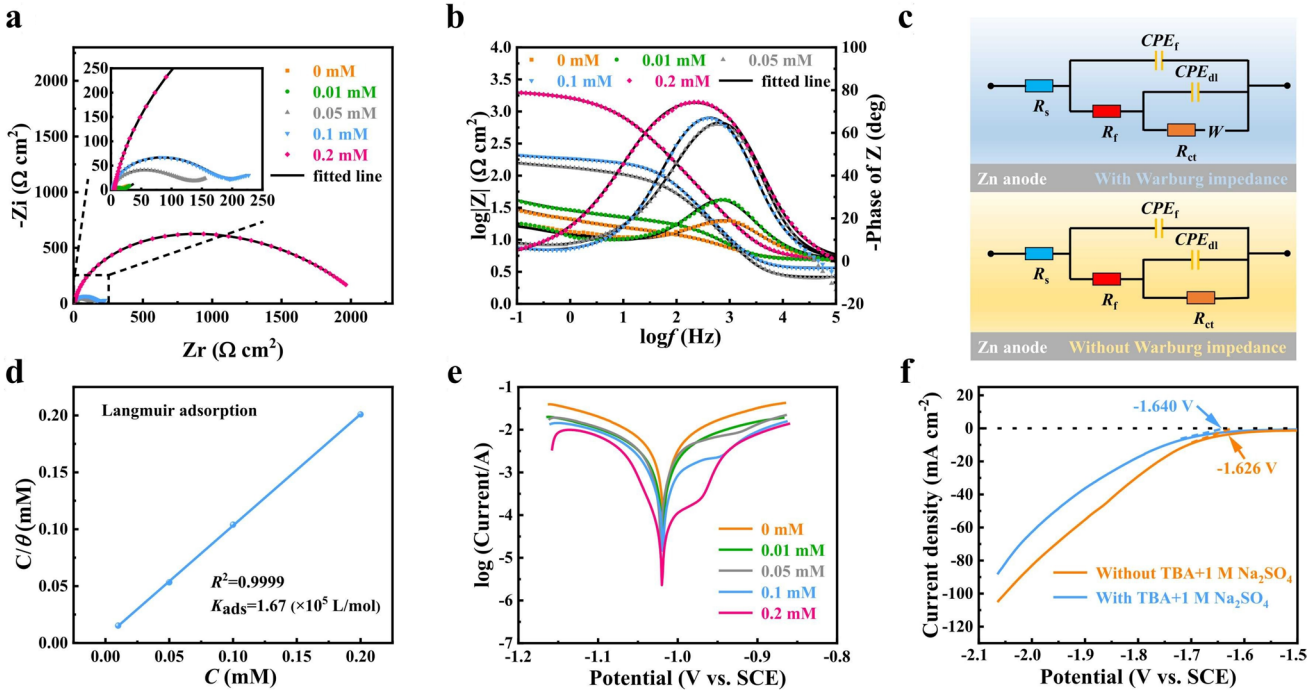

Fig. 13 **a** Nyquist curve, **b** Bode curve, **c** Equivalent circuit diagram, **d** Langmuir isothermal adsorption curve, and **e** Tafel diagram of the Zn electrode in ZSO solution with varying TBA concentrations. **f** LSV curve [219] (Reproduced with permission. © 2025 Elsevier)

composite (CNF/GA) coatings demonstrated self-discharge retention of 99% after 24 h. Hybrid (organic and inorganic) coatings provide multifunctional protection for Zn anode in aqueous electrolytes [224, 228, 233, 234]. Some metal-based anticorrosive coatings have also been developed and tested, exhibiting slightly lower coulombic efficiency and capacity retention [235, 236].

The corrosion resistance, H_2 evolution, and electrochemical reversibility can also be tailored through alloying the Zn anode with suitable elements [238, 239]. The literature study reveals that the presence of Ni, Bi, and Sn additives significantly improves performance. Jo et al. showed that the presence of 1-5wt.% of Ni and Bi reduced the C_R, i_{corr}, and H_2 evolution remarkably [240, 241]. A similar finding was reported elsewhere by Kang et al. [242], Da et al. [243], and Wang et al. [244] for Bi alloyed Zn anodes. The alloying not only improves corrosion resistance but also enhances battery performance, including capacity retention and high coulombic efficiency over 1000 cycles. Zhu and coworkers observed that the Sn-alloyed Zn anode showed 89.5% capacity retention [245]. They observed that for extended cycling, Sn alloying improves surface morphology and reduces H_2 evolution. LCSM images revealed that after 1000 cycles, the bare Zn surface becomes highly rough, covered with corrosion products, and exhibits surface pits, cracks, and dendrite growth (Fig. 15a). However, Fig. 15b shows that the ZnSn alloy surface remains significantly smoother and more uniform, with fewer surface defects. Figure 15c, d represents the roughness profile of bare Zn- and Sn-alloyed Zn surfaces, and Fig. 15e, f shows the underlying mechanisms. ZnSn alloy serves as an H_2 evolution inhibitor by reducing icorr and the H_2 evolution overpotential. The dendrite formation and growth were significantly reduced by uniform Zn^{2+} nucleation. Summaries of recent reports on the corrosion inhibition of Zn anodes using corrosion inhibitors, anticorrosive coatings, and alloying are presented in Tables 4, 5, and 6, respectively.

2.2 Electrochemical Corrosion and Corrosion Inhibition of Sustainable Aluminum-Based Batteries

Al-air batteries have attracted significant attention in energy storage systems owing to their low cost, high theoretical energy density, and eco-friendly nature [246, 247]. Nevertheless, like Zn-based batteries, the practical

https://doi.org/10.1007/s40820-026-02178-9

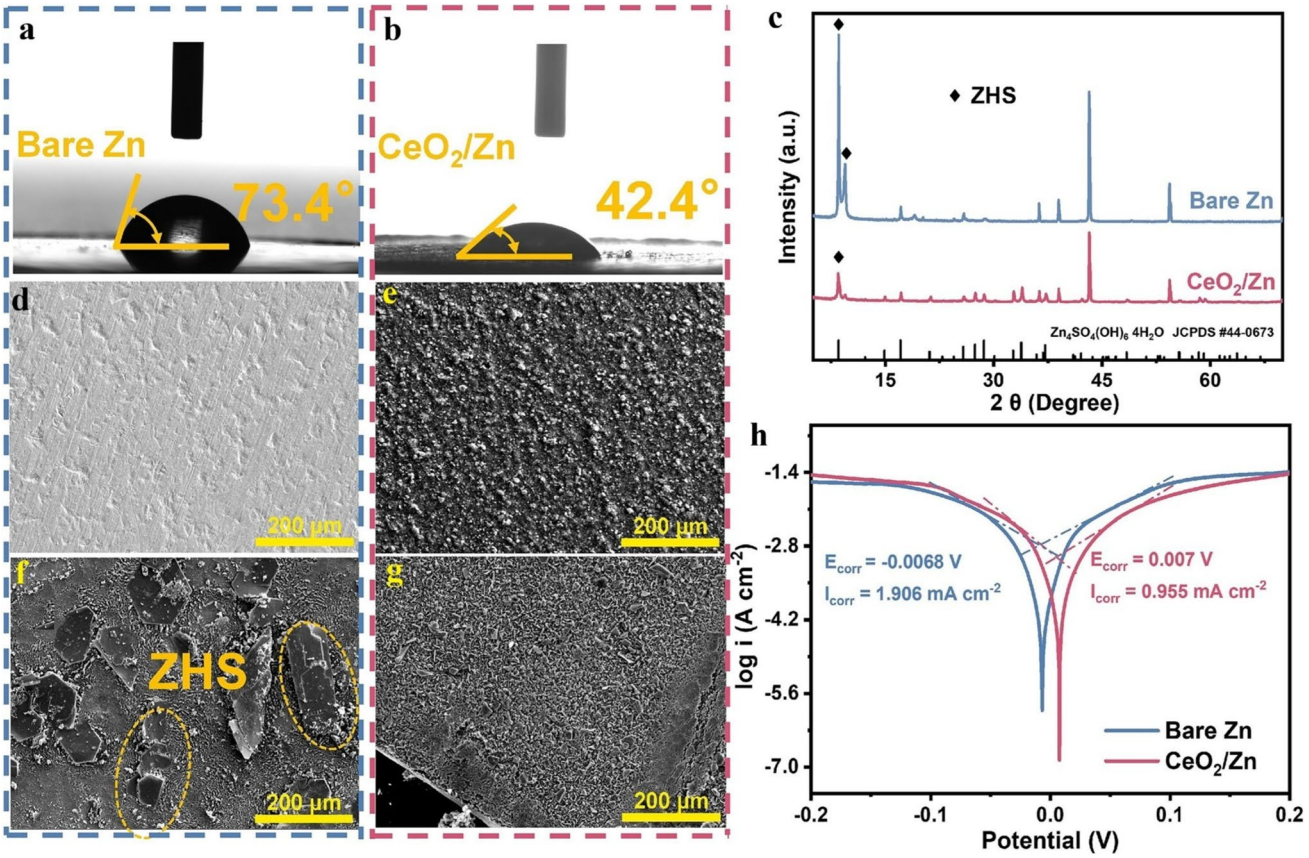

Fig. 14 Schematics showing **a** bare Zn and **b** CeO_2/Zn electrodes' water contact angle values. **c** Uncovered Zn and CeO_2/Zn anode XRD patterns following a 7-day immersion in 2 M $ZnSO_4$ electrolyte. Before and after immersion, SEM pictures of **d**, **e** bare Zn and **f**, **g** CeO_2/Zn. **h** Tafel curves of the CeO_2/Zn and bare Zn anodes [227] (Reproduced with permission. © 2025 Elsevier)

implementation of Al anode in electrode in alkaline electrolytes, mainly KOH and NaOH solutions, is constrained by its susceptibility toward corrosion [248, 249]. Al reacts with H_2O and OH^- and forms $Al(OH)_3$ and H_2 [250]. Corrosion leads to continuous, undesirable aluminum (Al) loss and hydrogen (H_2) evolution, resulting in poor anode utilization and coulombic efficiency. $Al(OH)_3$ layers serve as a barrier for discharge uniformity and electron transfer, resulting in a volatile voltage profile and reduced lifespan [251]. These circumstances increase C_R, i_{corr}, and H_2 evolution and enhance the probability of pitting corrosion. Recently, the use of organic compounds has emerged as an effective inhibitor for these undesirable reactions. Huo et al. studied and documented the inhibition potential of an amino acid derivative, namely N-α-Fmoc-N-epsilon-Boc-D-lysine (FDLH), for Al-5052 anode in 4M NaOH electrolyte [252]. They observed that FDLH significantly reduced AL-5052 anode dissolution and H_2 evolution. A careful inspection of Fig. 16 reveals that the electrochemical behavior is dramatically altered in the presence of FDLH. EOCP vs. time curves shifted to the positive (anodic) side, indicating the formation of protective films of FDLH.

PDP curves also showed a remarkable shift and reduction in icorr in the presence of FDLH. The tested inhibitor demonstrated 57.1% efficiency in inhibiting Al anode dissolution, serving as a mixed-type inhibitor. The increased diameter of the Nyquist plot and the enhanced impedance and phase angle of the Bode plot in the presence of FDLH suggest increased passivation and a higher R_{ct} for Al corrosion. EIS data were fitted using an equivalent circuit. In the absence of FDLH, the Al anode is freely attacked and corroded by H_2O and OH^-, leading to unrestricted corrosion and dissolution. However, FDLH forms a stable protective film using Al–O–C and Al-O-N bonds (Fig. 17). The dense, uniform, and hydrophobic film exhibits multifunctional

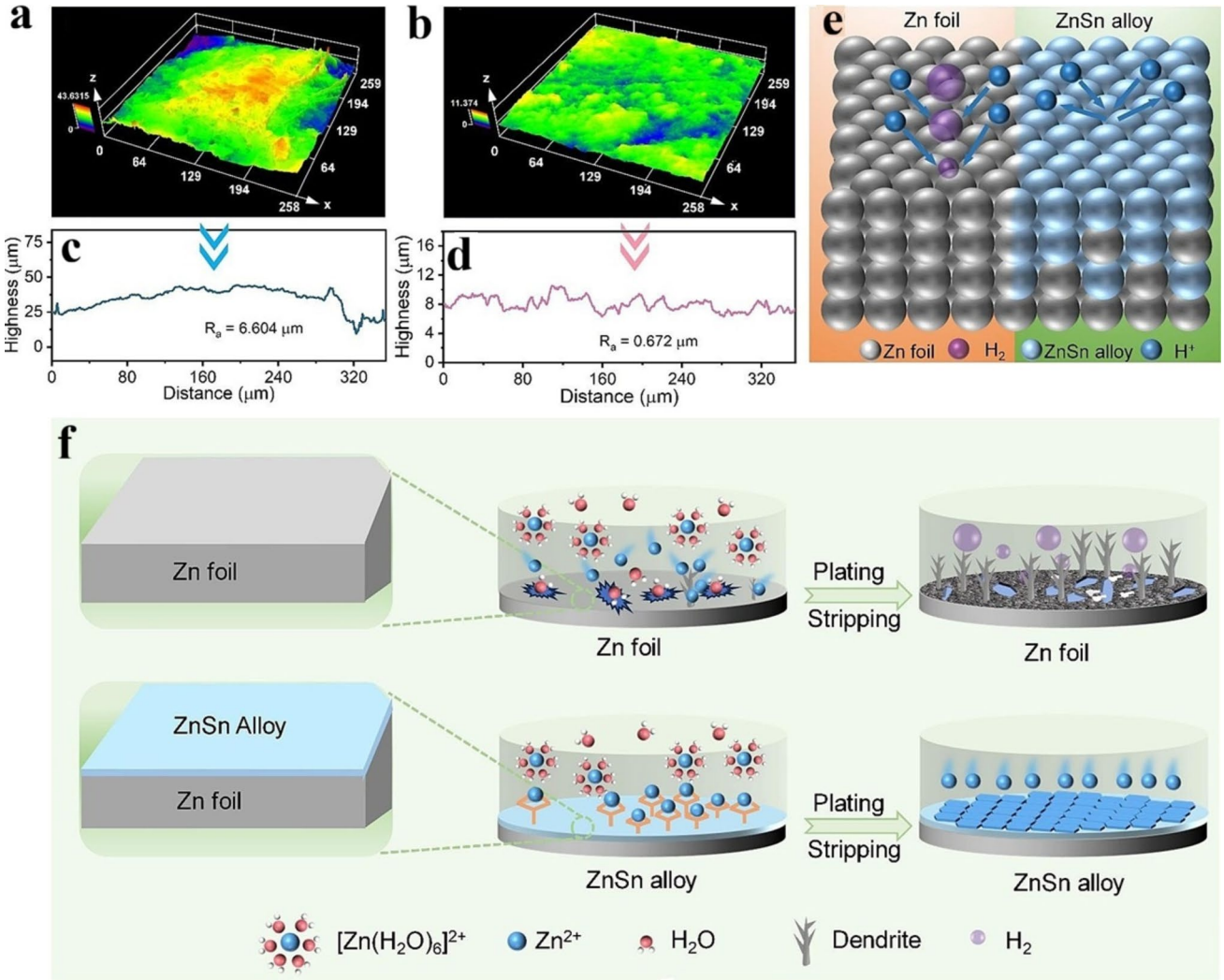

Fig. 15 3D LCSM images of **a** Zn foil and **b** ZnSn alloy after 1000 cycles. **c** and **d** roughness profile. **e** Schematic diagram of H_2 inhibition of ZnSn alloy. **f** Diagram of the modification mechanism of ZnSn alloy [245] Reproduced with permission. © 2025 Elsevier)

properties, enhancing both corrosion resistance and battery performance. FDLH inhibits both anodic and cathodic reactions. These observations showed that the FDLH inner layer serves as a chemical passivator while its outer layer retards the diffusion of corrosive species, including OH^- and H_2O. The inhibition potential of organic and polymeric inhibitors, including PVA, CTAB, heterocycles, sodium octanoate (SO), sodium benzoate (SB), and sodium citrate hydrate (SC), has been studied and described widely [253–258]. They effectively adsorb at the interface between the Al anode and the alkaline electrolyte via their electron-rich coordination sites, thereby inhibiting corrosion.

El-Alouani et al. showed that the electronic structures of inhibitors played a crucial role in their adsorption and inhibition potential [254]. They showed that HOMO and LUMO were distributed over $–NO_2$ and –CN groups of Z4 molecules, indicating that these sites were involved in the charge transfer and adsorption (Fig. 18). The careful inspection also reveals that electron density regions are mainly located around O and N atoms, suggesting that they serve as sites for coordination bonding and chemisorption. These molecules retard the self-corrosion of the Al anode and form protective films. Many studies reported the inhibition potential of tannic acid (TA) [259], [Amim][TFSI] (ILs) [260], ZnO + PEG

 https://doi.org/10.1007/s40820-026-02178-9

Table 4 A summary of some recent reports on corrosion inhibition of Zn anode using corrosion inhibitors

S/N	Anode material	Battery type	Battery Electrolyte	Corrosion inhibitor(s)	Inhibition properties		Salient features	References
					Concentration	Efficiency		
1	Hg-free Zn powder	Alkaline Zn-MnO_2 batteries	1 M KOH	Diphenylglyoxim, Tripropylene glycol, Diaminepyridine, 2,4-Dinitrophenol, PEG-200, and PEG-600	1.0%	NA	a) Reduced anodic dissolution b) Improved cycling c) Reduced H_2 evolution	[159]
2	Hg-free pure Zn and Zn alloy (Mg &Pb)	Alkaline Zn-MnO_2 and Zn-air batteries	10 M NaOH- additives	sodium stannate, CaO, and sodium citrate	0.02 M, 0.3 and 15 wt.%	Up to 99.0%	a) Hg-free anodes b) Reduced anodic dissolution c) Corrosion under anodic control (i.e., anodic-type inhibition)	[160]
3	Zn plate (99.99%)	Alkaline Zn-MnO_2 and Zn-air batteries	ZnO saturated 8.5 M KOH	GAFAC RA600 (polyoxyethylene alkyl phosphate ester acid) and PEG-600	400–4000 ppm	RA600: 800–2000 ppm	a) PEG retard anodic reactions and H_2 evolution b) Protection effectiveness increases with time	[161]
4	Zn powder coated with Nb	Alkaline Zn-based batteries	ZnO saturated 6 M KOH	Nb nitrate covering ($Nb(NO_3)_3$)	0.045 M $Nb(NO_3)_3$	90.9% (10 min US)	a) Uniform Nb-rich protective covering was formed b) Reduced corrosion current density (i_{corr}) c) Increased transfer charge resistance (R_{ct})	[162]
5	Zn (99.35%)	Zn-Mn dry batteries	1 M $ZnCl_2$, 1 M NH_4Cl and their mixed	Amidopoly Ethylamines	1000 ppm	$ZnCl_2$ (84%; Comp-IV), NH_4Cl (68%; Comp-IV), and 79.8%	a) The inhibitors served as mixed types and adsorbed chemically b) Efficiency decreases with temperature	[163]
6	Zn sheet (99.99%	Alkaline Zn-MnO_2 batteries	3 and 8 M KOH	Tween 20 and PEG-600	500 ppm (Tween 20) + 500 PEG-600	89.7% (weight loss)	a) Tween and Peg-600 synergistically improve adsorption d) Self-discharge was greatly hindered along with HER	[164]

Table 4 (continued)

S/N	Anode material	Battery type	Battery Electrolyte	Corrosion inhibitor(s)	Inhibition properties		Salient features	References
					Concentration	Efficiency		
7	Zn sheet (99.99%	Alkaline Zn-MnO_2 batteries	ZnO saturated 3 M KOH	PEG-600 + IMZ (imidazole)	0.05 wt.% PEG-600 + 0.05 wt.% IMZ	83% (WL) & 79.9 (PDP)	a) IMZ retards anodic reactions b) PEG-600 reduced cathodic reactions c) Synergistic combination of IMZ and PEG-600 showed better performance than Hg-based inhibitors	[165]
8	Zn sheet	Alkaline Zn-MnO_2 batteries	ZnO saturated 7 M KOH	DTAB: (dodecyl trimethylammonium bromide)	0.07wt.%	80.2%	a) DTAB acted as an anodic inhibitor b) Delayed Zn passivation c) Forms a fluffy and diffusive protective film, allowing ion diffusion	[166]
9	Zn sheet	Alkaline Zn-MnO_2 (Zn-C) batteries	26% NH_4Cl	HEC (Hydroxyethyl cellulose)	300 ppm	93.90%	a) Reduced corrosion rate b) Improved anodic stability c) Improved shelf life and safe operation d) Reduced H_2 evolution and self-discharge	[157]
10	Zn (98.55%) alloy	Alkaline Zn-MnO_2 (Zn-C) batteries	7 M KOH	Polyoxyethylene (40) nonylphenyl ether(PNE)	0.25 mM	98.01%	a) Enhanced stability and specific capacity b) Reduced Zn corrosion c) Increased performance and greenness	[167]
11	Zn (bare)	Zn-based alkaline batteries	25 g L^{-1} KOH + 6 M KOH	CMC (carboxymethyl cellulose)	10–20 g L^{-1}	43.5%	a) Decreased C_R, dendrites, and surface roughness d) CMC replaces OH-/H_2O and self-adsorbs	[168]

https://doi.org/10.1007/s40820-026-02178-9

Table 4 (continued)

S/N	Anode material	Battery type	Battery Electrolyte	Corrosion inhibitor(s)	Inhibition properties		Salient features	References
					Concentration	Efficiency		
12	Zn (bare) powder	Alkaline Zn-Ni secondary batteries	ZnO saturated 6 M KOH	OED (2-octanone ethylene diamine)	4wt.%	95.1%	a) 70% theoretical capacity was maintained for Zn-Ni after 30 cycles b) OED enhances discharge voltage and cyclic capability c) Using N and O, OED forms hydrophobic films	[169]
14	Zn battery grade	Leclanché primary cell (Zn-C)	26% NH_4Cl	SDBS (Sodium dodecyl benzene sulfonate)	0.8 mM	89.7%	a) Adsorbs at positive potential and forms a protective film b) Smoothened Zn surface c) Outperform $HgCl_2$ benchmark	[170]
15	Zn and Zn-Ni alloys	Zn-Ni and Zn-MnO_2 alkaline batteries	8 M KOH	PEG-400 and CTMAB (cetyltrimethylammonium bromide)	250 ppm PEG + 250 ppm CTMAB	96.8% (Zn-10Ni alloy)	a) PEG-400 and CTMAB synergistically enhance their adsorption b) Reduced self-discharge and anodic dissolution c) Improved corrosion resistance and lifetime	[171]
16	Zinc	Aqueous Zn batteries	1 M $ZnSO_4$	AQS (sodium anthraquinone-2- sulfonate)	–	Coulombic efficiency: > 99.6%	a) Self-retention capacity was 92% after 500 cycles b) Showing stable cycling for 470 h	[174]
17	Zn (bare)	Hybrid aqueous batteries	1 M $ZnSO_4$ + 1 M $LiSO_4$	Pb^{2+} ions ($PbSO_4$)	5.0 wt.%	i_{corr} reduced 20%	a) Self-discharge retention was nearly 18% b) A 74.4% capacity retention was observed after 300 cycles c) Float charge current reduced to 65%	[177]

Table 4 (continued)

S/N	Anode material	Battery type	Battery Electrolyte	Corrosion inhibitor(s)	Inhibition properties		Salient features	References
					Concentration	Efficiency		
18	Zn (bare)	Rechargeable Zn-$LiMn_2O_4$ (aqueous) batteries	2 M $ZnSO_4$ + 1 M $LiSO_4$	Pyrazole + 5 wt.% fumed silica	0.2wt.% Pyrazole + 5 wt.% fumed silica	i_{corr} decreased from 5.25 to 0.9 mA cm^{-2} (~ 83%)	a) Increased recharge capacity b) 83.7% self-retention after 500 cycles d) Self-discharged reduced to 20% after 24 h	[178]
19	Zn metal	Rechargeable Zn-MnO_2 (aqueous) batteries	2 M $ZnSO_4$ with $MnSO_4$ and gelatine	Mn^{2+} ions + gelatine	0.2 M (Mn_2) + ions + 0.5 wt.% gelatine	i_{corr} decreased to 75 times	a) Increased specific capacity to 86 mAh g^{-1} b) Increased retention to 79.6% after 1000 cycles c) Gelatine forms a protective film and increases corrosion resistance	[179]
20	Zn (bare)	Rechargeable $LiMn_2O_4$ (aqueous) batteries	2 M $ZnSO_4$ + 1 M $LiSO_4$	PEG-200, 300, and 400	1 vol% PEG-200	i_{corr} reduced from 1.05 to 0.29 mA cm^{-2} (~ 72%)	a) Deposition current density decreased from 8.64 to 3.89 mA cm^{-2} b) Ecorr shifted in the positive direction, retarding H_2 evolution	[176]
21	Zn (bare)	Alkaline Zn batteries	25 g/L ZnO + 8.5 M KOH	PEG-600 (di acid)	800 ppm PEG-600 di acid	i_{corr} decreased from 90 to 10 mA cm^{-2} (9 times)	a) At 65 °C, PEG-600 forms a protective film, increasing the corrosion resistance b) The PEG films also reduced C_R, water permeability, and HER	[175]
22	Zn (bare) granules	Zn-air flow batteries	7 M KOH	Pluronic F-127 (P127) and sodium Dodecyl Sulfate (SDS)	SDS: 0.2 mM and P127: 100 ppm	i_{corr} decreased from 15.54 to 10.51 mA cm^{-2} (SDS)	a) SDS and P127 inhibited passivation and corrosion b) They hinder HER and ZnO film formation c) Charge transfer increases, and current density decreases	[180]

https://doi.org/10.1007/s40820-026-02178-9

Table 4 (continued)

S/N	Anode material	Battery type	Battery Electrolyte	Corrosion inhibitor(s)	Inhibition properties		Salient features	References
					Concentration	Efficiency		
23	Zn-Bi composite	Alkaline Zn-air batteries	6 M KOH	Benzotriazole (BTA), thiourea (CH_4N_2S), and SDBS	BTA and SDBS: 60 mg L^{-1} & CH_4N_2S: 7.6 g L^{-1}	76.9% (BTA) and 69.2% (SDBS)	a) Their %IE followed the sequence: BTA (76.9%) > SDBS (69.2%) > CH_4N2S (61.5%) b) They form surface protective coordination complexes c) Retention capacity was 96% after 60 cycles	[181]
24	Zn (bare) particles	Alkaline Zn-air batteries	45 wt.% KOH	Tween 20, PEG-600, and SDBS (Sodium dodecyl benzenesulfonate)	5–15 wt.%	Their effectiveness followed the order: SDBS > Tween 20 > PEG-600	a) SDBS, Tween 20, and PEG-600 showed the best performance at 10, 5, and 15 wt.%, respectively b) SDBS forms laminar protective films and improved conductivity c) Suppressed ZnO passivation	[182]
25	Zn (bare)	Zn-air batteries	6 M KOH + additives	$Zn(OAc)_2$ (zinc acetate) and Zn(Glu) (zinc gluconate	0.1 M $Zn(OAc)_2$ + 0.1 M Zn(Glu)	C_R decreased from 0.463 to 0.0467 g m^{-2} h^{-1}	a) They adsorb and form a thick film b) They increase the impedance and reduce dissolution c) Dendrite-free surface, longer lifecycle (297 h), and specific capacity (94%)	[183]
26	Zn (bare)	Alkaline Zn-air batteries	0.3 M ZnO + 6 M KOH	PEI (polyethylenimine) MW-600	50 ppm	52.2%	a) PEI adsorbs and reduces dendrites and C_R with a slight enhancement of HER b) Surface analyses showed the formation of dense inhibitive films c) Ecorr shifted to the positive side	[184]

Table 4 (continued)

S/N	Anode material	Battery type	Battery Electrolyte	Corrosion inhibitor(s)	Inhibition properties		Salient features	References
					Concentration	Efficiency		
27	Zn (bare)	Zn-I_2 batteries	2 M $ZnSO_4$	$(Zn_3(BTC)_2)$ MOFs	Ionic Sieve Membrane	C_R and H_2 evolution were reduced	d) C_R, HER, and dendrite formation were reduced e) Self-retention was 84.6% after 6000 cycles f) Coulombic efficiency was 99.65%	[64]
28	Zn (bare) (99.99%)	Zn-ion batteries	2 M $ZnSO_4$	BD (1-butyl-3-methylimidazolium phosphate dibutyl ester salt)	2.5 mM	91.3%	a) Forms stable inhibitive films b) Reduced dendrites and corrosion c) Adsorption follows the LAI model	[185]
29	Zinc (bare)	Zn-ion batteries	1 M $ZnSO_4$	EG (ethylene glycol)	25 v/v%	–	a) Decreased corrosion and reduced corrosion product formation	[186]
30	Zinc (bare)	Zn-ion batteries	2 M $ZnSO_4$	NH_4OH	1 mM	Decreased HER and C_R	a) Lowered HER, C_R, dendrites, and rough surface b) > 70% capacity retention was observed after 1500 cycles	[173]
31	Zinc (bare)	Zn/Cu, Zn/Zn	2 M $Zn(OTf)_2$	scandium (Sc^{3+}) ions	0.5 M	99.5% coulombic efficiency	a) Sc^{3+} provides effective cycling, dendrite-free, and very long life, i.e., after 5000 cycles	[187]
32	Zinc (bare)	Zn-MnO_2 batteries	2 M $ZnSO_4$	polyhydroxylated sugar (Trehalose)	100 mM	i_{corr} reduced 45%	b) Trehalose chemically adsorbs, altering Zn dissolution c) HER was significantly reduced d) Self-retention capacity was 89% after 1000 cycles and 1600 h	[188]

https://doi.org/10.1007/s40820-026-02178-9

Table 4 (continued)

S/N	Anode material	Battery type	Battery Electrolyte	Corrosion inhibitor(s)	Inhibition properties		Salient features	References
					Concentration	Efficiency		
33	Pure Zn	Zn-air and Zn-ion batteries	3.5% NaCl	Na_2SO_4 (sodium sulfate)	0.5 g L^{-1}	C_R = 4.26 mpy	a) 0.5 g L^{-1}increases resistance, and 1.0 g L^{-1} decreases it b) At 0.5 g L^{-1}, Na_2SO_4 serves as an anodic-type inhibitor and forms $ZnSO_4$ film c) Cl- ions integration destabilizes protective films	[204]
34	Zn (bare)	Zn-ion and Zn-V_2O_5 batteries	1 M $ZnSO_4$	SPS (anionic sodium 3,30-dithiodipropane sulfonate)	10 mM	i_{corr} reduced from 23 to 10 mA cm^{-2} (56.5%)	a) SPS adsorbs on the surface and doesn't produce any effect of Zn^{2+} ions' solvation b) Zn nucleation, HER, and C_R were reduced	[203]
35	Zn (bare)	Zn-ion batteries	2 M $ZnSO_4$	NTA (nitrilotriacetic acid)	0.15 wt.%	93.9%	a) NTA forms chemisorbed protective films b) C_R was reduced 16 times c) Coulombic efficiency 99.4% -99.6%	[205]
36	Zn (bare)	Zn-ion batteries	2 M $ZnSO_4$	BHB (6-bromo-1 H-benzimidazole)	2.0 mM	99.1%	a) Forms stable inhibitive films b) Reduced anodic dissolution c) Reduced H_2 evolution	[206]
37	Pure Zn (99.99%)	Zn-air batteries	6 M KOH	OP-10P (octylphenol polyoxyethylene ether phosphate) and DD (1,10-decanedithiol)	200 mg L^{-1} (OP-10P): 100 mg L^{-1} (DD)	99.9%	a) OP-10P forms the inner layer, and DD forms the outer layer b) Reduced dendrites c) Stabilized discharge	[207]

Table 4 (continued)

S/N	Anode material	Battery type	Battery Electrolyte	Corrosion inhibitor(s)	Inhibition properties		Salient features	References
					Concentration	Efficiency		
38	Zn (bare)	Zn-ion batteries	2 M $ZnSO_4$	Pyr (pyrazine), Pym (pyrimidine), and Pyd (pyridazine)	6.94 mM	i_{corr} reduced from 0.58 to 0.09 μA cm^{-2} (85%; Pyd)	a) 90% and 78% self-retention after 500 and 3000 cycles, respectively b) Pyd absorbs, and nucleation occurs through N-atom c) Reduced desolvation, H_2O activities, HER, and byproducts formation	[208]
39	Zn (bare)	Zn-I_2 batteries	1 M $ZnSO_4$	FCD (Fucoidan)	25 mM	Impedance increased from 380 to 776 Ω cm^{-2}	a) FCD suppressed dendrites and passivation b) Protective film of FCD shielded electrolyte d) C_R was reduced nearly 50%	[155]
40	Zn (bare)	Zn-MnO_2 batteries	2 M $ZnSO_4$	ggg (triglycine)	0.2 mM	Reduced i_{corr} values	a) Ggg coordinates with Zn^{2+} ions, forming a stable film b) Suppressed C_R and HER e) Zn life was extended > 4000 h	[209]
41	Zn (bare)	Aqueous Zn-I_2 batteries	1 M $Zn(OAc)_2$	EG (ethylene glycol) + I_2 (iodine)	10 V% EG + 0.05 wt.% I_2	C_R reduced from 514.7 to 43.7 mpy (15 times)	a) Reduced C_R and dendrites b) Self-retention was 91% after 250 cycles and 64.5% after 3000 cycles c) Specific capacity was 1210 mAh g^{-1}	[210]
42	Zn (bare)	Zn-V_2O_5 batteries	2 M $ZnSO_4$	C_5SeCN (Crown ether)	0.3 wt.%	Impedance rose 3 times	a) C_5SeCN reduces H_2O activities, and a Zn–O film was developed b) Coulombic efficiency was 99.4% after 4500 h c) Self-retention was 92% after 300 cycles	[211]

https://doi.org/10.1007/s40820-026-02178-9

Table 4 (continued)

S/N	Anode material	Battery type	Battery Electrolyte	Corrosion inhibitor(s)	Inhibition properties		Salient features	References
					Concentration	Efficiency		
43	Zinc (bare)	Aqueous Zinc batteries	1 M $ZnSO_4$	BD (1,2 butanediol) and PD (1,2- pentanediol)	1 vol%	i_{corr} reduced from 116.8 to 44.9 μA cm^{-2}	a) Zn retention was 98% after 24 h soaking b) BD and PD form an inhibitive film c) Coulombic efficiency was over 99.6%	[212]
44	Zn (bare)	Seawater-based Zn-ion batteries	2 M $ZnSO_4$ + 3.5% NaCl	PBTCA (2 phosphonobutane-1,2,4-tricarboxylic acid)	1.0 mM	–	a) Columbic efficiency was over 99.6% after 2000 cycles b) HER reduced to nearly 88% and cycle life rose from 200 to 2000 h d) Protective film retards the diffusion of Cl^- and H_2 evolution	[213]
45	Zn (bare)	Zn-ion batteries	2 M $ZnSO_4$	$[Zn(AcAc)_2]$ (zinc acetylacetonate)	5.6 g L^{-1}	i_{corr} dropped from 146 to 67 μA cm^{-2}	a) Decreased C_R, wettability, HER, and contact angle b) Self-retention of 52.9% after 12,000 cycles c) Reduced H_2O activities	[214]
46	Zn (bare)	Zn-ion batteries	2 M $ZnSO_4$ + 0.15 $MnSO_4$	DA-PPy (dopamine-functionalized polypyrrole)	DA: PPy = 1:10 (20 h)	E_{corr} shifted from −0.023 to −0.017 (more positive)	a) Decreased H_2 evolution, charge transfer, and activation energy b) N and O coordinate with the Zn^{2+} ions and form surface protective films	[215]
47	Zn (bare)	Aqueous Zn–S batteries	2 M $ZnSO_4$	PCA (pyrrolidone carboxylate)	30–60 mM	E_{corr} shifts were observed	a) Inhibits Zn corrosion b) The self-retention was 87% after 30,000 cycles c) Specific capacity was 211 mAh g^{-1}	[216]

Table 4 (continued)

S/N	Anode material	Battery type	Battery Electrolyte	Corrosion inhibitor(s)	Inhibition properties		Salient features	References
					Concentration	Efficiency		
48	Zn (bare)	Zn-V_2O_5 batteries	1 M $ZnSO_4$	IP (Imidazo[1,2-b] pyridazine)	0.2 mg L^{-1}	i_{corr} reduced from 1.293 to 0.368 mA cm^{-2}	a) Nearly 70.5% efficiency was derived by IP b) Adsorption of IP anchor Zn^{2+} ions and block H_2O diffusion c) Coulombic efficiency was 98.72% and highly stable for 2200 h	[217]
49	Zn (bare)	Zn-ion batteries	2 M $ZnSO_4$	SG (sodium gluconate)	0.2 M	46%	a) Cycle life increased from 170 to 1800 h b) Attained the specific capacity of 97.4% c) SG forms a protective, highly stable chelating complex	[218]
50	Zn metal	Zn-ion batteries	2 M $ZnSO_4$	TBA (2-amino-6-Trifluoromethoxy-benzothiazole)	0.1 mM	99.1%	a) TBA forms a hydrophobic film b) Serves as a mixed-type inhibitor c) Reduced H_2 evolution and dendrites	[219]
51	Zn (bare)	Aqueous Zn-ion batteries	1 M $ZnSO_4$	URT (Urotropine)	5 mM	i_{corr} decreases from 0.97 to 0.28 mA cm^{-2}	a) Formed bilayer, inhibits HER and dendrites b) Improved wettability, self-life, and self-discharge retention c) Reduced nucleation overpotential	[220]

https://doi.org/10.1007/s40820-026-02178-9

Table 5 A summary of some recent reports on corrosion inhibition of Zn anode using anticorrosive coatings

S/N	Anode material	Battery type	Battery electrolyte	Coating matrix	Coating medium	Efficiency	Salient features	References
1	Zn (bare) particles	Flexible Zn-air batteries	9 M KOH	Al_2O_3-based coatings (1.5 wt.%)	via the sol–gel technique	i_{corr} reduced from 525.4 to 112.1 μA cm^{-2} (78.7%)	a) Al_2O_3 films retards corrosion and H_2 evolution b) Best performance was observed at 1.5 wt.% after this segregation starts c) Retention capacity was 85% after 7 days	[221]
2	Zn (bare)	Zn-MnO_2 batteries	3 M $Zn(SO_3CF_3)_2$	Al_2O_3 and ALD-based ultra-thin coatings	Thickness: 0.2 mm	Decreased i_{corr} from 8.20 to 4.91 mA cm^{-2} (~41%)	a) 89.4% self-retention after 1000 cycles b) Reduced dendrites and contact angles	[222]
3	TiO_2-coated Zn (TiO_2@Zn)	Zn-MnO_2 batteries	Aqueous 3 M $Zn(OTf)_2$	Ultrathin TiO_2 coating (ALD)	Thickness: 8 nm	H_2 evolution was slowed	a) Reduced HER and formed $Zn(OH)_2$ passive film b) Increased self-discharge stability c) Self-retention was 85% after 1000 cycles d) 99% coulombic efficiency was achieved under long-term exposure	[223]
4	anti-corrosion elastic constraint (AEC)-Zn	Zn-MnO_2 batteries	2 M $ZnSO_4$	TiO_2 NPs + PVDF coatings	Thickness: 5 μm	Polarization decreased > 60%	a) Coulombic capacity was 99.4% b) PVDF blocks H_2O/O_2 diffusion c) Stable up to 2000 h cycling	[224]

Table 5 (continued)

S/N	Anode material	Battery type	Battery electrolyte	Coating matrix	Coating medium	Efficiency	Salient features	References
5	Zn particles	Zn-air batteries	6 M KOH	SiO_2-based coatings	CVD and CSD coatings	~40% reduced H_2 evolution	a) Reduced Zn dissolution and H_2 evolution b) Semiconductive Zn_2SiO_4 coatings were derived from CVD c) Insulating SiO_2 coatings were derived from CSD d) Coatings improved oxidation stability	[225]
6	Zn coated with ZrO_2	Zn-MnO_2 batteries	2 M $ZnSO_4$	ZrO_2-based coatings	Thickness: 4 μm	C_R reduced 3 times	a) Coulombic efficiency of 99.36% was derived b) C_R and HER were reduced c) Stable up to 3800 h cycling	[226]
7	Zn (bare) with CeO_2	Zn-ion batteries	2 M $ZnSO_4$	CeO_2-based non-conductive coatings	Thickness: 10 μm	i_{corr} decreased from 1.906 to 0.955 mA cm^{-2}	a) Coating decreased the contact angle (42.4°) and increased the wettability b) Very low polarization decreased gas evolution and surface bubbling c) Retention capacity was 98.5% after 4000 cycles	[227]

https://doi.org/10.1007/s40820-026-02178-9

Table 5 (continued)

S/N	Anode material	Battery type	Battery electrolyte	Coating matrix	Coating medium	Efficiency	Salient features	References
8	Zn with	Aqueous Zn batteries	2 M $ZnSO_4$	$ZnNb_2O_6^-$basec coatings	Thickness: 5 µm	C_R decreased nearly 16%	a) Cycle life of > 2000 h was attained after 3000 cycles b) Coulombic efficiency was 99.54% to 99.99%, with a retention capacity of 80.2% after 3000 cycles c) $ZnNb_2O_6$ serves as a multifunctional artificial solid electrolyte interphase (SEI)	[228]
9	Zn (bare)	Zn-MnO_2 batteries	2 M $ZnSO_4$	$Al_2Si_2O_5(OH)_4$ (Kaolin coating)	Thickness: 18–27 µm	Impedance increased 2 times	a) Excellent anticorrosion property b) Dendrite-free surface c) Long cycle stability, i.e., 800 h and 600 cycles	[229]
10	Zn particles	Zn-air batteries	7 M KOH	PANI coatings (20PANI@Zn)	20 mL HCl	85%	a) Reduced self-discharge b) Reduced HER c) 97.8% retention capacity after 24 h	[230]
11	Zn@C core shells	Rechargeable Zn-MnO_2 batteries	0.125 M ZnO + 6 M KOH	Carbon (C) shell coatings	Electrochemical reduction method (ZnO@C-A)	ZnO leaching decreased from 12.5 to 2.5%	a) 98.8% retention capacity was observed after 400 cycles b) Coulombic efficiency was 84% after 400 cycles c) ZnO leaching decreased from 12.5% to 2.5%	[231]

Table 5 (continued)

S/N	Anode material	Battery type	Battery electrolyte	Coating matrix	Coating medium	Efficiency	Salient features	References
12	Zn (bare)	Zn-MnO_2 batteries	2 M $ZnSO_4$	sCNT-based coatings	0.0125 wt.% sCNT; Thickness: 15 µm	i_{corr} reduced from 2.16 to 0.52 mA cm^{-2}	a) Reduced C_R and HER and dendrites free Zn deposition b) High self-discharge stability up to 1600 h c) Coulombic efficiency was 99.4%	[232]
13	Zn (bare)	Zn-ion batteries	2 M $ZnSO_4$	Cellulose nanofillers (CNF) + graphene acid (GA) coatings	Thickness: 30 µm (0.5 wt.% GA + 2 wt.% CNF	i_{corr} reduced from 1.74 to 0.25 mA cm^{-2} (85.6%)	a) 99% retention after 24 h b) The -COOH of GA helps in desolvation through adsorption d) Increased mechanical strength, reduced HER, and E_a	[233]
14	Zn (bare)	Zn-ion batteries	3 M $ZnSO_4$	Cellulose-based coatings	Thickness: 5 µm	C_R decreased by 62%	a) Overpotential decreased from 220 to 65 mV b) Self-life increased to 500 h from 57 h c) Attained a specific capacity of 89.4%	[234]
15	Zn coated with Cu–Zn (Zn-Cu/Zn)	Rechargeable Zn batteries	3 M $ZnSO_4$	Zn-Cu-based coatings	Thickness: 20.1 ± 0.9 µm	C_R was reduced 6 times 86% efficiency	a) Coulombic efficiency increased to 91.8% and HER reduced to nearly 80% b) Cu-coating decreased Zn oxidation and dissolution c) Long cycle life even after 1500 cycles	[235]
16	Zn (bare)	Aqueous Zn-MnO_2 batteries	2 M $ZnSO_4$ + 0.1 M $MnSO_4$ and 6 M KOH (ZnO)	$InCl_3$ (indium chloride)-based coating;	Ion exchange (150 mM; thickness: 8 µm)	Decreases i_{corr} to 7.7 mA cm^{-2}	a) Suppressed HER and corrosion rate b) Decreased current and dendrites c) Long-life and 72% retention capacity	[236]

https://doi.org/10.1007/s40820-026-02178-9

Table 6 A summary of some recent reports on corrosion inhibition of Zn anode using Zn anode alloying

S/N	Anode alloy	Battery type	Battery Electrolyte	Alloying element and ratio	Efficiency	Salient features	Refs
1	Zn powder	Alkaline Zn-air batteries	7 M KOH + 2 wt.% PAA	3 wt.% Bi and Ni	i_{corr} reduced from 1.2718 to 0.8490 mA cm^{-2}	a) Bi improves efficiency and reduces HER (4 times) b) E_{corr} slightly shifted in the positive direction c) Bi inclusion delays spontaneous corrosion	[240]
2	Zn powder	Alkaline Zn-air batteries	7 M KOH + 2 wt.% PAA	5 wt.% Bi and 5 wt.% Ni	R_{ct} increased from 55.4 to 602.2 Ω (ZnBi-2) (90.8%)	a) Bi decreased H_2 overpotential and shifted E_{corr} in a slightly negative direction b) Ni mostly helped in the reduction of H_2 evolution c) Bi and Ni improve the surface morphology	[241]
3	Zn-Bi (98:2) alloy	Zn-air batteries	7 M KOH + 2 wt.% PPA	2 wt.% Bi	91.1%	a) The lowest current density (0.326 mA cm^{-2}) was derived from Zn-Bi alloy b) 99.5% discharge capacity was retained c) KOH-PAA reduced self-discharge	[242]
4	Zn powder	Alkaline Zn-air batteries	6 M KOH	1.5 wt.% Bi	53.8%	a) Specific capacity and energy density increased to 21.7% and 28.7%, respectively b) 84.6% capacity retention was observed after 60 cycles c) Bi reduced dendrites and H_2 evolution and overpotential	[243]

Table 6 (continued)

S/N	Anode alloy	Battery type	Battery Electrolyte	Alloying element and ratio	Efficiency	Salient features	Refs
5	Zn-Bi alloy	Zn-ion batteries	1 M $ZnSO_4$	Bi	i_{corr} reduced from 3.589 to 0.333 mA cm^{-2}	d) Nearly 90% reduction in i_{corr} was observed, and HER overpotential raised to -1.81 from 1.72 V e) Coulombic efficiency was 99.6% after 1000 cycles f) No dendrite formation occurs	[244]
6	Zn and Zn-Sn alloy	Zn-ion batteries	2 M $ZnSO_4$	Sn	31%	g) Sn reduced C_R and HER h) Sn increased the lifecycle by 150% as compared to pure Zn i) Zn-Sn manifests a heat capacity of 89.5% after 1000 cycles	[245]

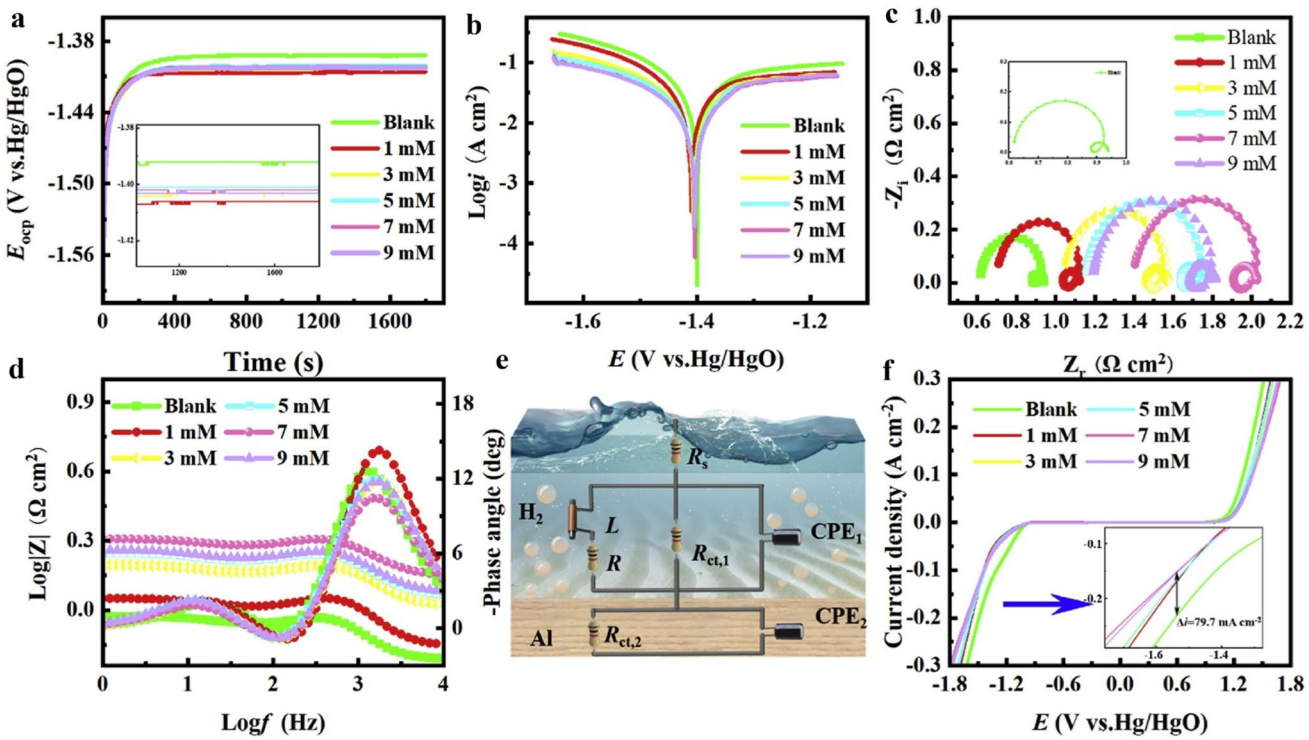

Fig. 16 Al-5052 anode's **a** EOCP-time curves and **b** PDP curves in 4 M NaOH with and without FDLH. Nyquist and Bode graphs of Al-5052 in 4 M NaOH with and without FDLH are shown in **c** and **d**, respectively. **e** Equivalent in correspondence. **f** Window for electrochemical stabilization using various electrolytes [252] (Reproduced with permission. © 2025 Elsevier)

https://doi.org/10.1007/s40820-026-02178-9

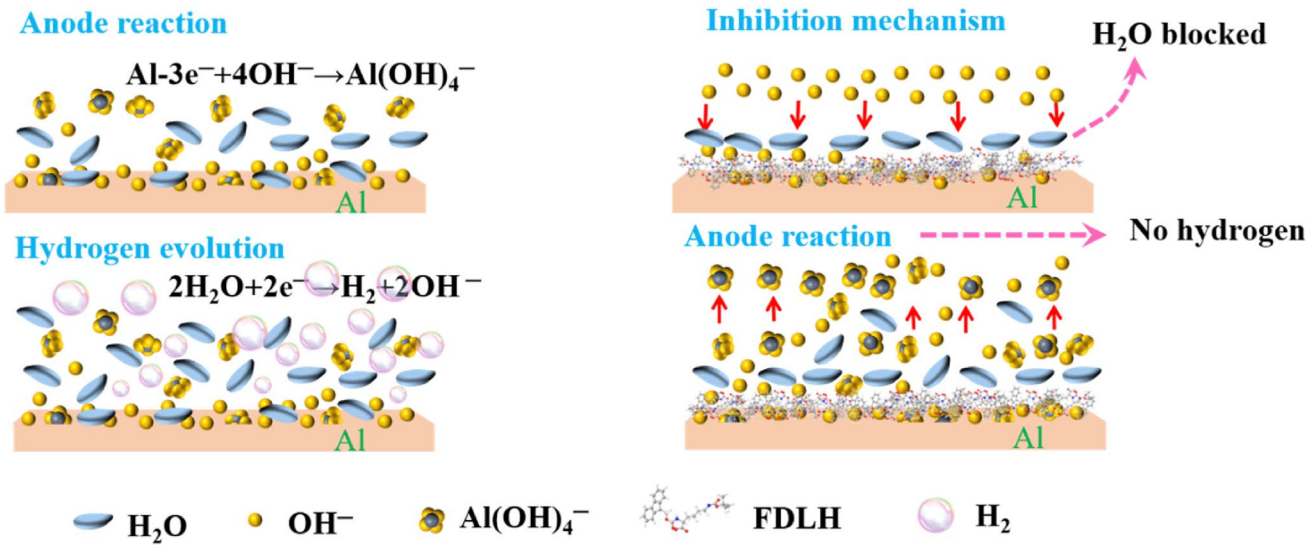

Fig. 17 Schematic illustration of the FDLH corrosion inhibition process [252] (Reproduced with permission. © 2025 Elsevier)

diacid [261], nonoxynol-9 (a non-ionic surfactant) [262], and CTAB [263]. They adsorb on the Al surface using their polar functional groups, such as –OH, $–NH_2$, –SH, and –COOH, as well as the π-electrons of aromatic systems or side chains. Their adsorption results in the retardation of anodic and cathodic reactions. Protein- and biopolymer-based inhibitors have emerged as promising, effective, and eco-friendly alternatives to aluminum corrosion inhibition. These green molecules, including L-cysteine, alkyl polyglucosides (APG), L-aspartic acid (Asp), fulvic and humic acids, and casein protein, are associated with numerous polar functional groups that coordinate with the Al surface and form a chelating complex to inhibit corrosion [264–269]. They achieve more than 80% efficiency by developing corrosion-protective inhibitive films.

Surfactants and ILs have also demonstrated outstanding potential for inhibiting Al anode corrosion in alkaline electrolytes by altering the electrochemical potential, retarding self-corrosion, and inhibiting H_2 evolution. For the development of corrosion-protective films, the heteroatoms (N, O, and S) of ILs coordinate with the Al surface, demonstrating more than 96% efficiency [260]. Nonoxynol-9 and quaternary ammonium surfactants manifest reasonably high efficiency and serve as mixed-type corrosion inhibitors [262, 263]. Some studies also documented the synergistic effects of organic–inorganic hybrid additives for Al anode corrosion protection in battery environments. Their synergistic formulations are better inhibitors than their isolated counterparts. For example, the L-cysteine/ZnO hybrid manifests excellent protection for Al dissolution [270]. The authors observed and reported that cysteine coordinates on the Al surface, forming Al–Zn–S and Al–Zn–O, and significantly inhibit corrosion. Likewise, the 8-HQ /ZnO hybrid forms Al-O and Zn-N type complexes and inhibits corrosion and retard H_2 evolution [271]. The literature survey on composite materials on Al anode corrosion inhibition shows that NiAl-vanadate(LDH/PVA) hybrid [272], PGA + K_2SnO_3 [267], and decyl glucoside + decanedithiol + K_2SnO_3 [273] have been effectively used.

Zhang et al. studied the synergistic performance of decyl glucoside (DG), decanedithiol (DD), and K_2SnO_3 for Al-1080 corrosion in 4 M KOH [273]. The PDP and OCP analyses revealed that the presence of DG, DD, and K_2SnO_3 shifts E_{corr} toward the positive direction, indicating control over H_2 evolution kinetics. EIS analyses validate the PDP results, showing that the Nyquist plots for a synergistic combination of DD, DG, and K_2SnO_3 exhibit the largest semicircle diameter (Fig. 19). This finding suggests that DD + DG + K_2SnO_3 exhibits the highest resistance and the lowest corrosion rate. The presence of different components in the formulation enhances their adsorption and film-forming ability, which is responsible for reduced C_R, i_{corr}, and H_2 evolution, as well as increased R_{ct} values. Figure 20 shows the corrosion inhibition mode of the DD + DG + K_2SnO_3 system. SnO_3^{2-} ions are first released from K_2SnO_3 and form a Sn-based protective film through their deposition.

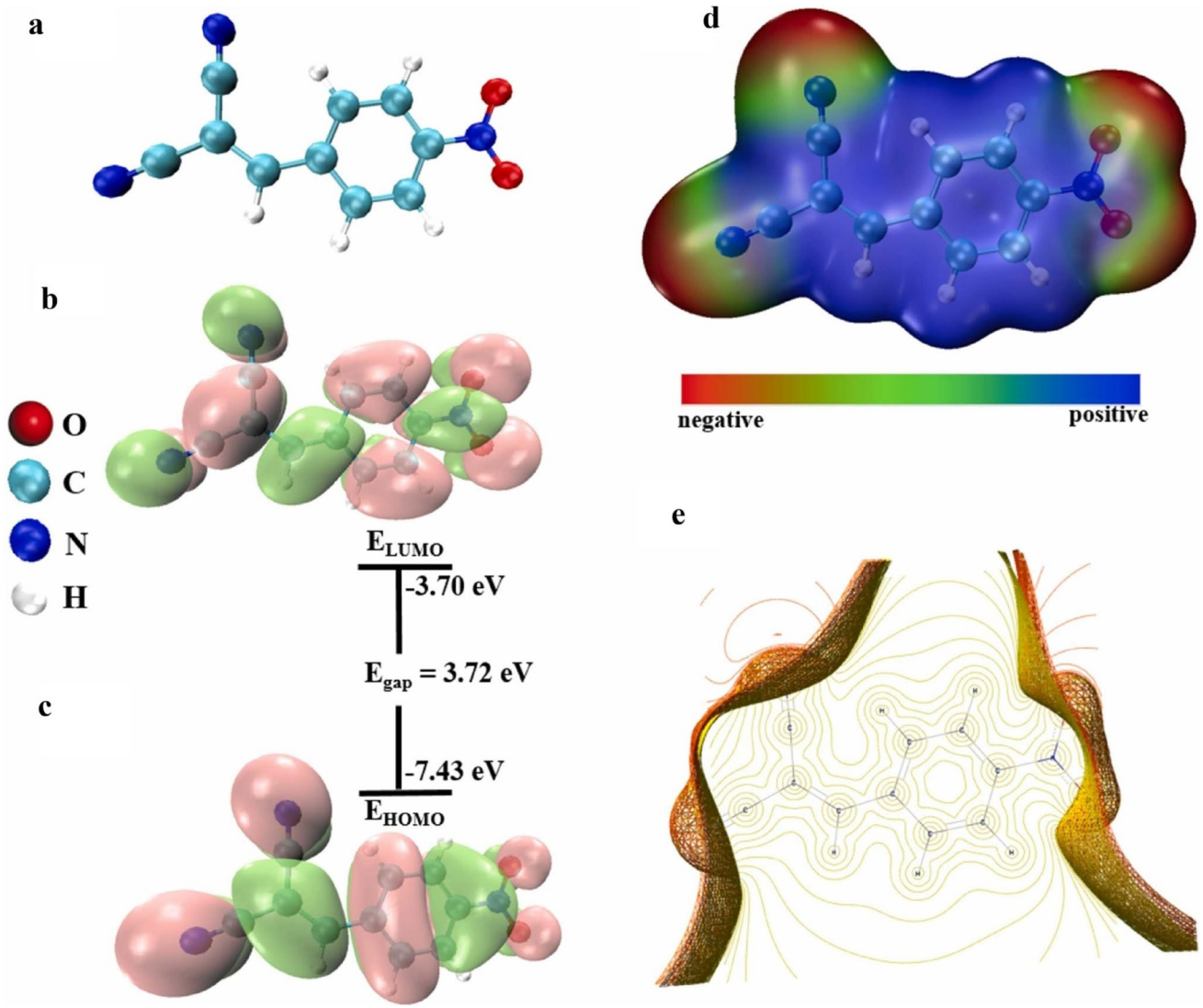

Fig. 18 Electronic structure analysis of the Z4 monomer displaying: **a** optimized geometry, and **b** orbital distributions of LUMO and **c** HOMO. **d** ESP and **e** MESP visualization [254] (Reproduced with permission. © 2025 Elsevier)

The adsorption of DG follows this step to enhance the hydrophobic character of the protective films and fill the surface defects and cracks. Lastly, DD coordinates with Al and adsorbed Sn through S atoms, forming Al-S and Sn-S bonds to increase the protection of existing films and their density. More so, DFT-based analyses showed that DG is associated with a smaller ΔE ($E_{LUMO} - E_{HOMO}$) and a higher dipole moment than DD. This results in a higher binding affinity of DG for Al^{3+} ions than for DD. Nevertheless, the DD + DG + K_2SnO_3 system develops Al-Sn-S-C-O-based multifunctional layers to retard anodic dissolution and cathodic H_2 evolution.

Bio-based QDs and plant extracts have emerged as carbon-rich and green corrosion inhibitors for the Al anode in alkaline batteries [259, 274–276]. Gao and coworkers studied the inhibition efficiency of Toona sensis extract (TSE) containing different active phytochemicals for Al anodic dissolution [274]. They observed that the active constituents bind to the Al surface, forming O–Al and N–Al bonds and thereby forming inhibitive films. Figure 21 presents the

https://doi.org/10.1007/s40820-026-02178-9

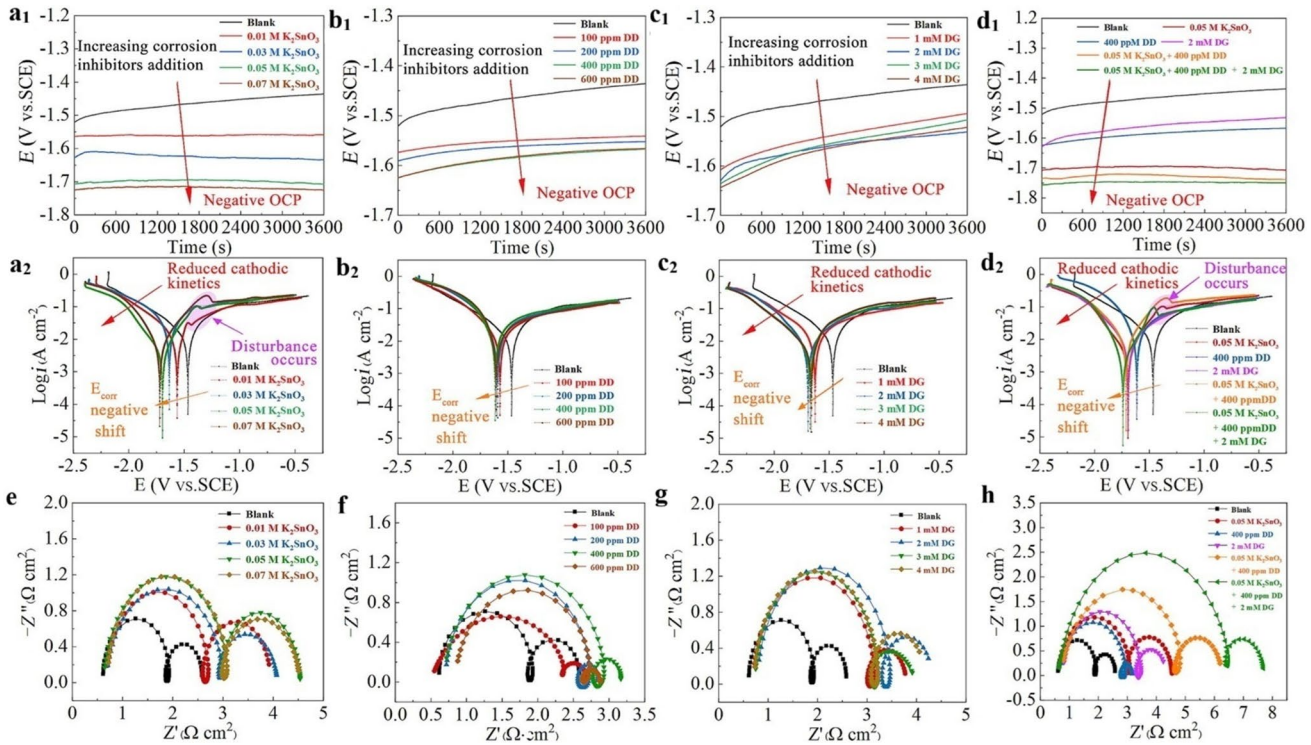

Fig. 19 E_{OCP} versus time curves and dynamic polarization curves for the Al-1080 anode in 4 M KOH with and without additives **a** K_2SnO_3, **b** DG, **c** DD, and **d** summary of K_2SnO_3, DD, DG, K_2SnO_3 + DD, and K_2SnO_3 + DD + DG. Electrochemical impedance spectra of the Al-1080 anode in 4 M KOH with and without additives and corresponding equivalent circuits **e** K_2SnO_3, **f** DD, **g** DG, and **h** summary of K_2SnO_3, DD, DG, K_2SnO_3 + DD, and K_2SnO_3 + DD + DG [273] (Reproduced with permission. © 2025 Elsevier)

distributions of the HOMO, LUMO, and FMOs, their energy gaps, electrostatic potential maps (EPMs), and adsorption energies for different active phytochemicals. The authors observed that kaempferol and quercetin were associated with the lowest energy gap, highest chemical reactivity, and the best coordination ability. EPMs were mainly located around N and O atoms, indicating they form Al–O and Al–N complexes. Careful observation shows that quercetin had the most negative E_{ads} value, followed by kaempferol and nicotinic acid. Based on different outcomes, they proposed that different constituents adsorbed on the Al surface via chemisorption. Polymer-based protective layer including PVA [253], NiAl-vanadate-based LDH/PVA [272], and Prussian blue integrated PAA [277] also manifested reasonable Al protection in alkaline electrolytes. Chung et al. showed that alkali metal cations such as Rb^+, K^+, Na^+, and Li^+ affect the discharge and corrosion properties of Al in KOH-based electrolyte [278]. The outcomes suggest that Rb^+ showed the best corrosion resistance and discharge capacity, validating that large cations provide superior electrochemical stability. Other reports also documented the inhibition of the Al anode in battery electrolytes [254, 256, 257, 279, 280].

The alloying approach for increasing the corrosion resistance of the Al anode in battery and saline environments has mainly been explored. Minor alloying elements, including Bi, Mg, Zn, Sn, In, and Ga, significantly enhance the corrosion resistance and anodic activities [281–284]. Different alloying elements perform various functions. For example, Sn decreases H_2 evolution and breaks oxide films, thereby activating Al. Mg decreases H_2 evolution, while Zn stabilizes dissolution and raises the H_2 evolution overpotential. Bi and In disrupt oxide layers, and Cu forms protective films (passivation). Additionally, Ga controls surface activities. Summaries of some representative results showing the effects of corrosion inhibitors and alloying are presented in Tables 7 and 8.

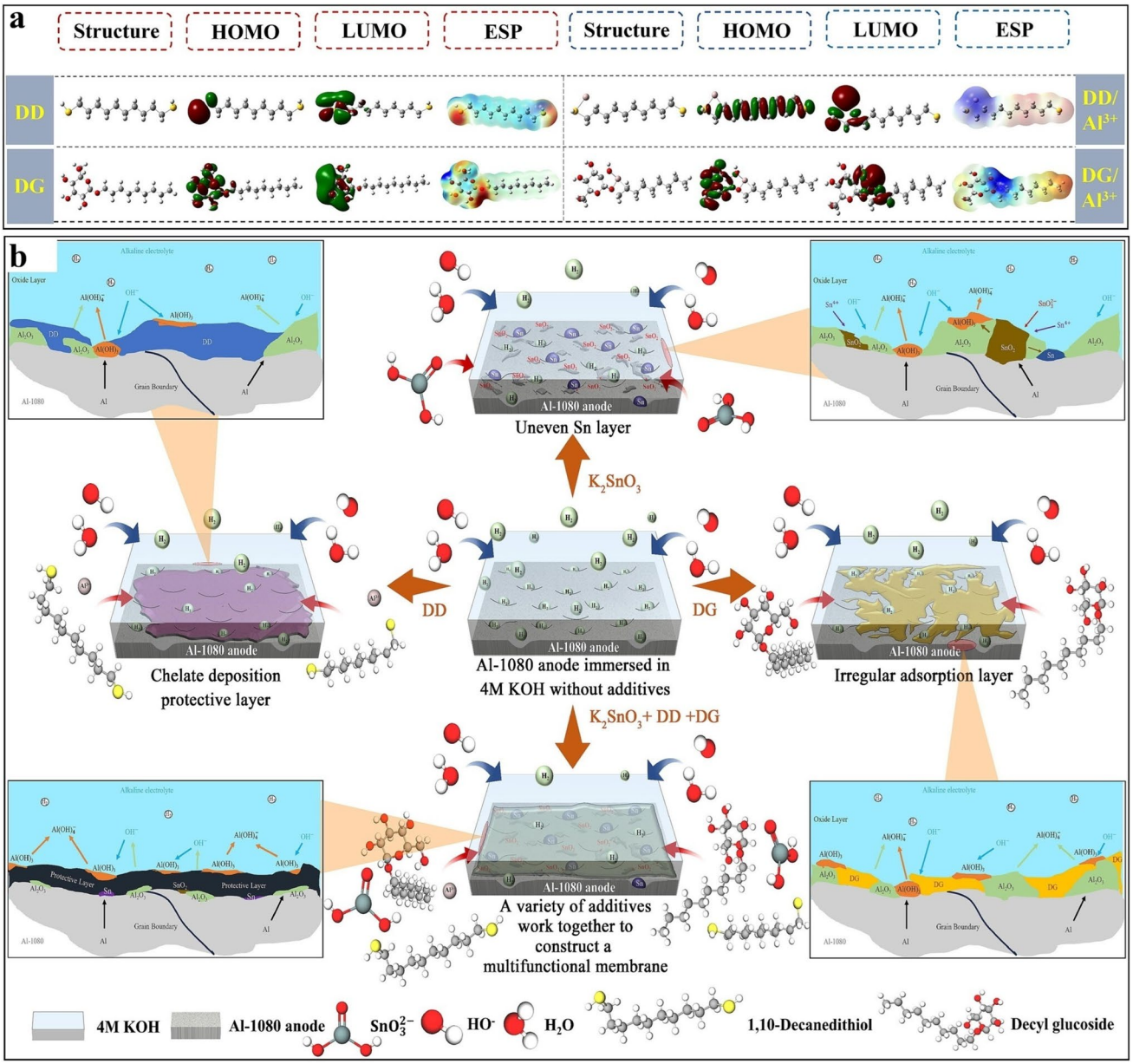

Fig. 20 DFT computation and the mechanism of corrosion inhibition. **a** Diagrammatic representation of the Al-1080 anode's corrosion inhibition process in 4 M KOH, both with and without additives. **b** LUMO, HOMO, and ESP structures optimized for DD, DG, DD/Al^{3+}, and DG/Al^{3+} [273] (Reproduced with permission. © 2025 Elsevier)

2.3 Electrochemical Corrosion and Corrosion Inhibition of Sustainable Magnesium-Based Batteries

Magnesium (Mg) is a highly reactive metal, and it readily oxidizes to form a passivating film of $Mg(OH)_2$, reducing electron transport and electrochemical stability [285, 286]. Corrosion can adversely affect the retention capacity, H_2 evolution, and self-discharge, which compromise the safety and integrity of batteries [113]. These adverse effects are more pronounced in aqueous, humid, or saline conditions [287, 288]. The corrosion mitigation of Mg anode has

 https://doi.org/10.1007/s40820-026-02178-9

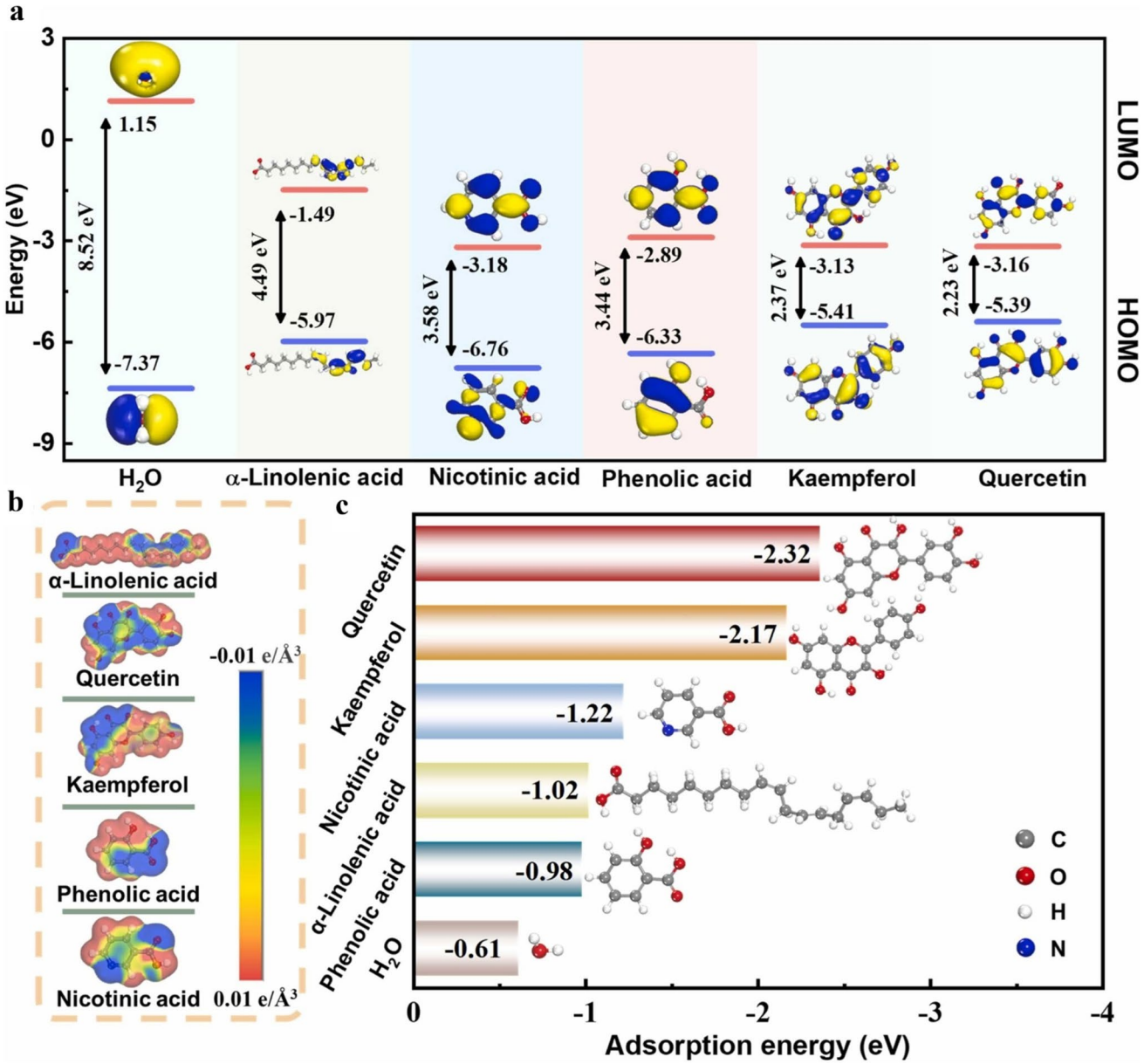

Fig. 21 Schematics showing **a** FOMs of H_2O and different active constituents of TSE extract; **b** EPM of TSE constituents; and **c** E_{ads} of TSE constituents on the Al surface [274] (Reproduced with permission. © 2025 Elsevier)

already gained significant advancement through corrosion inhibitors, anticorrosive coatings, and alloying approaches [289, 290]. These strategies have been proven essential for achieving reasonable electrode stability, enhancing battery performance, corrosion resistance, and prolonging cycle life. Deyab noticed that the presence of 2.5 mM of DG (decyl glucoside) in 3.5% NaCl (saline) solution reduced the corrosion rate significantly and showed the inhibition efficiency of 94% [291]. DG forms strong, compact inhibitive films via Mg-O bonding, thereby improving anode utilization, discharge voltage, and retention capacity. A binary mixture of 10 mM Na_3PO_4 and 30 mM NaF manifests 98.8% efficiency for the Mg anode in 2 M Na_2SO_4 [292]. Na_3PO_4 and NaF form protective films of $Mg_3(PO_4)_2$ and MgF_2,

Table 7 A summary of some recent reports on corrosion inhibition of Al anode using corrosion inhibitors

S/N	Anode material	Battery type	Battery electrolyte	Corrosion inhibitor(s)	Inhibition properties		Salient features	References
					Conce	Efficiency		
1	Al-5052 alloy	Alkaline Al-air batteries	4M NaOH	FDLH (N-α-Fmoc-N-epsilon-Boc-D-lysine)	7 mM	60.9%	a) FDLH adsorbs on the Al surface and coordinates by using the -COOH's oxygen Protective films contain $Al(OH)_3$ and Al_2O_3	[252]
2	Pure Al (99.99%)	Alkaline Al-air batteries	4M NaOH	PVA (polyvinyl alcohol)	1% (PVA; MW1099)	60.44%	b) -OH helps in adsorption and corrosion inhibition c) A 50% to 60% reduction in H_2 evolution was observed Reduces i_{corr}, C_R, and HER through a double-fold adsorption process	[253]
3	Al-5052 alloys (AlMgCr)	Alkaline Al-air batteries	4M NaOH	Z4 (2-n(4-nitrobenzylidene) malononitrile)	1×10^{-3} M	i_{corr} reduced from 29.0 to 19.6 mA cm^{-2} (~32.4%)	d) Reduced C_R, i_{corr}, and H_2 evolution e) Serves as a mixed-type inhibitor, and adsorption occurs through N and O Energy density improved by 2.5 times	[254]
4	Pure Al (99.99%)	Alkaline Al-air batteries	4M NaOH	MPA (2-mercapto-3-pyridinecarboxylic acid)	10 mM	i_{corr} reduced from 25.37 to 13.68 mA cm^{-2} (46.1%)	a) –SH–, pyridine N, and –COOH serve as adsorption centers, forming Al-O/S/N bonds b) Discharge lifetimes increase 1.5 times f) Specific capacity increased 65.7%	[255]
5	Al-5052 alloys (AlMgCr)	Alkaline Al-air batteries	4M NaOH	CPPE (cashew phenol polyoxyethylene ether)	0.2 mM	74.5%	g) CPPE adsorbs using the oxygen of -OH and ether groups to form Al-O h) Hydrophobic layer improves surface passivation CPPE films reduce C_R and HER	[256]
6	Al-5052 alloys (AlMgCr)	Alkaline Al-air batteries	4M NaOH	Hybrid inhibitor (8-hydroxyquinoline-5-sulfonic acid (H_2QS) and CTAB)	0.6 mM (CTAM) + 0.5 mM (H2QS)	94.19%	c) Increased R_{ct} and decreased i_{corr} values d) O and N coordinate and form chelating films Increase cycling stability	[257]

https://doi.org/10.1007/s40820-026-02178-9

Table 7 (continued)

S/N	Anode material	Battery type	Battery electrolyte	Corrosion inhibitor(s)	Inhibition properties		Salient features	References
					Conce	Efficiency		
7	Pure Al (99.99%)	Alkaline Al-air batteries	1M NaOH	SO (sodium octanoate)	10 wt.%	i_{corr} reduced from 32,000 to 16,800 μA cm^{-2} (47.4%)	e) Strongest binding energy (E_{bin}: 379 kcal mol^{-1}) f) Highest activity (ΔE = 3.577 eV) g) Form a stable chelating complex through chemisorption	[258]
8	Pure Al (99.99%)	Alkaline Al-air batteries	1M NaOH	SB (sodium benzoate)	5 wt.%	34.8%	h) The π-electrons and -COOH work together and form physicochemisorption i) Stronger binding energy (E_{bin}: 135 kcal/mol) j) Higher activity (ΔE = 3.708 eV)	[258]
9	Pure Al (99.99%)	Alkaline Al-air batteries	1M NaOH	SC (sodium citrate hydrate)	5 wt.%	36.6%	k) Multidentate adsorption l) Stronger binding energy (E_{bin}: 307 kcal mol^{-1})	[258]
10	Pure Al (99.99%)	Neutral Al batteries	5M NaCl solution + $Na_2S_2O_8$ (catholyte)	TA (tannic acid) green corrosion inhibitor	400 mg	i_{corr} reduced 0.0027 μA cm^{-2}	m) Suppressed C_R, pitting corrosion, i_{corr}, and dendrites n) Increase specific capacity, energy density, and recycling o) TA form Al-O-C coordinate bond through adsorption	[259]
11	Pure Al (99.99%)	Alkaline Al-air batteries	4M NaOH	Ionic liquids ([Amim][TFSI]))	1.5 mM	96.2%	a) IL predominantly serves as a mixed-type inhibitor b) Self-corrosion and H_2 evolution were reduced p) Improved operating voltage, energy density, and anodic efficiency	[260]
12	Pure Al (99.99%)	Alkaline Al-air batteries	4M NaOH	PEG diacid + ZnO	5000 ppm PEG diacid + 16 g L^{-1} ZnO	C_R was reduced 10 times	a) PEG diacid suppressed anodic dissolution and cathodic H_2 evolution c) Zn/PEG diacid film develops during the reaction	[261]

Table 7 (continued)

S/N	Anode material	Battery type	Battery electrolyte	Corrosion inhibitor(s)	Inhibition properties		Salient features	References
					Conce	Efficiency		
13	Pure Al (99.99%)	Alkaline Al-air batteries	4M NaOH	N9 (Nonoxynol-9)	2.0 mM	92.8%	d) Decreased i_{corr}, C_R, and H_2 evolution e) Adsorption followed the Freundlich adsorption model b) Improved discharge voltage, anode utilization, and energy capacity	[262]
14	Pure Al (99.99%)	Alkaline Al-air batteries	4M NaOH	CTAB, DDAB, and DDBAB	0.6 mM	i_{corr} reduced from 22.1 to 10.4 mA cm^{-2}	f) All surfactants serve as cathodic-type inhibitors g) Their effectiveness followed the sequence: DDBAB > DDAB > CTAB h) Discharge voltage and capacity density were increased	[263]
15	Pure Al (99.99%)	Alkaline Al-air batteries	5M NaOH	6-Thioguanine	0.5 mM	i_{corr} reduced from 9.725 to 61.70 mA cm^{-2} (~36.56%)	c) Decreased i_{corr}, C_R, and H_2 evolution. Served as a mixed-type inhibitor d) High concentration reduced efficiency i) –C = N–, –SH and $–NH_2$ serve as adsorption sites for adsorption of inhibitors	[264]
16	Al alloy (Mg-Mg-Ca-Zn-Sn)	Alkaline Al-air fuel cell	4M NaOH	Casein protein and Na_2SnO_3	0.6 g L^{-1} Casein + 0.05 M Na_2SnO_3	83.1%	j) Casein-mediated uniform deposition of Sn occurs, forming inhibitive films e) The amide and carbonyl groups of casein coordinate with Al^{3+} and Sn^{2+}	[265]
17	AA-5052 alloys	Alkaline Al-air batteries	4M NaOH	L-aspartic acid (Asp) and CaO	10 mM Asp and 4 mM CaO	i_{corr} reduced from 87.84 to 22.38 mA cm^{-2} (~74.5%)	k) $Ca(OH)_2$ forms, which provide coverage and corrosion protection l) Corrosion was reduced, while the reactivity of the anode remained unchanged m) Discharge voltage and capacity density were improved	[266]

https://doi.org/10.1007/s40820-026-02178-9

Table 7 (continued)

S/N	Anode material	Battery type	Battery electrolyte	Corrosion inhibitor(s)	Inhibition properties		Salient features	References
					Conce	Efficiency		
18	Al alloy (Al–Mg-Ga-Sn-Zn)	Alkaline Al-air batteries	4M NaOH	Alkyl polyglucoside (APG) and K_2SnO_3	2 mM APG and 0.05 M K_2SnO_3	H2 evolution reduced from 0.735 to 0.043 mL cm^{-2} min^{-1} (~94.14%)	n) APG boosts uniformity and protectiveness of Sn film o) SnO_3^{2-} and APG work together synergistically p) Discharge voltage, capacity, and anode utilization were improved	[267]
19	Pure Al (99.99%)	Alkaline Al-air batteries	5M NaOH	humic/fulvic acid mixture (Flax straw extract)	3 vol%	i_{corr} reduced nearly 50%	f) C_R, i_{corr}, H_2, and current were reduced, and they serve as mixed-type inhibitors g) R_p, discharge voltage, and capacity, and overall efficiency increased	[268]
20	Pure Al (99.9%)	Alkaline Al-air batteries	4M NaOH	Hybrid additives (agar + L-cysteine + $ZnCl_2$)	0.25 wt.% agar + 10 mM Cys + 10 mM $ZnCl_2$	HER reduced from 1.47 to 0.0833 mL cm^{-2} min^{-1}	i) Agar adsorbs and forms a uniform protective layer j) $ZnCl_2$ provides a blocking effect, avoids Zn dissolution, and retards H_2 evolution h) Using $–NH_2$ and –COOH groups, Cys links $Al(OH)_3$ and Zn^{2+}	[269]
21	Pure Al (99.99%)	Alkaline Al-air batteries	4M NaOH	Hybrid inhibitor (NiAl-vanadate LDH + Poly(vinyl acetal)	LDH: PVA = 85:15	i_{corr} reduced from 32.35 to 6.16 mA cm^{-2}	a) Reduced C_R, i_{corr}, and H_2 evolution b) Two-fold protection as LDH provides Al^{3+}/OH^- channels and PVA forms a hydrophobic film to retard H_2O diffusion q) Specific capacity, energy density, and power density were increased	[272]
22	Commercial Al-1060	Alkaline Al-air batteries	4M NaOH	L-cysteine + ZnO	0.03 M (L-cysteine) + ZnO (0.2 M)	i_{corr} reduced from 47.73 to 6.74 mA cm^{-2} (85%)	c) Reduced self-corrosion, H_2 evolution, and Zn^{2+} diffusion d) Dense Al-Zn-C-S films are formed r) Cys serve as multidentate ligand with $–NH_2$, –SH, and –COOH coordination sites	[270]

Table 7 (continued)

S/N	Anode material	Battery type	Battery electrolyte	Corrosion inhibitor(s)	Inhibition properties		Salient features	References
					Conce	Efficiency		
23	AA-5052 alloys	Alkaline Al-air batteries	4M NaOH	8HQ (8hydroxyquinoline) + ZnO	10.0 mM 8HQ + 4.0 mM ZnO	i_{corr} reduced from 77.3 to 22.0 mA cm^{-2} (~71.6%)	s) R_p increased 3 times, and the H_2 evolution greatly reduced t) Improved energy density, discharge voltage, capacity density, and anode utilization u) 8-HQ adsorbs and forms a chelating complex	[271]
24	Al-1080 alloy	Alkaline Al-air batteries	4M KOH	Hybrid inhibitor (1, 10-decanedithiol (DD); Decyl glucoside (DG), and K_2SnO_3 (potassium stannate)	0.05 mM K_2SnO_3 + 400 ppm DD + 2 mM DG	H_2 evolution from 0.2095 to 0.0406 mL cm^{-2} min^{-1} (80.62%)	q) A multicomponent system works synergistically r) The system increases battery capacity, energy density, and recycling v) C_R and HER were suppressed, and the contact angle was increased	[273]
25	High-purity Al	Alkaline Al-air batteries	4M NaOH	TSE (*Toona Sinensis* extract)	0.4 g L^{-1}	51.9%	k) Self-corrosion and HER were significantly reduced l) R_p increased from 1.44 to 2.55 Ω cm^2 w) Phytochemicals form Al-N and Al-O complexes	[274]
26	Al (bare)	Alkaline Al-air batteries	4M NaOH	N-doped C-quantum dots (Tannic acid and L-tryptophan-based)	150 mg L^{-1}	68.4%	m) N-CQDs adsorb through π-Al and N-Al and inhibit corrosion n) Adsorption followed physicochemisorption x) Adsorption reduced H_2 evolution	[275]
27	Pure Al (99.99%)	Alkaline Al-air batteries	4M NaOH	Sophora japonica leaves (SCDs) based C-quantum dots (SCDs)	0.2 g L^{-1}	41.5%	s) Increased R_{ct} and decreased i_{corr} values t) SCDs adsorb by forming S-Al and O–Al coordinate bonds e) Reduced anodic dissolution and HER	[276]

https://doi.org/10.1007/s40820-026-02178-9

Table 7 (continued)

S/N	Anode material	Battery type	Battery electrolyte	Corrosion inhibitor(s)	Inhibition properties		Salient features	References
					Conce	Efficiency		
28	Pure Al (99.99%)	Alkaline Al-air batteries	PAA hydrogels with KOH solute	Prussian blue (PB)	12 mg cm^{-2}	81.2%	f) PB forms conductive and stable protective film, preventing the formation of $Al(OH)_3$ g) Increased anode efficiency, energy density, battery capacity, and power density	[277]
29	Al–Mg-Sn-Gd-P alloy	Alkaline Al-air batteries	1 M KOH	Li^+, Na^+, K^+ and Rb^+	1 M (LiOH, NaOH, KOH, and KbOH)	Best efficiency for KbOH	o) They all form surface protective oxides that block the diffusion of corrosive species p) Larger size decreases water activities h) C_R and H_2 evolution decrease as the size increases	[278]
30	Al-5052 alloy	Alkaline Al-air batteries	4 M NaOH	ZK5 (maltoheptaose)	1×10^{-3} M	60.9%	q) Smother surface reduced C_R and H_2 evolution r) Forms the Al-O complex and becomes effective by surface adsorption s) ZK5 serves as a mixed-type inhibitor	[279]
31	High purity Al (99.999%)	Alkaline Al-air batteries	4 M NaOH	L-cysteine	0.5 M L^{-1}	i_{corr} reduced from 2.27×10^{-2} to 7.86×10^{-3} μA cm^{-2}	i) Cys increases anodic activity and forms a protective film j) –SH, $–NH_2$, and –COOH serve as adsorption centers k) Al_2O_3 was replaced by hydrated $Al(OH)_3$	[280]

Table 8 A summary of some recent reports on corrosion inhibition of Al anode using elemental alloying

S/N	Anode alloy	Battery type	Battery Electrolyte	Alloying element and ratio	Efficiency	Salient features	Refs
1	Al-1 Mg-1Zn-0.1Bi-0.02In alloy	Al-AgO battery	7 M KOH and 4 M NaOH	Mg (1 wt.%), Zn (1 wt.%), Bi (0.1 wt.%), In (0.02 wt.%)	C_R reduced from 17.162 to 4.273 mg cm^{-2} h^{-1}	d) Bi and In provide activation to Al by segregation and oxide disruption e) Zn raises the potential of hydrogen evolution f) Mg reduced cracking and increased strength	[281]
2	Al–Mg-Sn-Ga-In alloy	Alkaline Al-air batteries	2 M NaCl and 4 M NaOH	0.05 wt.% In	i_{corr} reduced from 4.1 to 2.9 mA cm^{-2}	g) Decreased C_R and H_2 evolution h) Alloying improves electrochemical activities in NaCl but decreases them in NaOH i) Cl^- ions adsorb on the surface and stabilize anodic dissolution	[282]
3	Pure Al and Al 7075 alloys	Al-AgO battery	1 M NaOH	Cu-deposited	Self-corrosion decreased from 1280 to 766 mm/y	j) Cu layer serves as a barrier for alkaline attacks k) The galvanic couple of Al-Cu stabilizes dissolution l) Reduced C_R and H_2 evolution and increased energy density and resistance	[283]
4	Pure Al (4N6)	Alkaline Al-air batteries	4 M KOH	NA	C_R:10.86 mg cm^{-2} h^{-1}	a) Lowest i_{corr} (16.8 mA cm^{-2}) and highest R_{ct} (2.79 Ω cm^{-2})	[284]
5	Al-Sn	Alkaline Al-air batteries	4 M KOH	0.1 wt.% Sn	C_R: 5.78 mg cm^{-2} h^{-1}	a) Sn improves activity b) Promote segregation and local pitting corrosion c) Retards H_2 evolution	[284]
6	Al–Mg	Alkaline Al-air batteries	4 M KOH	1.05wt.%Mg	C_R: 1.25 mg cm^{-2} h^{-1}	a) Best activity with the highest R_{ct} value b) It was associated with the lowest surface energy	[284]
7	Al–Mg-Sn	Alkaline Al-air batteries	4 M KOH	1.06 wt.% Mg and 0.09 wt.% Sn	C_R: 3.06 mg cm^{-2} h^{-1}	m) Moderate corrosion rate n) Reasonable corrosion inhibition	[284]

https://doi.org/10.1007/s40820-026-02178-9

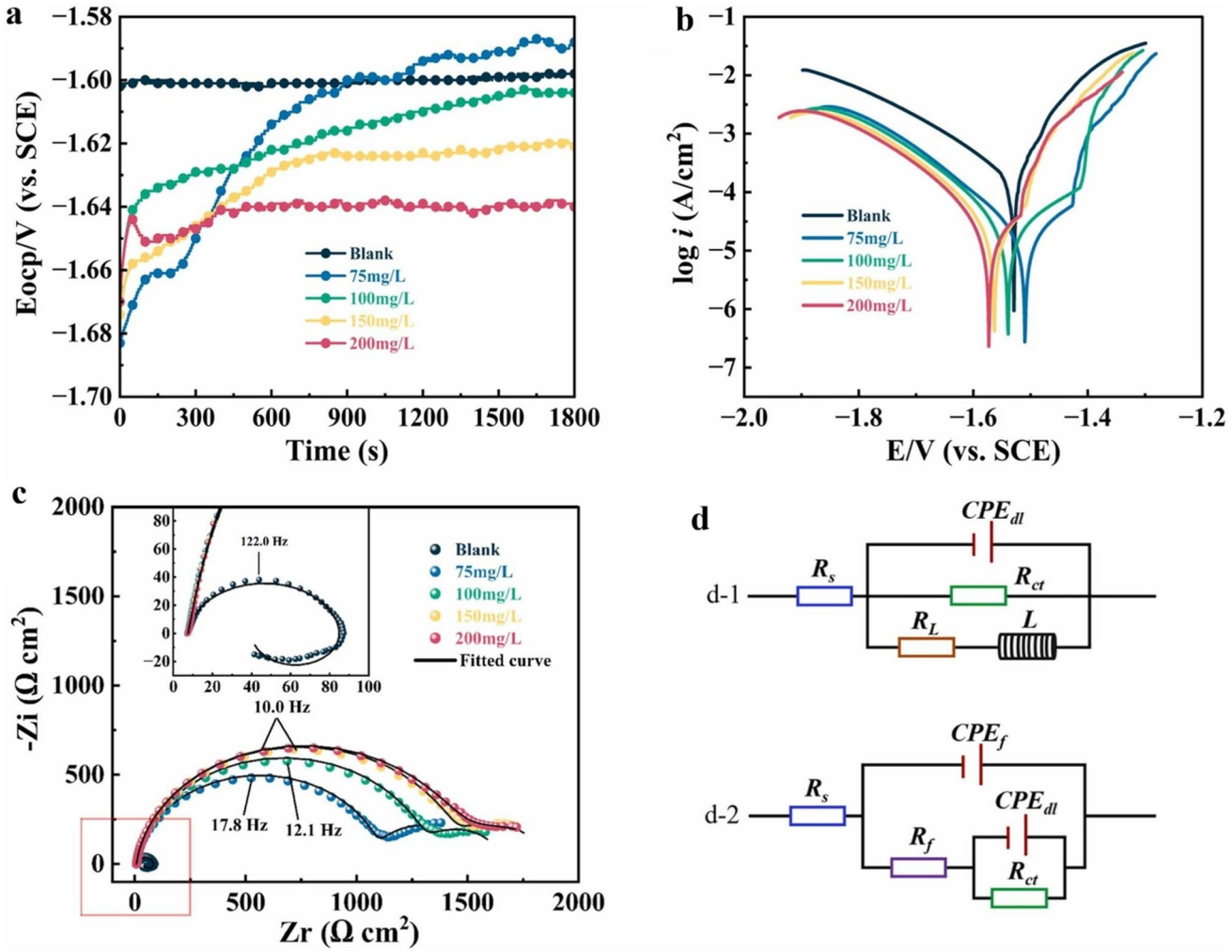

Fig. 22 Schematic illustration of AZ31B anode corrosion in 3.5% NaCl with different P-CD levels using **a** OCP, **b** Tafel, **c** Nyquist, and **d** equivalent circuit models [295] (Reproduced with permission. © 2025 Elsevier)

which delay the voltage drop and reduce self-corrosion. The inhibition potentials of phosphate additives for Mg corrosion have been reported in other studies [293, 294].

Zhao et al. reported the inhibition effectiveness of P-doped carbon QDs (P-CDs) for Mg-air batteries [295]. Electrochemical analyses revealed that P-CDs significantly reduced the i_{corr} value, achieving an inhibition efficiency of 85.2%. The formation of protective films of $Mg(OH)_2$ and $Mg_3(PO_4)_4$ reduced both anodic dissolution and cathodic H_2 evolution, resulting in a change in the shape of the Tafel polarization curves and Nyquist and Bode EIS plots (Fig. 22). In the presence of P-CDs, the battery showed a 70% increase in the anodic utilization. Jiang et al. studied and reported the use of sodium citrate (NaCA) to improve corrosion resistance and discharge property of Mg-based anodes in a chloride-free electrolyte [296]. As conventional NaCl-based electrolytes increase anodic dissolution and decrease efficiency due to the formation of $Mg(OH)_2$ and aggressive Cl^- ions, the authors propose using 0.1 M NaCA as an electrolyte. In such electrolytes, Mg anodes can be stabilized by the formation of a protective chelating complex by Mg^{2+} ions.

The corrosion resistance and battery performance of the Mg anodes can be significantly enhanced by alloying. Numerous alloying elements, including Sn, Pb, Al, Ge, Bi, Zn, In, and Ca, significantly reduced self-corrosion and H_2 evolution, while enhancing anodic efficiency. Wang and coworkers showed that the addition of 1–3 wt.% Sn to AZ61

Mg alloys reduced H_2 evolution and refined grains, proving improved discharge efficiency and corrosion resistance [297]. Another study showed that as serves as a cathodic poison, retarding H_2 evolution in Cl^- environments [298]. Pb and Al alloying improved electrochemical stability and discharge activity [299]. The presence of 14 and 15 elements, including Sn, Ge, Bi, Sb, and Pb, reduces corrosion rates via cathodic activation [300]. Ge and Zn enhanced the mechanical strength and corrosion resistance of Mg alloys [301]. Ca improves specific energy, cell voltage, and corrosion resistance [302, 303]. Summaries of some representative results showing the effects of corrosion inhibitors and alloying on Mg anode dissolution are presented in Tables 9 and 10.

2.4 Miscellaneous: Sustainable Na/K-Ion, Solid-State, Recyclable Li-Ion, and Organic Batteries

The practical implementation of sodium-ion batteries (SIBs) and potassium-ion batteries (KIBs) in energy storage is greatly challenged and hindered by undesirable corrosion [304–307]. Due to their weaker Lewis acidity, greater ionic radii, and unique solvation structures, Na^+ and K^+ exhibit different interfacial chemistries compared to Li^+, despite sharing numerous electrochemical properties. The literature inspection shows that the cycling instability of SIBs and KIBs is mainly caused by interfacial corrosion of the hard carbon anodes and layered oxide cathodes [308, 309]. Unlike Li-ion batteries, Na/K systems reveal more aggressive electrolyte-mediated decomposition due to narrower electrochemical stability windows [310, 311]. This makes corrosion mitigation an essential design requirement in SIBs and KIBs. In layered potassium transition metal oxides, including P′3- and P3-type K_xMnO_2, they represent a beautiful class of materials owing to their favorable K + diffusion kinetics, cost-effectivity, electrochemical reversibility, and exceedingly high theoretical capacity [312]. Nevertheless, their electrochemical stability and reversibility were greatly hindered in conventional ester-based electrolytes, especially in the presence of KPF_6, due to adverse interfacial reactions.

PF_6^- ions induce oxidative instability and hydrolysis by producing HF and several other corrosive species that aggressively attack Mn–O frameworks, causing lattice distortion, Mn disintegration and dissolution, rapid voltage decay, and structural stress [313]. More so, in carbonate-based electrolytes, the solvent molecules can intercalate into the layered oxide galleries and destabilize the structure by producing thick resistive cathode–electrolyte interface (CEI) layers [314]. The combined action of solvent diffusion and HF-mediated dissolution constitutes a severe, irreversible corrosion pathway that undermines the electrode's integrity and exacerbates its losses. In F-modified KMOF-7 and related systems, the incomplete replacement of O^{2-} by F^- ions enhances interfacial stability and retards HF attacks by minimizing CEI overgrowth and solvent ingress. This represents a practical, cost-effective cathode-side corrosion mitigation that is highly compatible with the high-voltage K-ion battery. Hard carbon (HC) has emerged and established itself as one of the most viable anode materials for Na/K batteries due to its low cost, tunable porous structure, and compatibility with the larger ions [315–318]. However, as HC surfaces are highly reactive, their performance is significantly influenced by the nature and stability of the solid-electrolyte interphase (SEI).

In KPF6/carbonate-based electrolyte systems, at low potential, electrolyte decomposition produces highly unstable SEI layers that fracture and lead to continuous consumption of electrolyte and battery capacity fading [318]. KPF6/DME and other ester-based electrolytes form unstable SEIs, leading to interfacial corrosion. Conversely, KFSI-based electrolytes form KF-rich, inorganic SEI films, enhancing anode stability by reducing solvent reduction and thereby maintaining cycle life and coulombic efficiency. The solvent-mediated corrosion in these battery systems can be minimized by implementing synergistic mitigation approaches, including anion-engineered salts [318], surface fluorination [313], polyanionic frameworks [309], nitrate stabilizers [319], aqueous gels [320], solid-state designs [321], and optimized hard carbon [308]. The literature studies show that electrolyte engineering provides an effective pathway for corrosion mitigation [322–325]. A shift from conventional KPF6/carbonate-based electrolytes to advanced electrolytes can reduce solvent decomposition, stabilize the SEI/CEI layer, and enhance current-collector passivation [326]. The use of binary salt electrolytes offers an effective method for corrosion control in KIBs. In KPF_6/KFSA carbonate electrolytes, a co-salt, KFSA ($K[N(SO_2F)_2]$), is introduced, and its anion decomposes more rapidly than PF6-, producing F- and S-containing species that precipitate in SEI formation [323].

https://doi.org/10.1007/s40820-026-02178-9

Table 9 A summary of some recent reports on corrosion inhibition of Mg anode using corrosion inhibitors

S/N	Anode material	Battery type	Battery electrolyte	Corrosion inhibitor(s)	Inhibition properties		Salient features	References
					Conc	Efficiency		
1	Pure Mg (99.99%)	Mg-air battery	3.5% NaCl	DG (Decyl glucoside)	2.5 mM	94.2%	a) i_{corr} decreased, and R_p increased b) DG forms a compact hydrophobic film by coordinating with Mg to form a Mg-O bond c) IR peaks for C–O–C and –O–H confirm the adsorption	[291]
2	AZ31 Mg alloy	Primary Mg-MnO_2 battery	2 M Na_2SO_4	Na_3PO_4 + NaF (binary mixture)	10 mM Na_3PO_4 + 30 mM NaF	98.8% (EIS)	d) R_p increased more than 81 times e) Developed MgF_2 and $Mg_3(PO_4)_2$ protective layers, preventing self-corrosion f) Improved battery performance	[292]
3	AZ31 Mg alloy	Mg-air battery	0.6 M NaCl	Vanadate and phosphate	0.02 M of each	i_{corr} reduced from 79.43 to 1.98 μA cm^{-2}	g) i_{corr} decreased, and R_p increased h) 65.5% increase in anodic efficiency i) Phosphate forms $Mg_3(PO_4)_2$ and $Mg(OH)_2$ compact layer j) Vanadate forms V_2O_3 + $Mg(OH)_2$ porous, cracked and less protective films	[293]
4	AZ31 Mg alloy	Mg-air battery	3.5% NaCl	Sodium phosphate (Na_3PO_4) and SDBS	0.5 g L^{-1} Na_3PO_4 + 0.5 g L^{-1} SDBS	C_R reduced from 0.063 to 0.003 g cm^{-2} h^{-1} (95.2%)	k) Na_3PO_4 forms a strong protective covering of $Mg_3(PO_4)_2$ l) SDBS adsorbs on $Mg_3(PO_4)_2$ and develops a hydrophobic film for the diffusion of Cl^- m) Improved potential stability and decreased byproduct formation	[294]

Table 9 (continued)

S/N	Anode material	Battery type	Battery electrolyte	Corrosion inhibitor(s)	Inhibition properties		Salient features	References
					Conc	Efficiency		
5	AZ31B Mg alloys	Neutral Mg-air battery	3.5% NaCl	PCDs (phosphorus-doped carbon quantum dots)	200 mgL^{-1}	i_{corr} reduced from 172.6 to 25.5 μA cm^{-2} (~ 85.2%)	n) P-CDs retard anodic dissolution and cathodic H_2 evolution o) Battery performance was significantly improved p) P-CDs adsorb and form corrosion-inhibitive films ($Mg_3(PO_4)_2$ and $Mg(OH)_2$)	[295]
6	Mg0.5-Zn0.2-Ge alloys	Aqueous Mg-air battery	3.5% NaCl	Sodium citrate (NaSC)	0.1 M (NaSC)	Utilization efficiency improved by 91.4%	q) Decreased self-corrosion (~ 50%), H_2 evolution, and film resistance (3 times) r) Reduced passivation and byproducts formation s) NaSC forms a soluble complex with $Mg^{2+/}$ Mg surface	[296]

https://doi.org/10.1007/s40820-026-02178-9

Table 10 A summary of some recent reports on corrosion inhibition of Mg anode using elemental alloying

S/N	Anode alloy	Battery type	Battery electrolyte	Alloying element and ratio	Efficiency	Salient features	References
1	AZ61-Sn alloys (AZ61: Mg-6Al-1Zn)	Seawater-based Mg-air battery	3.5% NaCl	Sn (1–3 wt.%)	i_{corr} reduced from 1.0×10^{-1} to 1.58×10^{-1} mA cm^{-2}	o) Shifts E_{corr} in the positive direction, reduced H_2 evolution, and improved current efficiency p) The best performance was derived at 3.0 wt.% q) Mg anode manifests uniform corrosion	[297]
2	Pure Mg and Mg-As (0.37wt.%) alloys	Seawater-based Mg battery	0.1 and 2.0 M NaCl	As (0.3 wt.%)	C_R was reduced 5 times	a) As serves as a strong cathodic poison b) Prevents cathodic polarization and retards H_2 evolution (10 times). Shift E_{corr} to the negative side c) Increase charge efficiency and corrosion resistance	[298]
3	Mg–Al-Pb alloys (Mg-3-9Al-2.5–7.5 Pb)	Seawater-based Mg battery	3.5% NaCl	Pb + Al alloying additives	3, 6, and 9.0 wt.% Al and 2.5, 5.0 & 7.5wt. Pb	d) The alloying elements synergistically improve battery and corrosion resistance performance e) Passivation film of $Mg(OH)_2$ forms to provide protection	[299]
4	Pure Mg and Mg-X alloys (x: Bi, Ge, Sn, Pb, and Sb)	Mg primary battery	0.1 M NaCl	Bi, Ge, Sn, Pb, and Sb (group 14 and 15 elements)	C_R reduced by ~ 1 order of magnitude	f) 0.3 wt.% Ge provided the best corrosion resistance g) Mass loss and H_2 evolution were suppressed with no filiform corrosion h) Mg-0.3Ge sample showed the best resistance	[300]
5	Mg-1Zn-xGe alloys (x: 0, 0.3 and 0.5 wt.%)	Mg primary battery	0.1 M NaCl	Ge with low Zn (1.0 wt.%)	C_R decreased nearly 10 times	r) No filiform corrosion with reduced H_2 evolution and HER s) Inhibits anodic polarization and cathodic activation t) Improve mechanical strength and corrosion resistance	[301]

Table 10 (continued)

S/N	Anode alloy	Battery type	Battery electrolyte	Alloying element and ratio	Efficiency	Salient features	References
6	Mg-Ca binary alloy	Mg-air battery	3.5% NaCl	Ca (01 wt.%)	i_{corr} reduced from 84.1 to 63.0 μA cm^{-2}	i) Low Ca concentration favors protection, but not high concentration j) Mg_2Ca provides detrimental galvanic effects u) The battery performance, including discharge potential, efficiency, specific capacity, and self-corrosion, was greatly improved	[303]
7	Mg-Sn binary alloys	Mg primary battery	0.6 M NaOH	1.5 mM	95.1% (10 Sn)	v) Sn increases corrosion and polarization resistance w) 10SN forms a strong barrier film with the lowest i_{corr} value x) Sn also decreased cathodic polarization, H_2 evolution, and HER	[302]

https://doi.org/10.1007/s40820-026-02178-9

The mismatch in electrochemical potential, mechanical properties, and electronic structures between electrodes and solid electrolytes leads to electrochemical corrosion in sustainable solid-state batteries [327–330]. Unlike liquid electrolyte-based systems, which are associated with wet surfaces and maintain dynamic contact, solid interfaces generally accumulate stress, space-charge layers, and micropores/microcracks that accelerate corrosive reactions and increase interfacial resistance. In solid-state battery systems, high-voltage cathodes can oxidize halide, polymer, or sulfide-derived electrolytes. At the same time, alkali metal anodes can reduce hybrid or oxide electrolytes, forming brittle byproducts that can promote electrode degradation [331, 332]. These undesirable reactions are particularly problematic in sustainable solid-state battery systems that utilize bio-derived polymers, recyclable materials, or low-toxic ceramics, as these materials possess reactive surface groups and exhibit narrower stability windows [333–335]. Interfacial corrosion in solid-state batteries has been identified as a primary failure mechanism that adversely affects their safety, integrity, and cycle life in next-generation alkali-ion battery systems [336, 337]. Corrosion mitigation of electrodes in solid-state batteries has been significantly advanced by engineering the ion-conductive interfaces. One of the most effective approaches to corrosion mitigation in such systems is the use of thin anticorrosive coatings, including metal oxides, fluorides, and phosphates. The coatings shield the electrolyte from attacks and minimize the corrosion reactions [338–340]. Polymeric buffer layers and artificial interphases can be used to accommodate strain, maintain continuous contact, and mitigate crack propagation by retarding the formation of interfacial voids and fragmentation, thereby slowing corrosion reactions [341]. Simultaneously, electrolyte-centered approaches, such as anion substitution, aliovalent doping, and polymer blending, offer alternative pathways to mitigate electrode degradation and enhance electrochemical stability by reducing corrosive interactions [342–344].

In Li-ion batteries (LIBs), electrochemical corrosion initiates from the destructive reactions at the electrode (Li)–electrolyte interfaces [345, 346]. These reactions include reduction of electrolyte, oxidation of electrolyte at the cathode, and current-collector attacks, transition metal dissolution, and destabilization of SEI and CEI [45]. These corrosion mechanisms are greatly accelerated and intensified by moisture-induced LiPF6 hydrolysis, thermal stress, and high voltage, as these processes accelerate the formation of HF and interphase breakdown [347–349]. Continuous corrosion leads to lithium loss, cracking, and thickening of the SEI and CEI, resulting in successive capacity decay and increased cell impedance. The cathodic corrosion can be directly linked to anodic instability [89, 350]. These challenges can be effectively addressed by implementing appropriate corrosion-mitigating strategies that minimize electrode–electrolyte interactions. External additives, including vinylene carbonate (VC), lithium difluoro(oxalato)borate (LiDFOB), and fluoroethylene carbonate (FEC), accelerate the formation of mechanically stable SEI/CEI layers that minimize the metal dissolution from high-voltage cathodes [351–353]. Similarly, protective coatings of metal oxides, such as ZrO_2 and Al_2O_3, niobate, and phosphates, provide physical barriers for electrolyte attacks and mitigate dissolution [354, 355]. Highly concentrated electrolytes, especially fluorinated ones, are associated with reduced HF production, promoting uniform interphase, cycle life, and anodic stability [356, 357]. The corrosion mitigation in recyclable Li-ion batteries is significant as it not only enhances the lifetime for operation but also reduces contamination, enhances structural retention, and enables effective materials recovery in second-life uses [358, 359].

In organic batteries, corrosion originates from redox and chemical reactions that attack metallic current collectors and organic electrode frameworks [360–362]. Organic electrodes, including Schiff base polymers, imides, conjugated redox polymers, and quinones, are susceptible to radical fragmentation, degradation from continuous charge/discharge cycling, protonation, and nucleophilic attack [363]. These reactions trigger the formation of anion radicals, enhanced electrolyte decomposition, and destabilization of the SEI and CEI, particularly when less stable salts or reactive solvents are employed [364]. For example, carbonyl (>C=O)-rich organic cathodes may undergo ring-opening or enolization reactions, while dissolved radical intermediates can diffuse into the electrolyte, resulting in rapid capacity fading and material degradation [365, 366]. The breakdown of organic electrodes, especially at high voltages, can produce aggressive species, such as HF, which can attack the current collectors and compromise their structural and interfacial integrity [45, 367]. These degradation processes lead to increased polarization, reduced cycle life, destruction of structural and interfacial stability, and decreased coulombic efficiency, despite their eco-friendly behavior [368]. Owing to these adverse effects and processes, corrosion mitigation has

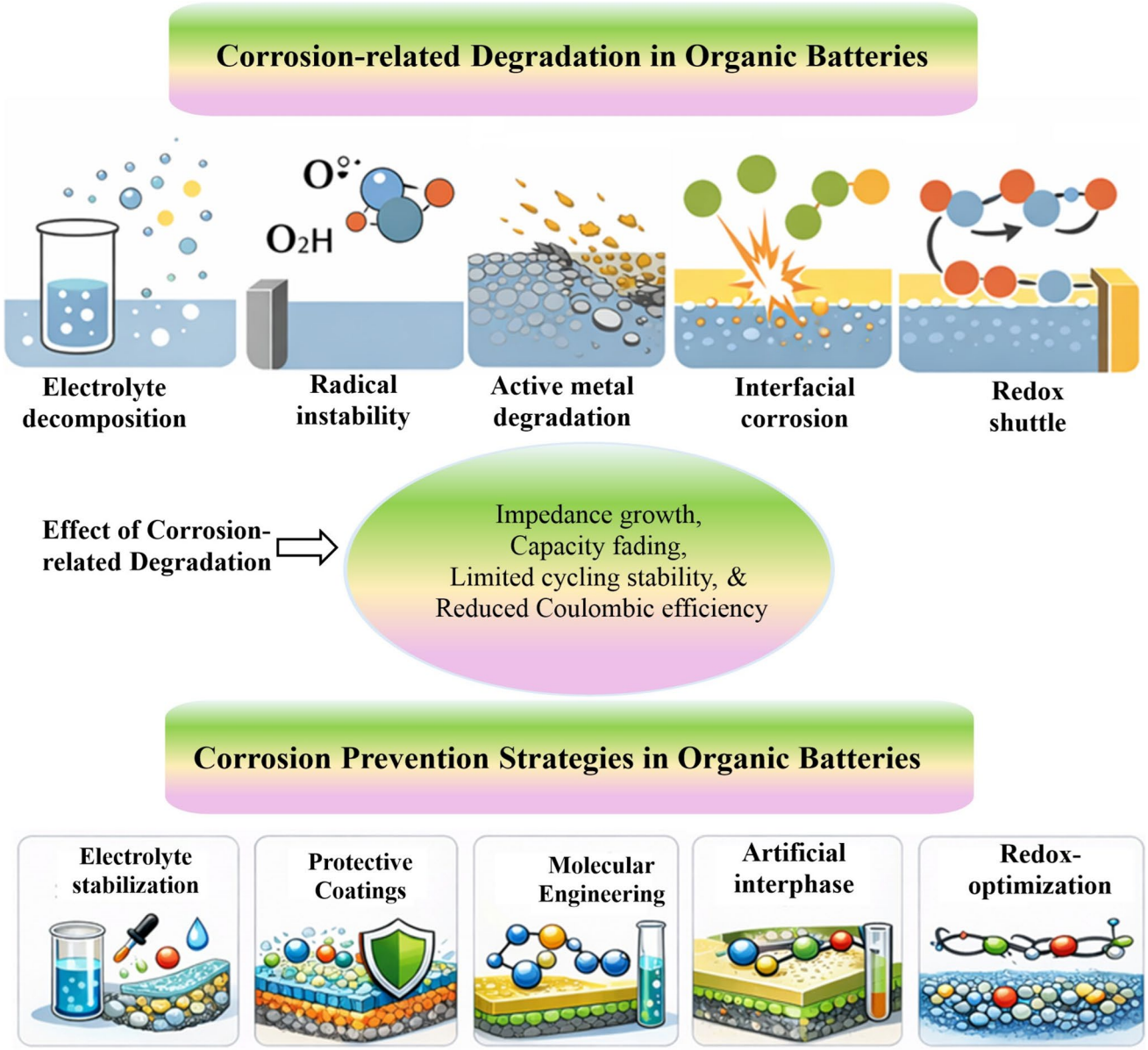

Fig. 23 Diagram showing pathways of corrosion-related degradation in organic battery systems and various corrosion prevention strategies. The upper panel shows the central corrosion mechanisms, and the lower panel shows the prevention strategies in such systems to suppress corrosion-mediated degradation and improve electrochemical stability

been essential in sustainable organic batteries (Fig. 23). Unlike corrosion in metal-anode systems, degradation in organic batteries mainly manifests through electrochemical reactions and chemical instability of redox-active molecules. Figure 23 schematically illustrates the major degradation pathways, including interfacial side reactions, active metal dissolution, electrolyte instability, and radical decomposition. These processes are directly involved in several adverse effects, including impedance growth, capacity fading, limited cycling stability, and reduced Coulombic efficiency. Therefore, different corrosion prevention strategies focus on electrolyte engineering, suppression of active metal corrosion, molecular-level stabilization, and the design of artificial interphases to enhance chemical and electrochemical stability. Molecular designing, especially hydrogen-bond stabilization, π-extension, adding of electron-withdrawing substituents, and polymer backbone cross-linking, minimizes the solubility of the materials and retard degradation [369–371]. Meanwhile, the implementation of corrosion-resistant salts, such as FSI- and

https://doi.org/10.1007/s40820-026-02178-9

TFSI-, localized high-concentration and highly concentrated electrolytes, water-in-salt formulations, and ionic liquids, can improve corrosion and degradation resistance [372–374]. The diffusion of electrolytes and subsequent corrosive attacks can be further minimized by using anticorrosive protective coatings [375, 376].

3 Next-Generation Corrosion Resistance Materials and Strategies: Self-Healing, Smart, and Nanostructured Materials

Corrosion in batteries is a complex and broader process that not only includes metal rusting but also electrode (anode/cathode)–electrolyte interactions and degradation, reactions between electrode and current collectors, binder and polymer degradation, degradation of cooling plates, tabs, and cell casing, and high voltage/temperature corrosion [49]. Corrosion challenges are particularly severe in modern energy storage systems that operate at relatively high voltages and use aggressive electrolytes [377, 378]. The modern energy storage systems also include replacing traditional Fe, Cu, Al, Zn, and Ni-based electrodes and chemistries that are reaching their limits. Recently, several attempts have been made to develop and implement next-generation corrosion-resistant materials for battery applications (Fig. 24). One of the major attempts involves alloying Cu and Al current collectors with different elements [379, 380]. The literature shows that Al–Zr, Al–Mn, or Al–Mg–Si alloys exhibit superior passive film stability and enhanced pitting resistance in LiPF6 electrolytes [381–383]. The presence of alloying elements enhances the stability and adherence of fluoride or oxide films. Similarly, micro-alloyed steels, such as Cu–Ni and Cu–Cr, possess better corrosion resistance and mechanical stability. The tailored microstructures and presence of alloying elements enhance passivity, facilitating the repair of local breakdowns.

Carbon coatings on current collectors (Cu or Al) are emerging attempts to enhance their corrosion resistance [384, 385]. The carbon coatings, including graphene (G), carbon nanotubes (CNTs), and amorphous carbon on Al or Cu, enhance their chemical inertness, electrical conductivity, and serve as a physical barrier against oxidative and HF attacks [386–388]. Metal carbide (MC) and metal nitride (MN) coatings, such as TiC, CrN, TiN, and NbN, improve the hardness and corrosion resistance of the current collectors [389, 390]. These coatings can be applied by atomic layer deposition (ALD) or physical vapor deposition (PVD). Coatings with conductive polymers, such as poly(3,4-ethylenedioxythiophene) (PEDOT) or related polymers, improve flexibility, adhesion, and corrosion resistance [391, 392]. The presence of metal oxides such as TiO_2 and Al_2O_3 provides additional pitting resistance, especially at high potentials. Instead of traditional tabs, busbars, and cell casings that utilize aluminum, copper, and nickel-plated steel cans, high-performance steels such as super-austenitic or duplex steels can be used [393]. These next-generation materials exhibit high resistance to HF, chloride, and pitting attacks.

Ceramic coatings improve the chemical resistance and mechanical properties of Al alloys [394, 395]. Alloying also improves the corrosion resistance of tabs and busbars. Artificial interphases and protective interfaces enhance material stability by modifying interfaces rather than bulk material. These phases and faces retard the direct contact of metals with aggressive electrolytes and allow the ion transport to occur freely. These include cathode-electrolyte interphases (CEI), solid-electrolyte interphases (SEI), or polymer-ceramic hybrids [396, 397]. They are nanometer-thin and significantly improve interfacial stability and corrosion resistance. In solid-state batteries, corrosion problems arise from oxide- and sulfide-based electrolytes that react with Li metal and with oxygen in air. Recently, the use of Li-phosphate protective layers, doped garnet, and stable Li-ion conductors has emerged as non-corrosive and safe electrolytes [398]. They improve interfacial resistance, reduce electrochemical decomposition, and enhance chemical stability.

Pristine metal anodes are highly susceptible to corrosion, particularly through passivation, oxygen evolution, and hydrogen evolution. The next-generation approach involves allowing suitable elements to pass through. For example, Al-, In-, Mg-, and Bi-based alloying of the Zn anode minimizes H_2 evolution and dendrite growth and increases corrosion resistance [238, 399]. The corrosion resistance of Zn anodes can also be improved by applying inorganic, organic, or polymer coatings. Allowing Mg with Al and Zn (Mg–Al–Zn) improves corrosion resistance without decreasing the electrochemical activities. Polymer components, such as separators, binders, adhesives, and gaskets,

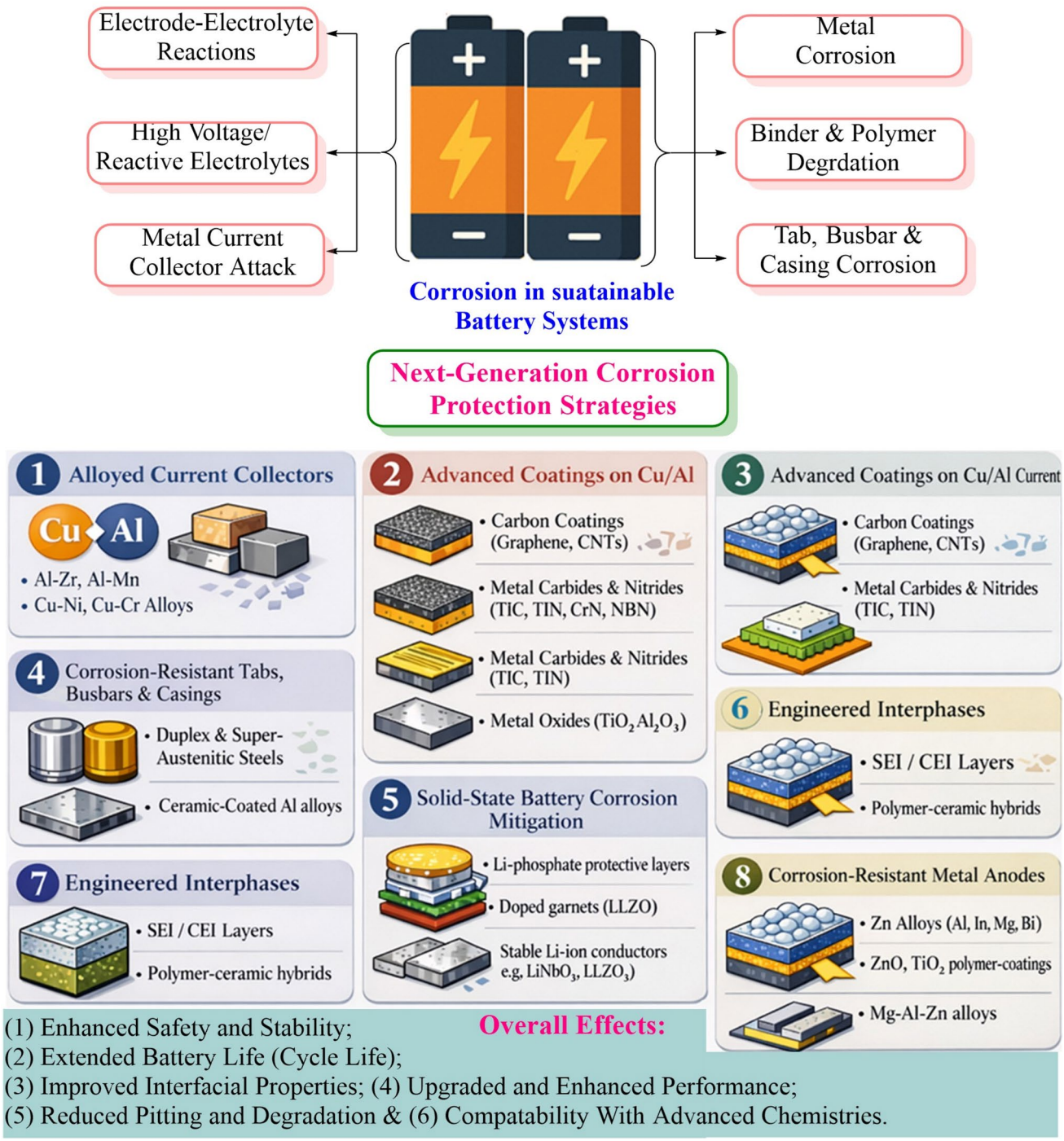

Fig. 24 Schematic illustration of attempts made toward the development and implementation of next-generation corrosion-resistant materials for battery applications

also undergo severe degradation, although attention has been focused on metallic corrosion. Therefore, suitable tailoring of these components can improve the lifespan of batteries by retarding the risks of corrosion. For example, cross-linked or fluorinated binders exhibit remarkable resistance to pitting attack at high-voltage cathodes [400, 401]. Likewise, ceramic-coated separators reveal resistance against oxidative degradation and improved thermal and mechanical stability [402].

https://doi.org/10.1007/s40820-026-02178-9

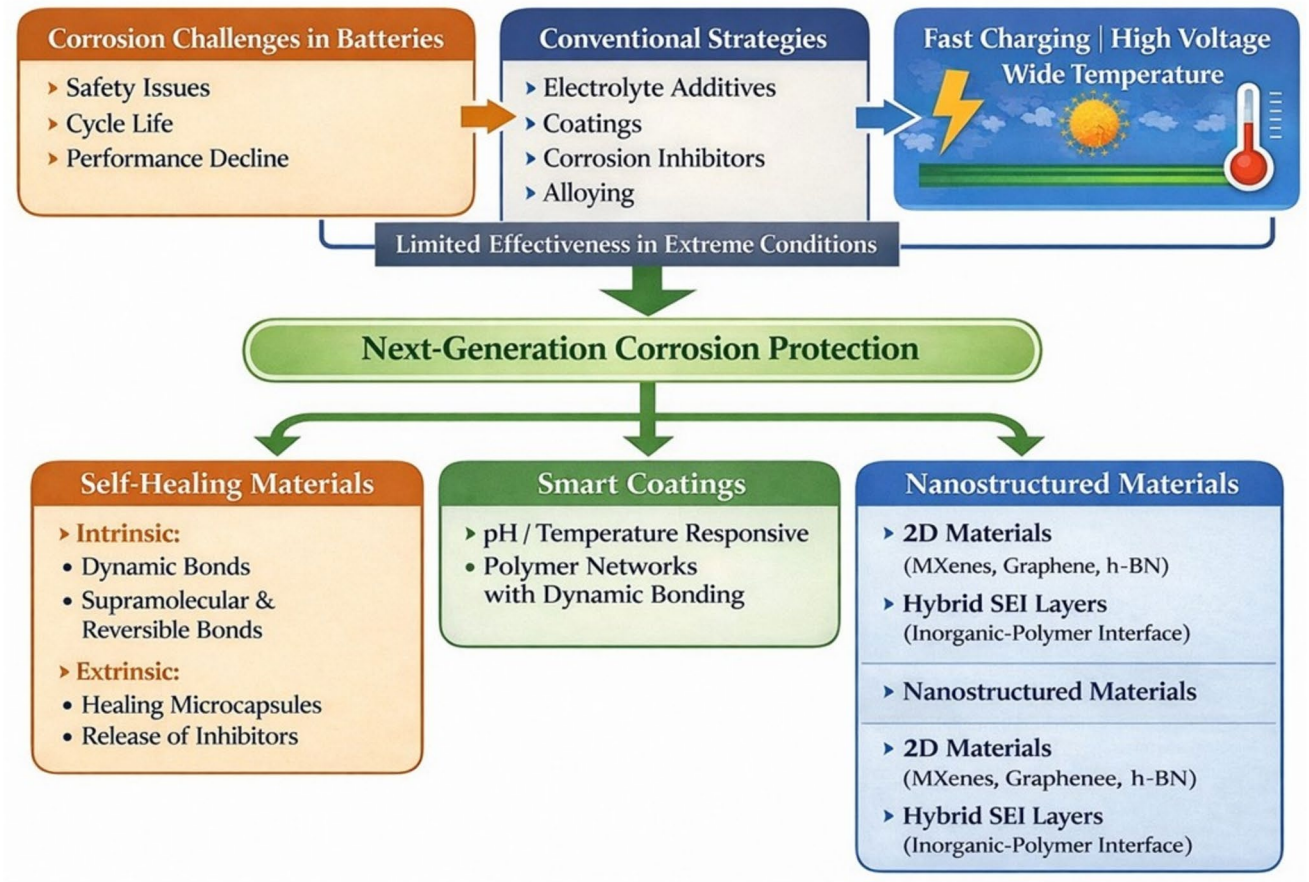

Fig. 25 Schematic illustration showing next-generation corrosion protection strategies in modern-day battery systems

The ongoing discussion reveals that corrosion has been a significant challenge and a notable barrier to the development of sustainable batteries. As corrosion adversely affects the safety, cycle life, and performance of the battery, several strategies have been developed to mitigate the consequences [403]. Conventional strategies, such as electrolyte additives, coatings, corrosion inhibitors, and alloying, are largely inadequate in modern-day battery systems that operate under relatively extreme conditions, including fast charging, high voltage, and wide temperature ranges. These demand next-generation corrosion protection strategies, including self-healing materials and coatings, innovative or stimuli-responsive systems, and nanostructured architectures in modern-day battery systems (Fig. 25). Self-healing materials are characterized by their ability to restore functional and structural integrity after chemical degradation or mechanical loss at the battery interfaces [404–406]. Self-healing can be of two types: intrinsic and extrinsic. Intrinsic self-healing reversible chemical bonds, including supramolecular interactions, dynamic covalent bonds, and ionic cross-linking, reform spontaneously at the damaged or corroded sites. On the other hand, in extrinsic self-healing, healing agents are encapsulated in micro- or nanocapsules or in polymer networks to become effective at the damage site in response to external stimuli.

Self-healing coatings incorporating suitable healing agents have been used for corrosion protection. In these coatings, corrosion inhibitors such as organic species, cerium salts, and monomers are encapsulated in microcapsules. These microcapsules are stimuli-responsive, i.e., they rupture in response to external stimuli, such as pH and temperature changes, at damaged sites and release active corrosion inhibitors/healing agents to provide self-healing protection [404–406]. In polymer-based self-healing coatings, external stimuli trigger dynamic network changes, including hydrogen and disulfide bonding, to provide instantaneous,

automatic healing at damaged sites [407–410]. In traditional batteries, SEI layers are highly unstable and experience electrolyte decomposition and corrosion. However, the next-generation dynamic polymer components automatically repair seal cracks and pores generated during cycling. Hybrid (inorganic-polymer) SEI interfaces, incorporating borate, Li_3N, or LiF, reorganize under electrochemical stress [411–413]. Recently, the use of nanostructured materials in sustainable corrosion protection in battery environments has been significantly enhanced. Due to their ability to minimize localized reaction sites, enhance surface uniformity, control electron and ion transport, offer tunable surface chemistry, and possess a high surface area, their use in protecting against battery corrosion is gaining particular attention. 2D material-based, including MXenes, graphene, and h-BN, are effectively employed in nanostructured coatings [39, 414–416]. Polymers and ceramic nanocomposites offer synergistic effects that enhance both corrosion protection and flexibility [417–419].

The literature investigation shows that several strategies and corrosion-resistant materials, including surface coatings, corrosion inhibitors, ionic liquids (ILs), bio-based corrosion inhibitors, and alloying, have been extensively employed to provide significant enhancements in corrosion resistance and cycling stability; several inherent shortcomings remain. Most ILs, surfactants, and organic corrosion inhibitors become effective by adsorbing onto the anode surface and forming hydrophobic protective films. Their adsorption and effectiveness may be compromised by competitive adsorption with aggressive ions or by instability under high-voltage, high-temperature conditions. Likewise, though alloying improves corrosion resistance, it may also adversely affect electrochemical potential, increase the risk of galvanic corrosion due to coupling effects, or increase cost. Oxide- and polymer-based protective coatings improve interfacial stability; however, excessive coating thickness may adversely affect ion transport and increase internal resistance. Moreover, though advanced materials such as ILs and MOFs are highly effective at the laboratory scale, they may face challenges in commercial-scale production, long-term stability, economic feasibility, and environmental compatibility. Though next-generation protection strategies, such as nanostructured interphases, self-healing coatings, and multifunctional hybrid systems, offer performance advantages, they still face numerous challenges. These challenges include economic feasibility, synthetic scalability, recyclability, and interfacial stability in real working conditions. Moreso, their complex structure may introduce additional mechanical instability, undesirable complexity, or interfacial resistance over prolonged use.

4 Challenges and Future Directions

The ongoing discussion shows that corrosion imposes numerous challenges in the development of sustainable battery systems. These challenges arise from the inherent susceptibility of metallic anodes and current collectors to corrosion via electrochemical reactions. Battery corrosion manifests as galvanic reactions, hydrogen evolution, localized pitting corrosion, and surface passivation. These undesirable processes accelerate the loss of active metal (anode), increase impedance, and reduce the coulombic efficiency of batteries. These processes become particularly destructive in aqueous batteries, where oxygen reduction and water spitting generate extremely corrosive environments. Another serious challenge arises from dendrite formation and growth, which concentrates current at microscopic tips, produces regions of local alkalinity or acidity, and ruptures protective (passive) films. Corrosion also produces recycling and environmental challenges to sustainable battery systems. As the battery ages, mixed-metal deposits, oxides, and hydroxides migrate to the separator membranes and active materials. The contamination reduces battery efficiency by lowering the purity of recovered metals, including Mg, Co, Mn, Al, Fe, Ni, and Li. These impurities also diminish recycling efficiency, increase the amount of spent electrolyte, and increase chemical complexity. Moreover, oxygen-rich electrolytes are associated with high swelling risk, accelerated mechanical damage, and cracking of cell components.

In view of the above, recent studies have focused on addressing the challenges associated with traditional battery systems, offering substantial prospects. Future studies should concentrate substantially on interface engineering to optimize ion-surface interactions, thereby suppressing the corrosion pathway and stabilizing metallic electrodes.

https://doi.org/10.1007/s40820-026-02178-9

Recent reports suggest that the presence of functional additives can positively impact solvation structures, enhance the density and uniformity of passive films, and displace pre-adsorbed water molecules. Numerous bio-based molecules (such as triglycine, chitosan, fucoidan, and carboxymethyl cellulose), multidentate heterocycles (e.g., imidazoles), and chelating ligands (such as sodium gluconate and nitrilotriacetic acid) have been reported as relatively non-toxic inhibitors of hydrogen evolution and dendrite growth. These species provide significant corrosion protection and enhance metal-ion transport kinetics, which are essential for improved battery performance and sustainability. Nonetheless, the available reports on these aspects are limited and warrant further exploration in future studies.

Recently, the research direction in sustainable battery systems is transitioning toward solid-state and hybrid electrolyte systems, which utilize deep eutectic solvents (DESs), ionic liquids (ILs), metal–organic frameworks (MOFs), and polymer-inorganic composites as multifunctional stabilizers. With the rapid progress of artificial intelligence for science (AI4S), data-driven modeling and AI are emerging as powerful tools for understanding corrosion mechanisms and developing subsequent mitigation strategies in battery systems [420–422]. Machine learning (ML) has already been employed to assess stability windows and corrosion rates as a function of pH, anode (alloy) composition, electrolyte chemistry, and temperature, enabling accelerated screening of suitable corrosion inhibitors and corrosion resistance materials [423, 424]. In battery systems, AI-assisted analysis of surface characterization (e.g., SEM, EDS, AFM, XPS, ICP-MS) and electrochemical data (e.g., R_{ct}, R_p, E_{corr}, i_{corr}) can help identify hidden correlations among interfacial properties, long-term degradation, and dendrite formation. In battery systems, data-driven approaches can also be used to optimize the design of corrosion-protective coatings, molecular-level corrosion inhibitors, and electrolyte fabrication [421, 425]. However, as corrosion-related AI datasets are often heterogeneous, small, and generated under non-standardized (unrealistic) testing conditions, models can face challenges when used across different materials and real operating environments.

Several currently used ML models work like black boxes, i.e., they provide the results without providing significant insight into the mechanistic aspects. This makes it hard to fully trust and rely on the models, particularly when they are used in new environments or situations that differ significantly from the data on which they were trained. Therefore, in future investigations, a better approach could be to combine basic scientific principles, such as transport and electrochemical principles, with AI. These models are generally known as hybrid or physics-informed models [426]. The other practical methods include active learning, where developed models are used to determine which experiments to run next, and digital twins, which link real-time experimental data with predictive tools to identify and diagnose corrosion. These electrolytes are well-known for their ability to alter solvation energetics, produce self-healing interfaces, and minimize free water acidity. Thin anti-corrosive coatings provide physical shielding and corrosion protection, enabling prolonged cycling stability. The corrosion prevention strategies should be further explored due to the increasing demand for grid storage, seawater-based energy systems, and the use of EV batteries in a second life. Cost-effective production, recycling, and corrosion protection, primarily using green inhibitors, enhance performance and align with global NZE goals.

Several inorganic, organic, and bio-derived corrosion inhibitors have been used in corrosion protection in battery systems, and they manifest remarkable performance at the laboratory scale. However, their large-scale use in battery systems depends on several other factors beyond their protection (electrochemical) performance. Availability of raw materials, complexity in synthesis, cost-feasibility, compatibility with electrolyte composition, influence on ionic conductivity, and long-term chemical stability must be carefully considered. Several functionalized organic corrosion inhibitors, mainly heterocycles, while they exhibit remarkable effectiveness, may involve tedious multi-step syntheses or expensive starting materials associated with several workups and purification steps. These factors not only make synthesis tedious and costly but also adversely affect the environment and industrial scalability. Likewise, though bio-based alternatives can be considered eco-friendly and promising corrosion inhibitors due to their excellent interfacial properties, they may face challenges with long-term stability, especially in highly alkaline or acidic battery conditions and during extended cycling. Moreover, these external additives added as corrosion inhibitors can adversely affect ion transport kinetics, electrolyte viscosity and composition, downstream recycling processes, and separator compatibility.

Synergistic formulations, i.e., combining two or more active species in a single formulation, represent a promising

strategy for achieving multifunctional protection in battery systems. Nevertheless, whether their combination has a synergetic or antagonistic effect should be systematically tested. The literature outcomes suggest that synergistic protection is provided by a proper combination of corrosion inhibitors capable of retarding both anodic metal dissolution and cathodic hydrogen evolution or oxygen reduction, resulting in overall mixed-type protection. Hybrid formulations of polymers and chelating organic molecules with inorganic (metal) ions are typical examples of synergistic formulations. On the other hand, antagonistic effects may result from competitive adsorption, excessive surface hydration, complex formation, or destabilization of the inhibitor (passive) film. Therefore, for the practical uses, the priority design principles for effective corrosion inhibitor selection should include: (i) the inhibitor should form effective and strong inhibitive films, (ii) the inhibitor must be stable in the operating pH window, (iii) the inhibitor synthesis should be cost-effective and scalable, (iv) the inhibitor should provide minimum interference with kinetics of ion (Zn^{2+}/ Al^{3+}, Mg^{2+}) transport and (v) the inhibitor should be compatible with environmental and recycling rules and regulations. Therefore, effective formulation should be balanced by electrochemical efficiency, economic feasibility, interfacial stability, and synthesis to enable industry-scale production.

5 Conclusions

Corrosion remains one of the most persistent problems, adversely affecting the longevity, safety, efficiency, and sustainability of battery systems. Although sustainable batteries, such as Mg-, Al-, Na-, Zn-, and bio-based systems, offer some advantages in terms of availability, recyclability, and environmental performance, their real-world practical use is strictly hindered by complex corrosion pathways. These corrosion pathways promote degradation reactions, destabilize interfaces, enhance self-discharge, and compromise structural integrity, performance, and cycle life. Corrosion adversely affects energy efficiency, shortens service life, and reduces recycling processes, while also increasing safety risks by contaminating systems with corrosion products and impurities. Recent advancements show that corrosion mitigation strategies can significantly increase sustainable battery performance. These strategies include surface passivating coatings, alloy engineering (alloying), electrolyte optimization and tailoring, and use of multifunctional organic, inorganic, polymeric, ILs, DESs, and bio-based corrosion inhibitors. The corrosion protection strategies reduced hydrogen evolution, oxygen spitting, and electrode dissolution.

Many inhibitors, including PEG, gluconates, CMC, heterocycles, MOFs, and advanced surface-active (amphiphilic) molecules, manifested reasonably high protection efficiency, exceeding 90%. These species align with the principles of green chemistry, exhibiting high biodegradability, computability, and low toxicity, enabling dendrite-free cycling and extending the cycle life of metallic anodes. However, given the demands for high-performance, fully recyclable batteries and corrosion resistance, the current progress appears insufficient. Therefore, research and development on dynamic passivation behavior, electrode–electrolyte interactions, and interface chemistry across various battery environments need to be thoroughly studied and established. Future studies should also integrate rational molecular design, in situ testing, and predictive modeling with experimental approaches to develop and demonstrate practical, eco-friendly corrosion protection strategies.

Acknowledgements CV thankfully acknowledges Khalifa University of Science and Technology for providing financial support.

Author Contributions CV and IB contributed to conceptualization, formal analysis, data curation, and writing—original draft. AA and KYR contributed to resources, visualization, supervision, and writing—review and editing.

Declarations

Conflict of interest The authors declare no conflict of interest. They have no known competing financial interests or personal relationships that could have influenced the work reported in this paper.

References

1. K. Schmidt-Rohr, How batteries store and release energy: explaining basic electrochemistry. J. Chem. Educ. **95**(10), 1801–1810 (2018). https://doi.org/10.1021/acs.jchemed.8b00479
2. Y. Zhao, Y. Ding, Y. Li, L. Peng, H.R. Byon et al., A chemistry and material perspective on lithium redox flow batteries towards high-density electrical energy storage. Chem. Soc. Rev. **44**(22), 7968–7996 (2015). https://doi.org/10.1039/c5cs00289c
3. J.L. Castle, D.F. Hendry, Can the UK achieve net zero greenhouse gas emissions by 2050? Natl. Inst. Econ. Rev. **266**, 11–21 (2023). https://doi.org/10.1017/nie.2024.6
4. P. Plachinda, J. Morgan, M. Coelho, Towards net zero: modeling approach to the right-sized facilities. Sustainability **15**(1), 163 (2023). https://doi.org/10.3390/su15010163
5. https://www.iea.org/reports/batteries-and-secure-energy-transitions/outlook-for-battery-demand-and-supply
6. E.M. Melchor-Martínez, R. Macias-Garbett, A. Malacara-Becerra, H.M.N. Iqbal, J.E. Sosa-Hernández et al., Environmental impact of emerging contaminants from battery waste: a mini review. Case Stud. Chem. Environ. Eng. **3**, 100104 (2021). https://doi.org/10.1016/j.cscee.2021.100104
7. W. Mrozik, M.A. Rajaeifar, O. Heidrich, P. Christensen, Environmental impacts, pollution sources and pathways of spent lithium-ion batteries. Energy Environ. Sci. **14**(12), 6099–6121 (2021). https://doi.org/10.1039/d1ee00691f
8. D. Pavlov, *Lead-Acid Batteries: Science and Technology* (Elsevier, Amsterdam, 2011). https://doi.org/10.1016/c2009-0-16975-1
9. J.P. Nelson, S. Manhas, Environmental impact of discarded nickel-cadmium batteries and their effect on human beings: a review. In: Int. Conf. Recent Trends in Environment and Sustainable Development (Springer, 2023), pp. 1011–1037. https://doi.org/10.1007/978-3-031-93444-5_71
10. Bhawna, P. Phogat, Shreya, N.L. Singh, S. Singh, Advancing energy storage: a comparative review of nickel–cadmium, nickel–metal hydride, and sodium-ion batteries. React. Chem. Eng. **10**(12), 2764–2788 (2025). https://doi.org/10.1039/d5re00156k/v4/review1
11. M. Feki-Tounsi, A. Hamza-Chaffai, Cadmium as a possible cause of bladder cancer: a review of accumulated evidence. Environ. Sci. Pollut. Res. **21**(18), 10561–10573 (2014). https://doi.org/10.1007/s11356-014-2970-0
12. M.A.P. Mahmud, N. Huda, S.H. Farjana, C. Lang, Comparative life cycle environmental impact analysis of lithium-ion (LiIo) and nickel-metal hydride (NiMH) batteries. Batteries **5**(1), 22 (2019). https://doi.org/10.3390/batteries5010022
13. T.Z. Humsa, R.K. Srivastava, Impact of rare earth mining and processing on soil and water environment at Chavara, Kollam, *Kerala*: a case study. Proced. Earth Planet. Sci. **11**, 566–581 (2015). https://doi.org/10.1016/j.proeps.2015.06.059
14. M. Padhiary, R. Kumar, Assessing the environmental impacts of agriculture, industrial operations, and mining on agro-ecosystems. In: Smart Internet of Things for Environment and Healthcare (Springer Nature, Switzerland, 2024), pp. 107–126. https://doi.org/10.1007/978-3-031-70102-3_8
15. J.S. Guzolu, M. Gharabaghi, M. Mobin, H. Alilo, Extraction of Li and co from Li-ion batteries by chemical methods. J. Inst. Eng. Ind. Ser. D. **98**(1), 43–48 (2017). https://doi.org/10.1007/s40033-016-0114-z
16. X. Yang, H. Wen, Y. Liu, Y. Huang, Q. Zhang et al., Lithium pollution and its associated health risks in the largest lithium extraction industrial area in China. Environ. Sci. Technol. **58**(26), 11637–11648 (2024). https://doi.org/10.1021/acs.est.4c00225
17. A. Gulagi, D. Bogdanov, C. Breyer, The role of storage technologies in energy transition pathways towards achieving a fully sustainable energy system for India. J. Energy Storage **17**, 525–539 (2018). https://doi.org/10.1016/j.est.2017.11.012
18. M. Vujanović, Q. Wang, M. Mohsen, N. Duić, J. Yan, Recent progress in sustainable energy-efficient technologies and environmental impacts on energy systems. Appl. Energy **283**, 116280 (2021). https://doi.org/10.1016/j.apenergy.2020.116280
19. W.U. Rehman, Y. Ma, Z. Khan, F.Z. Ait Laaskri, J. Xu et al., Bioinspired materials for batteries: structural design, challenges and future perspective. Results Chem. **13**, 101997 (2025). https://doi.org/10.1016/j.rechem.2024.101997
20. B. Lee, Y. Ko, G. Kwon, S. Lee, K. Ku et al., Exploiting biological systems: toward eco-friendly and high-efficiency rechargeable batteries. Joule **2**(1), 61–75 (2018). https://doi.org/10.1016/j.joule.2017.10.013
21. F. Zhang, T. Liao, C. Yan, Z. Sun, Bioinspired designs in active metal-based batteries. Nano Res. **17**(2), 587–601 (2024). https://doi.org/10.1007/s12274-023-6102-3
22. H. Wang, Y. Yang, L. Guo, Renewable-biomolecule-based electrochemical energy-storage materials. Adv. Energy Mater. **7**(23), 1700663 (2017). https://doi.org/10.1002/aenm.201700663
23. E.S. Morais, A.M. da Costa Lopes, M.G. Freire, C.S.R. Freire, J.A.P. Coutinho et al., Use of ionic liquids and deep eutectic solvents in polysaccharides dissolution and extraction processes towards sustainable biomass valorization. Molecules **25**(16), 3652 (2020). https://doi.org/10.3390/molecules25163652
24. J. Zhang, J. Liu, Z. Xu, D. Cao, K. Chen, Enabling a sustainable future energy storage with cellulose-based solid-state electrolytes: a review. Mater. Today Energy **54**, 102091 (2025). https://doi.org/10.1016/j.mtener.2025.102091
25. H. Yang, L. Zhu, W. Li, Y. Tang, X. Li et al., Lignocellulose-mediated gel polymer electrolytes toward next-generation energy storage. Nano-Micro Lett. **18**(1), 84 (2025). https://doi.org/10.1007/s40820-025-01927-6
26. L. Zhang, H. Gao, G. Jin, S. Liu, J. Wu et al., Cellulose-based electrolytes for advanced lithium-ion batteries: recent advances and future perspectives. ChemNanoMat **8**(8),

e202200142 (2022). https://doi.org/10.1002/cnma.202200142

27. J. Jumadi, W.S.W. Harun, K. Kadirgama, L. Samylingam, N. Aslfattahi et al., Green energy materials: unlocking the potential of chitosan and cellulose in energy storage. J. Inorg. Organomet. Polym. Mater. (2025). https://doi.org/10.1007/s10904-025-04018-6
28. J. Yan, J. Qian, Y. Li, L. Li, F. Wu et al., Toward sustainable lithium iron phosphate in lithium-ion batteries: regeneration strategies and their challenges. Adv. Funct. Mater. **34**(44), 2405055 (2024). https://doi.org/10.1002/adfm.202405055
29. Z. Wang, D. Wu, X. Wang, Y. Huang, X. Wu, Green phosphate route of regeneration of $LiFePO_4$ composite materials from spent lithium-ion batteries. Ind. Eng. Chem. Res. **62**(2), 1181–1194 (2023). https://doi.org/10.1021/acs.iecr.2c03743
30. M.M. Mashfy, T.A. Alvy, N. Hossain, M.A. Haque, F.T. Mohsin et al., Sodium ion batteries: a sustainable alternative to lithium-ion batteries with an overview of market trends, recycling, and battery chemistry. Next Energy **10**, 100478 (2026). https://doi.org/10.1016/j.nxener.2025.100478
31. L. Fan, S. Wei, S. Li, Q. Li, Y. Lu, Recent progress of the solid-state electrolytes for high-energy metal-based batteries. Adv. Energy Mater. **8**(11), 1702657 (2018). https://doi.org/10.1002/aenm.201702657
32. M. Balaish, K.J. Kim, H. Chu, Y. Zhu, J.C. Gonzalez-Rosillo et al., Emerging processing guidelines for solid electrolytes in the era of oxide-based solid-state batteries. Chem. Soc. Rev. **54**, 8925–9007 (2025). https://doi.org/10.1039/D5CS00358J
33. A. Agrawal, C.M. Hussain, Green and sustainable metal–air batteries for powering flexible wearable electronics: current status and future prospects. Sustain. Energy Fuels **8**(20), 4687–4708 (2024). https://doi.org/10.1039/d4se00555d
34. D. Ahuja, V. Kalpna, P.K. Varshney, Metal air battery: A sustainable and low cost material for energy storage. J. Phys: Conf. Ser. **1913**, 012065 (2021). https://doi.org/10.1088/1742-6596/1913/1/012065
35. J. Thakur, C. Martins Leite de Almeida, A.G. Baskar, Electric vehicle batteries for a circular economy: second life batteries as residential stationary storage. J. Clean. Prod. **375**, 134066 (2022). https://doi.org/10.1016/j.jclepro.2022.134066
36. P. Slotte, E. Pohjalainen, J. Hanski, P. Kivikytö-Reponen, Effect of life extension strategies on demand and recycling of EV batteries–material flow analysis of Li and Ni in battery value chain for Finnish EV fleet by 2055. Resour. Conserv. Recycl. **215**, 108081 (2025). https://doi.org/10.1016/j.resconrec.2024.108081
37. L. Liu, N. Solin, O. Inganäs, Bio based batteries. Adv. Energy Mater. **11**(43), 2003713 (2021). https://doi.org/10.1002/aenm.202003713
38. B.E. Ibrahimi, J.V. Nardeli, L. Guo, An overview of corrosion. In: Sustainable Corrosion Inhibitors I: Fundamentals, Methodologies, and Industrial Applications, pp. 1–19 (2021). https://doi.org/10.1021/bk-2021-1403.ch001
39. S.P. Vinodhini, J.R. Xavier, Recent progress in graphene-based nanocomposites for enhanced energy storage and corrosion protection. J. Mater. Sci. **60**(34), 14837–14879 (2025). https://doi.org/10.1007/s10853-025-11307-5
40. H. Sun, Z. Wang, Q. Meng, S. White, Advancements in hydrogen storage technologies: enhancing efficiency, safety, and economic viability for sustainable energy transition. Int. J. Hydrog. Energy **105**, 10–22 (2025). https://doi.org/10.1016/j.ijhydene.2025.01.176
41. C. Han, G. Chen, Y. Ma, J. Ma, X. Shui et al., Strategies towards inhibition of aluminum current collector corrosion in lithium batteries. Energy Mater. (2023). https://doi.org/10.20517/energymater.2023.53
42. S. Ivanov, Corrosion of current collectors in metal-ion batteries. In: Corrosion and Degradation in Fuel Cells, Supercapacitors and Batteries, pp. 251–288. (Springer Nature Switzerland, 2024). https://doi.org/10.1007/978-3-031-57012-4_11
43. X. Zhang, B. Winget, M. Doeff, J.W. Evans, T.M. Devine, Corrosion of aluminum current collectors in lithium-ion batteries with electrolytes containing $LiPF_6$. J. Electrochem. Soc. **152**, B448 (2005). https://doi.org/10.1149/1.2041867
44. P. Ruetschi, Aging mechanisms and service life of lead–acid batteries. J. Power. Sources **127**(1–2), 33–44 (2004). https://doi.org/10.1016/j.jpowsour.2003.09.052
45. H. Du, Y. Wang, Y. Kang, Y. Zhao, Y. Tian et al., Side reactions/changes in lithium-ion batteries: mechanisms and strategies for creating safer and better batteries. Adv. Mater. **36**(29), 2401482 (2024). https://doi.org/10.1002/adma.202401482
46. X. Li, P. Liu, C. Han, T. Cai, Y. Cui et al., Corrosion of metallic anodes in aqueous batteries. Energy Environ. Sci. **18**(5), 2050–2094 (2025). https://doi.org/10.1039/d5ee00075k
47. M. Jiang, C. Fu, P. Meng, J. Ren, J. Wang et al., Challenges and strategies of low-cost aluminum anodes for high-performance Al-based batteries. Adv. Mater. **34**(2), 2102026 (2022). https://doi.org/10.1002/adma.202102026
48. X. Zhang, R. Lv, W. Tang, G. Li, A. Wang et al., Challenges and opportunities for multivalent metal anodes in rechargeable batteries. Adv. Funct. Mater. **30**(45), 2004187 (2020). https://doi.org/10.1002/adfm.202004187
49. M. Kim, L. Pompizii, J. Byun, A. Coskun, J.W. Choi, The challenge of corrosion in next-generation rechargeable metal batteries. Chem **11**(8), 102661 (2025). https://doi.org/10.1016/j.chempr.2025.102661
50. Y. Zhao, S. Guo, M. Chen, B. Lu, X. Zhang et al., Tailoring grain boundary stability of zinc-titanium alloy for long-lasting aqueous zinc batteries. Nat. Commun. **14**, 7080 (2023). https://doi.org/10.1038/s41467-023-42919-7
51. H. Yang, L. Wu, B. Jiang, W. Liu, J. Song et al., Clarifying the roles of grain boundary and grain orientation on the corrosion and discharge processes of α-Mg based Mg-Li alloys for primary Mg-air batteries. J. Mater. Sci. Technol. **62**, 128–138 (2021). https://doi.org/10.1016/j.jmst.2020.05.067
52. A. Kolesnikov, M. Kolek, J.F. Dohmann, F. Horsthemke, M. Börner et al., Galvanic corrosion of lithium-powder-based electrodes. Adv. Energy Mater. **10**(15), 2000017 (2020). https://doi.org/10.1002/aenm.202000017

 https://doi.org/10.1007/s40820-026-02178-9

53. B. Zhou, I. Stoševski, A. Bonakdarpour, D.P. Wilkinson, Suppressing chemical and galvanic corrosion in anode-free lithium metal batteries through electrolyte design. Adv. Funct. Mater. **34**(7), 2311212 (2024). https://doi.org/10.1002/adfm.202311212
54. J. Ma, J. Wen, Q. Li, Q. Zhang, Effects of acidity and alkalinity on corrosion behaviour of Al–Zn–Mg based anode alloy. J. Power. Sources **226**, 156–161 (2013). https://doi.org/10.1016/j.jpowsour.2012.10.075
55. X. Liu, Y. Guo, F. Ning, Y. Liu, S. Shi et al., Fundamental understanding of hydrogen evolution reaction on zinc anode surface: a first-principles study. Nano-Micro Lett. **16**(1), 111 (2024). https://doi.org/10.1007/s40820-024-01337-0
56. S. Thomas, N. Birbilis, M.S. Venkatraman, I.S. Cole, Corrosion of zinc as a function of pH. Corrosion **68**(1), 15009-1-015009–9 (2012). https://doi.org/10.5006/1.3676630
57. Z. Zembura, L. Burzynska, The corrosion of zinc in de-aerated 0.1 M NaCl in the pH range from 1.6 to 13.3. Corros. Sci. **17**(11), 871–878 (1977). https://doi.org/10.1016/0010-938x(77)90093-2
58. M. Gmytryk, J. Sedzimir, Corrosion of Zn in deaerated sulphate solutions at different pH values. Corros. Sci. **7**(10), 683–695 (1967). https://doi.org/10.1016/s0010-938x(67)80010-6
59. M. Mouanga, P. Berçot, J.Y. Rauch, Comparison of corrosion behaviour of zinc in NaCl and in NaOH solutions. Part I: Corrosion layer characterization. Corros. Sci. **52**(12), 3984–3992 (2010). https://doi.org/10.1016/j.corsci.2010.08.003
60. C. Qiao, L. Shen, L. Hao, X. Mu, J. Dong et al., Corrosion kinetics and *patina* evolution of galvanized steel in a simulated coastal-industrial atmosphere. J. Mater. Sci. Technol. **35**(10), 2345–2356 (2019). https://doi.org/10.1016/j.jmst.2019.05.039
61. L. Baugh, Corrosion and polarization characteristics of zinc in neutral–acid media–II. Effect of NH_4^+ ions and the role of battery zinc alloying constituents. Electrochim. Acta **24**, 669–677 (1979). https://doi.org/10.1016/0013-4686(79)87049-8
62. L.M. Baugh, A. Higginson, Passivation of zinc in concentrated alkaline solution: I. Characteristics of active dissolution prior to passivation. Electrochim. Acta **30**(9), 1163–1172 (1985). https://doi.org/10.1016/0013-4686(95)80008-5
63. M. Mokaddem, P. Volovitch, K. Ogle, The anodic dissolution of zinc and zinc alloys in alkaline solution. I. Oxide formation on electrogalvanized steel. Electrochim. Acta **55**(27), 7867–7875 (2010). https://doi.org/10.1016/j.electacta.2010.02.020
64. H. Yang, Y. Qiao, Z. Chang, H. Deng, P. He et al., A metal–organic framework as a multifunctional ionic sieve membrane for long-life aqueous zinc–iodide batteries. Adv. Mater. **32**(38), 2004240 (2020). https://doi.org/10.1002/adma.202004240
65. I. Boukerche, S. Djerad, L. Benmansour, L. Tifouti, K. Saleh, Degradability of aluminum in acidic and alkaline solutions. Corros. Sci. **78**, 343–352 (2014). https://doi.org/10.1016/j.corsci.2013.10.019
66. S.-M. Moon, S.-I. Pyun, The formation and dissolution of anodic oxide films on pure aluminium in alkaline solution. Electrochim. Acta **44**(14), 2445–2454 (1999). https://doi.org/10.1016/s0013-4686(98)00368-5
67. W.-J. Lee, S.-I. Pyun, Effects of sulphate ion additives on the pitting corrosion of pure aluminium in 0.01 M NaCl solution. Electrochim. Acta **45**(12), 1901–1910 (2000). https://doi.org/10.1016/s0013-4686(99)00418-1
68. J. Flis, L. Kowalczyk, Effect of sulphate anions on tunnel etching of aluminium. J. Appl. Electrochem. **25**(5), 501–507 (1995). https://doi.org/10.1007/BF00260695
69. S. Li, B.C. Church, Effects of sulfate and nitrate anions on aluminum corrosion in slightly alkaline solution. Appl. Surf. Sci. **440**, 861–872 (2018). https://doi.org/10.1016/j.apsusc.2018.01.108
70. R.G. Wymer, R.E. Blanco, Uranium-aluminum alloy dissolution. Ind. Eng. Chem. **49**(1), 59–61 (1957). https://doi.org/10.1021/ie50565a026
71. D. Singh, R. Chaudhary, C. Agarwal, Corrosion characteristics of some aluminum alloys in nitric acid. J. Electrochem. Soc. **129**, 1869 (1982). https://doi.org/10.1149/1.2124317
72. G.T. Burstein, R.M. Organ, Repassivation and pitting of freshly generated aluminium surfaces in acidic nitrate solution. Corros. Sci. **47**(12), 2932–2955 (2005). https://doi.org/10.1016/j.corsci.2005.05.054
73. K.F. Khaled, Electrochemical investigation and modeling of corrosion inhibition of aluminum in molar nitric acid using some sulphur-containing amines. Corros. Sci. **52**(9), 2905–2916 (2010). https://doi.org/10.1016/j.corsci.2010.05.001
74. R. Ambat, E.S. Dwarakadasa, Studies on the influence of chloride ion and pH on the electrochemical behaviour of aluminium alloys 8090 and 2014. J. Appl. Electrochem. **24**(9), 911–916 (1994). https://doi.org/10.1007/BF00348781
75. E. Gulbrandsen, J. Taftø, A. Olsen, The passive behaviour of Mg in alkaline fluoride solutions. Electrochemical and electron microscopical investigations. Corros. Sci. **34**(9), 1423–1440 (1993). https://doi.org/10.1016/0010-938x(93)90238-c
76. G.G. Perrault, Potentiostatic study of the magnesium electrode in aqueous solution. J. Electroanal. Chem. Interfac. Electrochem. **27**(1), 47–58 (1970). https://doi.org/10.1016/s0022-0728(70)80201-7
77. G.L. Song, A. Atrens, Corrosion mechanisms of magnesium alloys. Adv. Eng. Mater. **1**(1), 11–33 (1999). https://doi.org/10.1002/(sici)1527-2648(199909)1:111::aid-adem11%3e3.0.co;2-n
78. P. King, The role of the anion in the anodic dissolution of magnesium. J. Electrochem. Soc. **113**, 536 (1966). https://doi.org/10.1149/1.2424019
79. G. Hoey, M. Cohen, Corrosion of anodically and cathodically polarized magnesium in aqueous media. J. Electrochem. Soc. **105**, 245 (1958). https://doi.org/10.1002/(SICI)1527-2648(199909)1:1<11::AID-ADEM11>3.0.CO;2-N

80. N. Birbilis, A.D. King, S. Thomas, G.S. Frankel, J.R. Scully, Evidence for enhanced catalytic activity of magnesium arising from anodic dissolution. Electrochim. Acta **132**, 277–283 (2014). https://doi.org/10.1016/j.electacta.2014.03.133
81. M. Curioni, The behaviour of magnesium during free corrosion and potentiodynamic polarization investigated by real-time hydrogen measurement and optical imaging. Electrochim. Acta **120**, 284–292 (2014). https://doi.org/10.1016/j.electacta.2013.12.109
82. H. Wu, Z. Shi, X. Zhang, A.M. Qasim, S. Xiao et al., Achieving an acid resistant surface on magnesium alloy *via* bio-inspired design. Appl. Surf. Sci. **478**, 150–161 (2019). https://doi.org/10.1016/j.apsusc.2019.01.181
83. J. Liang, P.B. Srinivasan, C. Blawert, W. Dietzel, Influence of pH on the deterioration of plasma electrolytic oxidation coated AM50 magnesium alloy in NaCl solutions. Corros. Sci. **52**(2), 540–547 (2010). https://doi.org/10.1016/j.corsci.2009.10.011
84. B. Zhou, Z. Yang, L. Lu, B. Fang, D.P. Wilkinson et al., Corrosion mechanisms and mitigation strategies of lithium metal anodes for liquid lithium batteries. Matter **8**(3), 101996 (2025). https://doi.org/10.1016/j.matt.2025.101996
85. J.S. Edge, S. O'Kane, R. Prosser, N.D. Kirkaldy, A.N. Patel et al., Lithium ion battery degradation: what you need to know. Phys. Chem. Chem. Phys. **23**(14), 8200–8221 (2021). https://doi.org/10.1039/d1cp00359c
86. M. Alipour, C. Ziebert, F.V. Conte, R. Kizilel, A review on temperature-dependent electrochemical properties, aging, and performance of lithium-ion cells. Batteries **6**(3), 35 (2020). https://doi.org/10.3390/batteries6030035
87. H. Parangusan, J. Bhadra, N. Al-Thani, A review of passivity breakdown on metal surfaces: influence of chloride- and sulfide-ion concentrations, temperature, and pH. Emergent Mater. **4**(5), 1187–1203 (2021). https://doi.org/10.1007/s42247-021-00194-6
88. Y.-C. Liu, Y. Li, X. Fu, Z.-A. Xue, J.-J. Wang, Lithium dendrite growth, evolution, inhibition in lithium-ion batteries. J. Energy Storage **138**, 118559 (2025). https://doi.org/10.1016/j.est.2025.118559
89. M.D. Bouguern, A.K. M R, K. Zaghib, The critical role of interfaces in advanced Li-ion battery technology: a comprehensive review. J. Power. Sources **623**, 235457 (2024). https://doi.org/10.1016/j.jpowsour.2024.235457
90. H. Xu, Q. Shen, Y. Sun, F. Liu, Y. Zhang, Temperature dependence of water and salt transport in concentration gradient batteries: insight from membrane properties. J. Membr. Sci. **713**, 123382 (2025). https://doi.org/10.1016/j.memsci.2024.123382
91. T.R. Beck, Effect of hydrodynamics on pitting. Corrosion **33**(1), 9–13 (1977). https://doi.org/10.5006/0010-9312-33.1.9
92. Y. Wang, K. Wu, H. Zhao, J. Li, X. Sheng et al., Degradation prediction of proton exchange membrane fuel cell stack using semi-empirical and data-driven methods. Energy AI **11**, 100205 (2023). https://doi.org/10.1016/j.egyai.2022.100205
93. Y. Chang, J. Xiao, H. Yuan, J. Jin, Y. Lu et al., Synergistic dual additives enable highly safe and long-cycling lithium metal batteries. Chem. Eng. J. **521**, 166851 (2025). https://doi.org/10.1016/j.cej.2025.166851
94. Z.-P. Liang, K.-X. Jiang, B.-A. Feng, L. Li, T.-A. Zhang, Effect of anodic potential on the characteristics of passive films grown on a brass alloy in a soil environment. Mater. Corros. **73**(3), 404–413 (2022). https://doi.org/10.1002/maco.202112795
95. K. Guo, S. Qi, H. Wang, J. Huang, M. Wu et al., High-voltage electrolyte chemistry for lithium batteries. Small Sci. **2**(5), 2100107 (2022). https://doi.org/10.1002/smsc.202100107
96. W.-H. Hou, Y. Lu, Y. Ou, P. Zhou, S. Yan et al., Recent advances in electrolytes for high-voltage cathodes of lithium-ion batteries. Trans. Tianjin Univ. **29**(2), 120–135 (2023). https://doi.org/10.1007/s12209-023-00355-0
97. X. Dong, B. Wei, D. Legut, H. Zhang, R. Zhang, Electrochemical Pourbaix diagrams of Mg–Zn alloys from first-principles calculations and experimental thermodynamic data. Phys. Chem. Chem. Phys. **23**(35), 19602–19610 (2021). https://doi.org/10.1039/d1cp02754a
98. T. Dam, A.-G. Nguyen, G. Cao, C.-J. Park, Electrolyte development for enhancing sub-zero temperature performance of secondary batteries. Small **21**(35), 2500982 (2025). https://doi.org/10.1002/smll.202500982
99. M. Asiri, M. Kedhim, V. Jain, S. Ballal, A. Singh et al., Impact of temperature and state-of-charge on long-term storage degradation in lithium-ion batteries: an integrated P2D-based degradation analysis. RSC Adv. **15**(28), 22576–22586 (2025). https://doi.org/10.2139/ssrn.5272326
100. M. Liu, P. Wang, W. Zhang, H. He, G. He et al., Strategies for pH regulation in aqueous zinc ion batteries. Energy Storage Mater. **67**, 103248 (2024). https://doi.org/10.1016/j.ensm.2024.103248
101. Y. Chen, X. Yang, Y. Li, G. Liu, F. Ran, Mechanism and application of electrolyte additives in regulating stability of zinc anode interface in aqueous zinc metal batteries. Adv. Funct. Mater. (2026). https://doi.org/10.1002/adfm.202531039
102. I. Bösing, J. Thöming, M. Baune, Electrolyte composition for distinguishing corrosion mechanisms in steel alloy screening. Int. J. Corros. **2017**, 9425864 (2017). https://doi.org/10.1155/2017/9425864
103. B. Li, N.M. Harrison, A.P. Horsfield, Uncovering the electrochemical stability and corrosion reaction pathway of Mg (0001) surface: insight from first-principles calculation. Corros. Sci. **241**, 112524 (2024). https://doi.org/10.1016/j.corsci.2024.112524
104. A. Zagalskaya, P. Chaudhary, V. Alexandrov, Corrosion of electrochemical energy materials: stability analyses beyond Pourbaix diagrams. J. Phys. Chem. C **127**(30), 14587–14598 (2023). https://doi.org/10.1021/acs.jpcc.3c01727
105. M.S. Venkatraman, I.S. Cole, B. Emmanuel, Corrosion under a porous layer: a porous electrode model and its implications for self-repair. Electrochim. Acta **56**(24),

 https://doi.org/10.1007/s40820-026-02178-9

8192–8203 (2011). https://doi.org/10.1016/j.electacta.2011.06.020

106. L. Su, L. Liu, B. Liu, J. Meng, X. Yan, Revealing the impact of oxygen dissolved in electrolytes on aqueous zinc-ion batteries. iScience **23**(4), 100995 (2020). https://doi.org/10.1016/j.isci.2020.100995
107. Y. Yuan, Z. Li, R. Deng, S.D. Pu, M. Walker et al., Identifying the role of Zn self-dissolution in the anode corrosion process in Zn-ion batteries. Energy Environ. Sci. **18**(11), 5610–5621 (2025). https://doi.org/10.1039/d5ee00485c
108. S.S. Zhang, A review on electrolyte additives for lithium-ion batteries. J. Power. Sources **162**(2), 1379–1394 (2006). https://doi.org/10.1016/j.jpowsour.2006.07.074
109. K. Xu, Electrolytes and interphases in Li-ion batteries and beyond. Chem. Rev. **114**(23), 11503–11618 (2014). https://doi.org/10.1021/cr500003w
110. T. Waldmann, M. Wilka, M. Kasper, M. Fleischhammer, M. Wohlfahrt-Mehrens, Temperature dependent ageing mechanisms in lithium-ion batteries–a post-mortem study. J. Power Sources **262**, 129–135 (2014). https://doi.org/10.1016/j.jpowsour.2014.03.112
111. Y.-Y. Wang, X.-Q. Zhang, M.-Y. Zhou, J.-Q. Huang, Mechanism, quantitative characterization, and inhibition of corrosion in lithium batteries. Nano Res. Energy **2**, e9120046 (2023). https://doi.org/10.26599/nre.2023.9120046
112. Z.N. Duan, Z.G. Qu, Q. Wang, J.J. Wang, Structural modification of vanadium redox flow battery with high electrochemical corrosion resistance. Appl. Energy **250**, 1632–1640 (2019). https://doi.org/10.1016/j.apenergy.2019.04.186
113. V.S. Saji, Corrosion and materials degradation in electrochemical energy storage and conversion devices. ChemElectroChem (2023). https://doi.org/10.1002/celc.202300136
114. J.N. Weker, M.F. Toney, Emerging *in situ* and operando nanoscale X-ray imaging techniques for energy storage materials. Adv. Funct. Mater. **25**(11), 1622–1637 (2015). https://doi.org/10.1002/adfm.201403409
115. D. Liu, Z. Shadike, R. Lin, K. Qian, H. Li et al., Review of recent development of in situ/operando characterization techniques for lithium battery research. Adv. Mater. **31**(28), 1806620 (2019). https://doi.org/10.1002/adma.201806620
116. J. Lu, T. Wu, K. Amine, State-of-the-art characterization techniques for advanced lithium-ion batteries. Nat. Energy **2**(3), 17011 (2017). https://doi.org/10.1038/nenergy.2017.11
117. J. Xu, J. Hu, S. Hu, Enhanced corrosion resistance and discharge performance of Mg-MnO_2 battery by Na_2SiO_3 additive. Chem. Res. Chin. Univ. **35**(4), 641–646 (2019). https://doi.org/10.1007/s40242-019-9049-x
118. R.-C. Zeng, Y. Hu, S.-K. Guan, H.-Z. Cui, E.-H. Han, Corrosion of magnesium alloy AZ31: the influence of bicarbonate, sulphate, hydrogen phosphate and dihydrogen phosphate ions in saline solution. Corros. Sci. **86**, 171–182 (2014). https://doi.org/10.1016/j.corsci.2014.05.006
119. J. Lin, C. Hsia, J. Uan, Characterization of Mg, Al-hydrotalcite conversion film on Mg alloy and Cl–and CO_3^{2-} anion-exchangeability of the film in a corrosive environment. Scr. Mater. **56**(11), 927–930 (2007). https://doi.org/10.1016/j.scriptamat.2007.02.020
120. P. Pei, K. Wang, Z. Ma, Technologies for extending zinc–air battery's cyclelife: a review. Appl. Energy **128**, 315–324 (2014). https://doi.org/10.1016/j.apenergy.2014.04.095
121. R. Bender, D. Féron, D. Mills, S. Ritter, R. Bäßler et al., Corrosion challenges towards a sustainable society. Mater. Corros. **73**(11), 1730–1751 (2022). https://doi.org/10.1002/maco.202213140
122. N. Qiu, J. Yang, W. Mou, M. Xiao, Study on mechanical properties of lithium-ion battery in hydrothermal salt spray environment under different mechanical abuse conditions. Thin-Walled Struct. **213**, 113273 (2025). https://doi.org/10.1016/j.tws.2025.113273
123. P. Du, D. Liu, X. Chen, H. Xie, X. Qu et al., Research progress towards the corrosion and protection of electrodes in energy-storage batteries. Energy Storage Mater. **57**, 371–399 (2023). https://doi.org/10.1016/j.ensm.2023.02.028
124. W.C. Munonye, G.O. Ajonye, S.O. Ahonsi, D.I. Munonye, I.O. Chigozie et al., Advancing circularity in battery systems for renewable energy: technologies, barriers, and future directions. Adv. Energy Sustain. Res. **7**, e202500255 (2026). https://doi.org/10.1002/aesr.202500255
125. M. Cerrillo-Gonzalez, M. Villen-Guzman, C. Vereda-Alonso, J. Rodriguez-Maroto, J. Paz-Garcia, Towards sustainable lithium-ion battery recycling: advancements in circular hydrometallurgy. Processes **12**(7), 1485 (2024). https://doi.org/10.3390/pr12071485
126. B.I. Chigbu, Advancing sustainable development through circular economy and skill development in EV lithium-ion battery recycling: a comprehensive review. Front. Sustain. **5**, 1409498 (2024). https://doi.org/10.3389/frsus.2024.1409498
127. Z. Chen, Q. Yu, W. Wang, J. Zhang, Interface engineering strategies for shuttle mitigation in alkali metal–sulfur batteries: a comparative review from Li–S to Na–S and K–S systems. Nano-Micro Lett. **18**(1), 167 (2026). https://doi.org/10.1007/s40820-025-02004-8
128. Z. Zhu, S. Xiong, J. Li, L. Wang, X. Tang et al., Hydrogel polymer electrolytes for aqueous zinc-ion batteries: recent progress and remaining challenges. Batteries **11**(10), 380 (2025). https://doi.org/10.3390/batteries11100380
129. Y. Liu, H. He, A. Gao, J. Ling, F. Yi et al., Fundamental study on Zn corrosion and dendrite growth in gel electrolyte towards advanced wearable Zn-ion battery. Chem. Eng. J. **446**, 137021 (2022). https://doi.org/10.1016/j.cej.2022.137021
130. X. Cai, X. Li, J. Liang, J. Qiu, W. Lin et al., Stabilizing the anode and cathode interface synchronously *via* electrolyte-triggered hydrogel interphase for zinc metal batteries. Nano-Micro Lett. **18**(1), 206 (2026). https://doi.org/10.1007/s40820-025-02051-1
131. H. Zhang, X. Gan, Y. Yan, J. Zhou, A sustainable dual cross-linked cellulose hydrogel electrolyte for high-performance

zinc-metal batteries. Nano-Micro Lett. **16**(1), 106 (2024). https://doi.org/10.1007/s40820-024-01329-0

132. L. Xu, L. Zhang, D. Liu, Z. Ren, W. Liu et al., A comprehensive review of the functionalized integrated application of gel polymer electrolytes in electrochromic devices. Nano-Micro Lett. **18**(1), 106 (2026). https://doi.org/10.1007/s40820-025-01909-8
133. A. Ortiz-Ozuna, F.A. Godínez, B. Ramírez-Barat, M.C. Garcia-Alonso, M.L. Escudero et al., pH evolution around the AZ31/steel galvanic couple under gelled-electrolytes: a numerical and experimental study. Corros. Sci. **178**, 109061 (2021). https://doi.org/10.1016/j.corsci.2020.109061
134. A. Ruiz-Garcia, V. Esquivel-Peña, J. Genesca, R. Montoya, Advances in galvanic corrosion of aluminum alloys. Electrochim. Acta **449**, 142227 (2023). https://doi.org/10.1016/j.electacta.2023.142227
135. T. Zhang, Y. Dai, S. Ren, Z. Huang, C. Han et al., Polymer–silicate composite gel systems for enhanced chloride resistance of cement-based materials. Gels **11**(12), 936 (2025). https://doi.org/10.3390/gels11120936
136. Y.-H. Lin, L.-T. Wu, Y.-T. Zhan, J.-C. Jiang, Y.-L. Lee et al., Self-assembly formation of solid-electrolyte interphase in gel polymer electrolytes for high performance lithium metal batteries. Energy Storage Mater. **61**, 102868 (2023). https://doi.org/10.1016/j.ensm.2023.102868
137. C. Fu, L. Song, Y. Feng, T. Zhang, L. Wu et al., Fluorophenyl-engineered gel electrolytes enabling 4.8 V lithium batteries with durable electrolyte-electrode interfaces. Adv. Funct. Mater. (2025). https://doi.org/10.1002/adfm.202525005
138. C. Huang, H. Li, Z. Teng, Y. Luo, W. Chen, MOF-modified dendrite-free gel polymer electrolyte for zinc-ion batteries. RSC Adv. **14**(22), 15337–15346 (2024). https://doi.org/10.1039/d4ra02200a
139. X. Shi, C. Dong, L. Ma, M. Yang, X. Chen et al., A sustainable and recyclable cellulose gel electrolyte enables stable zinc metal anode for green aqueous batteries. Chem. Eng. J. **504**, 158659 (2025). https://doi.org/10.1016/j.cej.2024.158659
140. M.-K. Zhang, W. Chen, M.-L. Xu, Z. Wei, D. Zhou et al., How buffers resist electrochemical reaction-induced pH shift under a rotating disk electrode configuration. Anal. Chem. **93**(4), 1976–1983 (2021). https://doi.org/10.1021/acs.analchem.0c03033
141. C. Örnek, F. Zhang, A. Larsson, M. Mansoor, G.S. Harlow et al., Understanding passive film degradation and its effect on hydrogen embrittlement of super duplex stainless steel–Synchrotron X-ray and electrochemical measurements combined with CalPhaD and ab-initio computational studies. Appl. Surf. Sci. **628**, 157364 (2023). https://doi.org/10.1016/j.apsusc.2023.157364
142. J. Ma, H. Luo, X. Hu, Z. Pan, X. Li, Electrochemical study on the effect of hydrogen on the passive film of selective laser melted 316L stainless steel in a proton exchange membrane water electrolyzer environment. Int. J. Hydrog. Energy **48**(51), 19396–19410 (2023). https://doi.org/10.1016/j.ijhydene.2023.02.045
143. P. Meng, J. Huang, Z. Yang, M. Jiang, Y. Wang et al., Air-stable binary hydrated eutectic electrolytes with unique solvation structure for rechargeable aluminum-ion batteries. Nano-Micro Lett. **15**(1), 188 (2023). https://doi.org/10.1007/s40820-023-01160-z
144. R.N. Mishra, A.K.M.R. Reddy, M.-A. Goulet, K. Zaghib, Water-in-salt electrolytes: advances and chemistry for sustainable aqueous monovalent-metal-ion batteries. Batteries **11**(4), 120 (2025). https://doi.org/10.3390/batteries11040120
145. F. Deißenbeck, S. Surendralal, M. Todorova, S. Wippermann, J. Neugebauer, Revealing the reaction pathway of anodic hydrogen evolution at magnesium surfaces in aqueous electrolytes. J. Am. Chem. Soc. **146**(44), 30314–30319 (2024). https://doi.org/10.1021/jacs.4c10086
146. Y. Wu, Z. Zhao, Y. Fei, H. Zhang, G. Li, Localized high-concentration electrolyte with water-miscible diluent enables stable zinc deposition and long-life aqueous zinc metal batteries. Adv. Funct. Mater. (2025). https://doi.org/10.1002/adfm.202526034
147. M.M. El-Naggar, Effects of Cl^-, $NO_3^-$and SO_4^{2-}anions on the anodic behavior of carbon steel in deaerated 0.50M $NaHCO_3$ solutions. Appl. Surf. Sci. **252**(18), 6179–6194 (2006). https://doi.org/10.1016/j.apsusc.2005.08.025
148. H. Yang, Z. Zhu, S. Zhou, T. Li, Progress in the study of corrosion characteristics of water-wall tubes of power station boilers by Cl^-/SO_4^{2-}. J. Phys.: Conf. Ser. (IOP Publ.) **2821**, 012008 (2024)
149. X. Guo, J. Shan, S. Gong, J. Xu, Q. Xu et al., Enhancing ionic conductivity and controlling lithium dendrite growth *via* ferroelectric ceramic $Bi_4Ti_3O_{12}$. J. Taiwan Inst. Chem. Eng. **161**, 105513 (2024). https://doi.org/10.1016/j.jtice.2024.105513
150. Y. Chen, K. Wang, H. Wang, T. Zhang, D. Zhong, Unlocking dendrite growth in metal batteries. Prog. Mater. Sci. **158**, 101633 (2026). https://doi.org/10.1016/j.pmatsci.2025.101633
151. S. So, Y.N. Ahn, J. Ko, I.T. Kim, J. Hur, Uniform and oriented zinc deposition induced by artificial Nb_2O_5 layer for highly reversible Zn anode in aqueous zinc ion batteries. Energy Storage Mater. **52**, 40–51 (2022). https://doi.org/10.1016/j.ensm.2022.07.036
152. T.-H. Wu, Y. Zhang, Z.D. Althouse, N. Liu, Nanoscale design of zinc anodes for high-energy aqueous rechargeable batteries. Mater. Today Nano **6**, 100032 (2019). https://doi.org/10.1016/j.mtnano.2019.100032
153. W. Haotian, Z. Tiansui, L. Guangfang, L. Hongfang, Corrosion inhibitor for Zn anode of neutral aqueous zinc ion batteries. J. Chin. Soc. Corros. Prot. **44**, 1089–1099 (2023)
154. X. Feng, P. Li, J. Yin, Z. Gan, Y. Gao et al., Enabling highly reversible Zn anode by multifunctional synergistic effects of hybrid solute additives. ACS Energy Lett. **8**(2), 1192–1200 (2023). https://doi.org/10.1021/acsenergylett.2c02455

 https://doi.org/10.1007/s40820-026-02178-9

155. B. Ren, X. Zhang, H. Wei, J. Jiang, G. Chen et al., Suppressing zinc metal corrosion by an effective and durable corrosion inhibitor for stable aqueous zinc batteries. Adv. Funct. Mater. **35**(17), 2418594 (2025). https://doi.org/10.1002/adfm.202418594
156. K. Guan, L. Tao, R. Yang, H. Zhang, N. Wang et al., Anti-corrosion for reversible zinc anode *via* a hydrophobic interface in aqueous zinc batteries. Adv. Energy Mater. **12**(9), 2103557 (2022). https://doi.org/10.1002/aenm.202103557
157. M.A. Deyab, Hydroxyethyl cellulose as efficient organic inhibitor of zinc–carbon battery corrosion in ammonium chloride solution: electrochemical and surface morphology studies. J. Power. Sources **280**, 190–194 (2015). https://doi.org/10.1016/j.jpowsour.2015.01.107
158. A. Singh, K.R. Ansari, M.A. Quraishi, Chondroitin sulfate as a green corrosion inhibitor for zinc in 26% ammonium chloride solution: electrochemical and surface morphological analysis. Colloids Surf. A Physicochem. Eng. Aspects **607**, 125465 (2020). https://doi.org/10.1016/j.colsurfa.2020.125465
159. V.K. Nartey, L. Binder, K. Kordesch, Identification of organic corrosion inhibitors suitable for use in rechargeable alkaline zinc batteries. J. Power. Sources **52**(2), 217–222 (1994). https://doi.org/10.1016/0378-7753(94)02010-8
160. A.R.S. Kannan, S. Muralidharan, K.B. Sarangapani, V. Balaramachandran, V. Kapali, Corrosion and anodic behaviour of zinc and its ternary alloys in alkaline battery electrolytes. J. Power. Sources **57**(1–2), 93–98 (1995). https://doi.org/10.1016/0378-7753(95)02225-2
161. Y. Ein-Eli, M. Auinat, D. Starosvetsky, Electrochemical and surface studies of zinc in alkaline solutions containing organic corrosion inhibitors. J. Power. Sources **114**(2), 330–337 (2003). https://doi.org/10.1016/s0378-7753(02)00598-0
162. L. Zhu, H. Zhang, W. Li, H. Liu, New modification procedure of zinc powder in neodymium nitrate solution for improving the electrochemical properties of alkaline zinc electrodes. J. Phys. Chem. Solids **70**(1), 45–54 (2009). https://doi.org/10.1016/j.jpcs.2008.09.005
163. M. Abdallah, A. El-Etre, M. Moustafa, Amidopoly ethylamines as corrosion inhibitors for zinc dissolution in different acidic electrolytes. Port. Electrochim. Acta **27**, 615–630 (2009). https://doi.org/10.4152/pea.200905615
164. M. Liang, H. Zhou, Q. Huang, S. Hu, W. Li, Synergistic effect of polyethylene glycol 600 and polysorbate 20 on corrosion inhibition of zinc anode in alkaline batteries. J. Appl. Electrochem. **41**(8), 991–997 (2011). https://doi.org/10.1007/s10800-011-0328-6
165. H. Zhou, Q. Huang, M. Liang, D. Lv, M. Xu et al., Investigation on synergism of composite additives for zinc corrosion inhibition in alkaline solution. Mater. Chem. Phys. **128**(1–2), 214–219 (2011). https://doi.org/10.1016/j.matchemphys.2011.02.061
166. K. Liu, P. He, H. Bai, J. Chen, F. Dong et al., Effects of dodecyltrimethylammonium bromide surfactant on both corrosion and passivation behaviors of zinc electrodes in alkaline solution. Mater. Chem. Phys. **199**, 73–78 (2017). https://doi.org/10.1016/j.matchemphys.2017.06.050
167. M.A. Deyab, Application of nonionic surfactant as a corrosion inhibitor for zinc in alkaline battery solution. J. Power. Sources **292**, 66–71 (2015). https://doi.org/10.1016/j.jpowsour.2015.05.040
168. C. Yang, Z. Zhang, Z. Tian, K. Zhang, J. Li, Y. Lai, Effects of carboxymethyl cellulose on the electrochemical characteristics and dendrite growth of zinc in alkaline solution. J. Electrochem. Soc. **163**, A1836 (2016). https://doi.org/10.1149/2.0101609jes
169. Z. Liu, Y. Zhao, G.-C. Han, J. Liu, Q. He et al., Preparation of Schiff base surfactant and its application in alkaline zinc-nickel batteries. Ionics **22**(12), 2391–2397 (2016). https://doi.org/10.1007/s11581-016-1785-z
170. Y. Qiang, S. Zhang, L. Guo, S. Xu, L. Feng et al., Sodium dodecyl benzene sulfonate as a sustainable inhibitor for zinc corrosion in 26% NH_4Cl solution. J. Clean. Prod. **152**, 17–25 (2017). https://doi.org/10.1016/j.jclepro.2017.03.104
171. H.M.A. El-Lateef, M. Elrouby, Synergistic inhibition effect of poly(ethylene glycol) and cetyltrimethylammonium bromide on corrosion of Zn and Zn: Ni alloys for alkaline batteries. Trans. Nonferrous Met. Soc. China **30**(1), 259–274 (2020). https://doi.org/10.1016/s1003-6326(19)65197-6
172. Y. Xia, R. Tong, J. Zhang, M. Xu, G. Shao et al., Polarizable additive with intermediate chelation strength for stable aqueous zinc-ion batteries. Nano-Micro Lett. **16**(1), 82 (2024). https://doi.org/10.1007/s40820-023-01305-0
173. R. Chen, W. Zhang, Q. Huang, C. Guan, W. Zong et al., Trace amounts of triple-functional additives enable reversible aqueous zinc-ion batteries from a comprehensive perspective. Nano-Micro Lett. **15**(1), 81 (2023). https://doi.org/10.1007/s40820-023-01050-4
174. R. Sun, D. Han, C. Cui, Z. Han, X. Guo et al., A self-deoxidizing electrolyte additive enables highly stable aqueous zinc batteries. Angew. Chem. Int. Ed. **62**(28), e202303557 (2023). https://doi.org/10.1002/anie.202303557
175. D. Gelman, H. Drezner, A. Kraytsberg, D. Starosvetsky, Y. Ein-Eli, Enhanced zinc corrosion mitigation *via* a tuned thermal pretreatment in an alkaline solution containing an organic inhibitor. J. Solid State Electrochem. **22**(7), 2217–2226 (2018). https://doi.org/10.1007/s10008-018-3922-2
176. A. Mitha, A.Z. Yazdi, M. Ahmed, P. Chen, Surface adsorption of polyethylene glycol to suppress dendrite formation on zinc anodes in rechargeable aqueous batteries. ChemElectroChem **5**(17), 2409–2418 (2018). https://doi.org/10.1002/celc.201800572
177. T.K.A. Hoang, M. Acton, H.T.H. Chen, Y. Huang, T.N.L. Doan et al., Sustainable gel electrolyte containing Pb^{2+} as corrosion inhibitor and dendrite suppressor for the zinc anode in the rechargeable hybrid aqueous battery. Mater. Today Energy **4**, 34–40 (2017). https://doi.org/10.1016/j.mtener.2017.03.003
178. T.K.A. Hoang, T.N.L. Doan, J.H. Cho, J.Y.J. Su, C. Lee et al., Sustainable gel electrolyte containing pyrazole as corrosion inhibitor and dendrite suppressor for aqueous Zn/$LiMn_2O_4$

battery. ChemSusChem **10**(13), 2816–2822 (2017). https://doi.org/10.1002/cssc.201700441

179. Y. Liu, Q. Shi, Y. Wu, Q. Wang, J. Huang et al., Highly efficient dendrite suppressor and corrosion inhibitor based on gelatin/Mn^{2+} co-additives for aqueous rechargeable zinc-manganese dioxide battery. Chem. Eng. J. **407**, 127189 (2021). https://doi.org/10.1016/j.cej.2020.127189
180. S. Hosseini, W. Lao-atiman, S.J. Han, A. Arpornwichanop, T. Yonezawa et al., Discharge performance of zinc-air flow batteries under the effects of sodium dodecyl sulfate and Pluronic F-127. Sci. Rep. **8**, 14909 (2018). https://doi.org/10.1038/s41598-018-32806-3
181. Y. Xiao, J. Shi, F. Zhao, Z. Zhang, W. He, Effects of electrolyte additives on the properties of zinc–bismuth electrodes in zinc–air batteries. J. Electrochem. Soc. **165**, A47 (2018). https://doi.org/10.1149/2.0251802jes
182. S. Thangavel, P.-T. Chen, W.-M. Yan, C.-J. Yang, K.D. Huang, Protection efficiencies ofsurface-activeinhibitorsin zinc-airbatteries. Int. J. Energy Res. **44**(14), 11883–11893 (2020). https://doi.org/10.1002/er.5831
183. H. Wu, T. Zhang, J. Zhu, G. Li, H. Liu, Highly efficient corrosion inhibitor for low charge voltage and long lifespan rechargeable aqueous zinc-air battery. Chem. Eng. J. **496**, 153819 (2024). https://doi.org/10.1016/j.cej.2024.153819
184. M.-H. Lin, C.-J. Huang, P.-H. Cheng, J.-H. Cheng, C.-C. Wang, Revealing the effect of polyethylenimine on zinc metal anodes in alkaline electrolyte solution for zinc–air batteries: mechanism studies of dendrite suppression and corrosion inhibition. J. Mater. Chem. A **8**(39), 20637–20649 (2020). https://doi.org/10.1039/d0ta06929a
185. Y. Gan, B. Tan, Q. Hu, S. Zhang, W. Li, Bi-functional inhibitors of zinc corrosion and dendrite formation in aqueous electrolyte: insights from experiments and theoretical calculations. Corros. Sci. **208**, 110619 (2022). https://doi.org/10.1016/j.corsci.2022.110619
186. T.N.T. Tran, M. Zhao, S. Geng, D.G. Ivey, Ethylene glycol as an antifreeze additive and corrosion inhibitor for aqueous zinc-ion batteries. Batteries Supercaps **5**(6), e202100420 (2022). https://doi.org/10.1002/batt.202100420
187. M. Kim, S.-J. Shin, J. Lee, Y. Park, Y. Kim et al., Cationic additive with a rigid solvation shell for high-performance zinc ion batteries. Angew. Chem. Int. Ed. **61**(47), e202211589 (2022). https://doi.org/10.1002/anie.202211589
188. H. Liu, Z. Xin, B. Cao, Z. Xu, B. Xu et al., Polyhydroxylated organic molecular additives for durable aqueous zinc battery. Adv. Funct. Mater. **34**(4), 2309840 (2024). https://doi.org/10.1002/adfm.202309840
189. X. Liu, K. Fan, X. Huang, J. Ge, Y. Liu et al., Recent advances in artificial intelligence boosting materials design for electrochemical energy storage. Chem. Eng. J. **490**, 151625 (2024). https://doi.org/10.1016/j.cej.2024.151625
190. X. Chen, M. Liu, S. Yin, Y.-C. Gao, N. Yao et al., Uni-electrolyte: an artificial intelligence platform for designing electrolyte molecules for rechargeable batteries. Angew. Chem. Int. Ed. **64**(30), e202503105 (2025). https://doi.org/10.1002/anie.202503105
191. C. Lin, L. Zhang, Y. Dong, Compositional machine learning and high-throughput screening aided discovery of novel anti-perovskite solid-state electrolytes. J. Energy Storage **125**, 116990 (2025). https://doi.org/10.1016/j.est.2025.116990
192. Y. Yan, F. Hai, B. Wang, W. Cao, M. Li et al., Machine learning accelerates high-voltage electrolyte discovery for lithium metal batteries. Energy Storage Mater. **79**, 104312 (2025). https://doi.org/10.1016/j.ensm.2025.104312
193. G. Yin, H. Zhu, S. Chen, T. Li, C. Wu et al., Machine learning-assisted high-throughput screening for electrocatalytic hydrogen evolution reaction. Molecules **30**(4), 759 (2025). https://doi.org/10.3390/molecules30040759
194. S.S. Manna, S. Manna, B. Pathak, Molecular dynamics-machine learning approaches for the accurate prediction of electrochemical windows of ionic liquid electrolytes for dual-ion batteries. J. Mater. Chem. A **11**(40), 21702–21712 (2023). https://doi.org/10.1039/d3ta04310j
195. Z. Xu, Y. Xia, H. Duan, J. Li, Y. Lin et al., High-throughput calculations and machine learning for discovering halide-type solid-state electrolyte materials. Chem. Mater. **37**(17), 6642–6654 (2025). https://doi.org/10.1021/acs.chemmater.5c01169
196. F. Zheng, B. Yuan, Y. Cai, H. Xiang, C. Tang et al., Machine learning tailored anodes for efficient hydrogen energy generation in proton-conducting solid oxide electrolysis cells. Nano-Micro Lett. **17**(1), 274 (2025). https://doi.org/10.1007/s40820-025-01764-7
197. J. Li, N. Wu, J. Zhang, H.-H. Wu, K. Pan et al., Machine learning-assisted low-dimensional electrocatalysts design for hydrogen evolution reaction. Nano-Micro Lett. **15**(1), 227 (2023). https://doi.org/10.1007/s40820-023-01192-5
198. I.B. Obot, D.D. MacDonald, Z.M. Gasem, Density functional theory (DFT) as a powerful tool for designing new organic corrosion inhibitors. Part 1: an overview. Corros. Sci. **99**, 1–30 (2015). https://doi.org/10.1016/j.corsci.2015.01.037
199. P. Liu, Q. Xu, Q. Zhang, Y. Huang, Y. Liu et al., A new insight into corrosion inhibition mechanism of the corrosion inhibitors: review on DFT and MD simulation. J. Adhes. Sci. Technol. **38**(10), 1563–1584 (2024). https://doi.org/10.1080/01694243.2023.2272318
200. E.E. Ebenso, C. Verma, L.O. Olasunkanmi, E.D. Akpan, D.K. Verma et al., Molecular modelling of compounds used for corrosion inhibition studies: a review. Phys. Chem. Chem. Phys. **23**(36), 19987–20027 (2021). https://doi.org/10.1039/d1cp00244a
201. N.U.S. Riyaz, M. Khaled, A. Alshami, I.A. Hussein, Machine learning-driven prediction of corrosion inhibitor efficiency: emerging algorithms, challenges, and future outlooks. Arab. J. Sci. Eng. **50**(24), 21329–21344 (2025). https://doi.org/10.1007/s13369-025-10386-5
202. H. Gong, L. Ma, D. Liu, D. Zhang, AI-driven discovery of high-performance corrosion inhibitors using a BERT-GPT

 https://doi.org/10.1007/s40820-026-02178-9

framework for molecular generation. Corros. Sci. **257**, 113327 (2025). https://doi.org/10.1016/j.corsci.2025.113327

203. Y. Lin, Z. Mai, H. Liang, Y. Li, G. Yang et al., Dendrite-free Zn anode enabled by anionic surfactant-induced horizontal growth for highly-stable aqueous Zn-ion pouch cells. Energy Environ. Sci. **16**(2), 687–697 (2023). https://doi.org/10.1039/d2ee03528f
204. R. Risheek, J. Aneesh, N. Gobinath, R. Radha, Investigation on corrosion inhibitors for zinc batteries: sodium sulphate. Mater. Today Proc. (2023). https://doi.org/10.1016/j.matpr.2023.03.108
205. Z. Liang, C. Li, D. Zuo, L. Zeng, T. Ling et al., Achieving stable Zn metal anode through novel interface design with multifunctional electrolyte additive. Energy Storage Mater. **63**, 102980 (2023). https://doi.org/10.1016/j.ensm.2023.102980
206. H. Li, Y. Gan, J. Zeng, M. Lv, B. Shang et al., Unveiling the mechanism of ultra-low-dose and ultra-high corrosion inhibition additive for enhancing zinc anode performance. Corros. Sci. **224**, 111544 (2023). https://doi.org/10.1016/j.corsci.2023.111544
207. H. Cen, Y. Gao, S. He, Z. Peng, C. Wu et al., Synergistic effect of surfactant and 1, 10-decanedithiol as corrosion inhibitor for zinc anode in alkaline electrolyte of zinc-air batteries. J. Colloid Interface Sci. **659**, 160–177 (2024). https://doi.org/10.1016/j.jcis.2023.12.142
208. D.-Q. Cai, H. Cheng, J.-L. Yang, H. Liu, T. Xiao et al., Understanding the structure–activity relationship of additives for durable Zn metal batteries: a case study of aromatic molecules. Energy Environ. Sci. **17**(21), 8349–8359 (2024). https://doi.org/10.1039/d4ee03232b
209. J. Zhang, Y. Liu, Y. Wang, Z. Zhu, Z. Yang, Zwitterionic organic multifunctional additive stabilizes electrodes for reversible aqueous Zn-ion batteries. Adv. Funct. Mater. **34**(34), 2401889 (2024). https://doi.org/10.1002/adfm.202401889
210. S. Mehta, S. Kaur, M. Singh, M. Kumar, K. Kumar et al., Unleashing ultrahigh capacity and lasting stability: aqueous zinc-sulfur batteries. Adv. Energy Mater. **14**(27), 2401515 (2024). https://doi.org/10.1002/aenm.202401515
211. R. Han, T. Jiang, Z. Wang, R. Xue, X. Liu et al., Reconfiguring Zn^{2+} solvation network and interfacial chemistry of Zn metal anode with molecular engineered crown ether additive. Adv. Funct. Mater. **35**(2), 2412255 (2025). https://doi.org/10.1002/adfm.202412255
212. Y. Shang, V. Kundi, I. Pal, H.N. Kim, H. Zhong et al., Highly potent and low-volume concentration additives for durable aqueous zinc batteries: machine learning-enabled performance rationalization. Adv. Mater. **36**(9), 2309212 (2024). https://doi.org/10.1002/adma.202309212
213. B. Shi, R. Meng, X. Jiang, Y. Liu, H. Wang et al., A highly stable zinc anode protected by a corrosion inhibitor for seawater-based zinc-ion batteries. J. Energy Chem. **97**, 332–341 (2024). https://doi.org/10.1016/j.jechem.2024.05.050
214. X. Xiao, X. Ye, Z. Wu, X. Wu, J. Yu et al., Trace small molecular/nano-colloidal multiscale electrolyte additives enable ultra-long lifespan of zinc metal anodes. Adv. Mater. **36**(38), 2408706 (2024). https://doi.org/10.1002/adma.202408706
215. X. Sun, X. Lv, M. Zhang, K. Shi, Z. Li et al., Construction of selective ion transport polymer at anode–electrolyte interface for stable aqueous zinc-ion batteries. ACS Nano **18**(11), 8452–8462 (2024). https://doi.org/10.1021/acsnano.3c13127
216. F. Wang, W. Liang, X. Liu, T. Yin, Z. Chen et al., A bifunctional electrolyte additive features preferential coordination with iodine toward ultralong-life zinc–iodine batteries. Adv. Energy Mater. **14**(21), 2400110 (2024). https://doi.org/10.1002/aenm.202400110
217. X. Gu, Y. Du, X. Ren, F. Ma, X. Zhang et al., Shielding-anchoring double protection tactics of imidazo [1, 2-b] pyridazine additive for ultrastable zinc anode. Adv. Funct. Mater. **34**(25), 2316541 (2024). https://doi.org/10.1002/adfm.202316541
218. B. Ma, K. Zhang, L. Li, R. Jia, B. Wang et al., Navigating highly reversible Zn metal anodes *via* a multifunctional corrosion inhibitor-inspired electrolyte additive. Chem. Eng. J. **500**, 157307 (2024). https://doi.org/10.1016/j.cej.2024.157307
219. H. Li, Y. Gan, X. Chen, J. Wang, T. Ling et al., New strategy for zinc anode corrosion protection: development of a benzothiazole-based inhibitor and its optimization for battery performance. Corros. Sci. **246**, 112762 (2025). https://doi.org/10.1016/j.corsci.2025.112762
220. W. Shao, C. Li, C. Wang, G. Du, S. Zhao et al., Stabilization of zinc anode by trace organic corrosion inhibitors for long lifespan. Chin. Chem. Lett. **36**(3), 109531 (2025). https://doi.org/10.1016/j.cclet.2024.109531
221. K. Wongrujipairoj, L. Poolnapol, A. Arpornwichanop, S. Suren, S. Kheawhom, Suppression of zinc anode corrosion for printed flexible zinc-air battery. Phys. Status Solidi B **254**(2), 1600442 (2017). https://doi.org/10.1002/pssb.201600442
222. H. He, H. Tong, X. Song, X. Song, J. Liu, Highly stable Zn metal anodes enabled by atomic layer deposited Al_2O_3 coating for aqueous zinc-ion batteries. J. Mater. Chem. A **8**(16), 7836–7846 (2020). https://doi.org/10.1039/d0ta00748j
223. K. Zhao, C. Wang, Y. Yu, M. Yan, Q. Wei et al., Ultrathin surface coating enables stabilized zinc metal anode. Adv. Mater. Interfaces **5**(16), 1800848 (2018). https://doi.org/10.1002/admi.201800848
224. R. Zhao, Y. Yang, G. Liu, R. Zhu, J. Huang et al., Redirected Zn electrodeposition by an anti-corrosion elastic constraint for highly reversible Zn anodes. Adv. Funct. Mater. **31**(2), 2001867 (2021). https://doi.org/10.1002/adfm.202001867
225. M. Schmid, U. Schadeck, M. Willert-Porada, Development of silica based coatings on zinc particles for improved oxidation behavior in battery applications. Surf. Coat. Technol. **310**, 51–58 (2017). https://doi.org/10.1016/j.surfcoat.2016.12.044
226. P. Liang, J. Yi, X. Liu, K. Wu, Z. Wang et al., Highly reversible Zn anode enabled by controllable formation of nucleation sites for Zn-based batteries. Adv. Funct. Mater. **30**(13), 1908528 (2020). https://doi.org/10.1002/adfm.201908528

227. C. Shu, Y. An, Y. Liu, Y. Xu, D. Ren et al., Construction of corrosion-resistant and dendrite-free zinc anode by coating nano-ceriumoxide for highly stable zinc battery. Chem. Eng. J. **509**, 161096 (2025). https://doi.org/10.1016/j.cej.2025.161096
228. H. Yang, J. Wang, P. Zhang, X. Cheng, Q. Guan et al., Dielectric-ion-conductive $ZnNb_2O_6$ layer enabling rapid desolvation and diffusion for dendrite-free Zn metal batteries. J. Energy Chem. **100**, 693–701 (2025). https://doi.org/10.1016/j.jechem.2024.09.010
229. C. Deng, X. Xie, J. Han, Y. Tang, J. Gao et al., A sieve-functional and uniform-porous Kaolin layer toward stable zinc metal anode. Adv. Funct. Mater. **30**(21), 2000599 (2020). https://doi.org/10.1002/adfm.202000599
230. Y.N. Jo, S.H. Kang, K. Prasanna, S.W. Eom, C.W. Lee, Shield effect of polyaniline between zinc active material and aqueous electrolyte in zinc-air batteries. Appl. Surf. Sci. **422**, 406–412 (2017). https://doi.org/10.1016/j.apsusc.2017.06.033
231. H. Wei, X. Hu, X. Zhang, Z. Yu, T. Zhou et al., Zn@C core–shell nanocomposite for rechargeable aqueous Zn// MnO_2 batteries with long lifetime. Energy Technol. **7**(4), 1800912 (2019). https://doi.org/10.1002/ente.201800912
232. J.H. Park, C. Choi, J.B. Park, S. Yu, D.-W. Kim, Fortifying zinc metal anodes against uncontrollable side-reactions and dendrite growth for practical aqueous zinc ion batteries: a novel composition of anti-corrosive and Zn^{2+} regulating artificial protective layer. Adv. Energy Mater. **14**(5), 2302493 (2024). https://doi.org/10.1002/aenm.202302493
233. K. Xia, L. Li, Y. Qiu, J. Weng, S. Shen et al., Graphene acid-enhanced interfacial layers with high Zn^{2+} ion selectivity and desolvation capability for corrosion-resistant Zn-metal anodes. J. Mater. Chem. A **12**(36), 24175–24187 (2024). https://doi.org/10.1039/d4ta03599b
234. V.-C. Ho, H.Y.N. Thi, T.H. Pham, H.-G. Jung, J.H. Kim et al., Functional cellulose interfacial layer on zinc metal for enhanced reversibility in aqueous zinc ion batteries. Chem. Eng. J. **496**, 153845 (2024). https://doi.org/10.1016/j.cej.2024.153845
235. Z. Cai, Y. Ou, J. Wang, R. Xiao, L. Fu et al., Chemically resistant Cu–Zn/Zn composite anode for long cycling aqueous batteries. Energy Storage Mater. **27**, 205–211 (2020). https://doi.org/10.1016/j.ensm.2020.01.032
236. K. Hu, X. Guan, R. Lv, G. Li, Z. Hu et al., Stabilizing zinc metal anodes by artificial solid electrolyte interphase through a surface ion-exchanging strategy. Chem. Eng. J. **396**, 125363 (2020). https://doi.org/10.1016/j.cej.2020.125363
237. T.K.A. Hoang, T.N.L. Doan, K.E.K. Sun, P. Chen, Corrosion chemistry and protection of zinc & zinc alloys by polymer-containing materials for potential use in rechargeable aqueous batteries. RSC Adv. **5**(52), 41677–41691 (2015). https://doi.org/10.1039/c5ra00594a
238. J. Sun, X. Zheng, K. Li, G. Ma, T. Dai et al., Scalable production of hydrogen evolution corrosion resistant Zn-Al alloy anode for electrolytic MnO_2/Zn batteries. Energy Storage Mater. **54**, 570–578 (2023). https://doi.org/10.1016/j.ensm.2022.10.059
239. W. Xie, K. Zhu, H. Yang, W. Yang, Advancements in achieving high reversibility of zinc anode for alkaline zinc-based batteries. Adv. Mater. **36**(5), 2306154 (2024). https://doi.org/10.1002/adma.202306154
240. Y.N. Jo, H.S. Kim, K. Prasanna, P.R. Ilango, W.J. Lee et al., Effect of additives on electrochemical and corrosion behavior of gel type electrodes for Zn-air system. Ind. Eng. Chem. Res. **53**(44), 17370–17375 (2014). https://doi.org/10.1021/ie5027315
241. H.S. Kim, Y.N. Jo, W.J. Lee, K.J. Kim, C.W. Lee, Coating on zinc surface to improve the electrochemical behavior of zinc anodes for zinc-air fuel cells. Electroanalysis **27**(2), 517–523 (2015). https://doi.org/10.1002/elan.201400457
242. Y.N. Jo, K. Prasanna, S.H. Kang, P.R. Ilango, H.S. Kim et al., The effects of mechanical alloying on the self-discharge and corrosion behavior in Zn-air batteries. J. Ind. Eng. Chem. **53**, 247–252 (2017). https://doi.org/10.1016/j.jiec.2017.04.032
243. Y. Da, F. Zhao, J. Shi, Z. Zhang, Effects of ultrafine bismuth powder on the properties of zinc electrodes in zinc-air batteries. J. Electron. Mater. **49**(4), 2479–2490 (2020). https://doi.org/10.1007/s11664-020-07978-2
244. M. Wang, Y. Meng, K. Li, T. Ahmad, N. Chen et al., Toward dendrite-free and anti-corrosion Zn anodes by regulating a bismuth-based energizer. eScience **2**(5), 509–517 (2022). https://doi.org/10.1016/j.esci.2022.04.003
245. X. Zhu, W. Zhang, Z. Peng, L. Pan, B. Li et al., Zinc-tin binary alloy interphase for zinc metal batteries. Chem. Eng. J. **499**, 156521 (2024). https://doi.org/10.1016/j.cej.2024.156521
246. M. Dilshad, T. Li, S.-L. Lee, L. Qin, Next-generation aluminum-air batteries: integrating new materials and technologies for superior performance. ACS Appl. Energy Mater. **8**(6), 3248–3275 (2025). https://doi.org/10.1021/acsaem.4c02926
247. X. Liu, H. Jiao, M. Wang, W.-L. Song, J. Xue et al., Current progresses and future prospects on aluminium–air batteries. Int. Mater. Rev. **67**(7), 734–764 (2022). https://doi.org/10.1080/09506608.2021.2006968
248. R. Harchegani, A. Riahi, Effect of cerium chloride on the self-corrosion and discharge activity of aluminum anode in alkaline aluminum-air batteries. J. Electrochem. Soc. **169**, 030542 (2022)
249. Y. Huang, W. Shi, L. Guo, Q. Zhang, K. Wang et al., Corrosion inhibition of L-tryptophan on Al-5052 anode for Al-air battery with alkaline electrolyte. J. Power. Sources **564**, 232866 (2023). https://doi.org/10.1016/j.jpowsour.2023.232866
250. H.-T. Teng, T.-Y. Lee, Y.-K. Chen, H.-W. Wang, G. Cao, Effect of $Al(OH)_3$ on the hydrogen generation of aluminum–water system. J. Power. Sources **219**, 16–21 (2012). https://doi.org/10.1016/j.jpowsour.2012.06.077
251. B. Liu, T. Lv, A. Zhou, X. Zhu, Z. Lin et al., Aluminum corrosion–passivation regulation prolongs aqueous batteries

 https://doi.org/10.1007/s40820-026-02178-9

life. Nat. Commun. **15**, 2922 (2024). https://doi.org/10.1038/s41467-024-47145-3

252. S. Huo, W. Zhang, Y. Qiang, Y. Zhang, S. Sundarrajan et al., An improved green high-efficiency strategy using an amino acid derivative as electrolyte additives for corrosion inhibition in alkaline Al-air battery. J. Power. Sources **629**, 236064 (2025). https://doi.org/10.1016/j.jpowsour.2024.236064
253. L. Xiong, W. Yang, Y. Zhu, Z. He, L. Li et al., On mechanism of corrosion inhibition of green inhibitor polyvinyl alcohol in aluminum-air batteries. J. Power. Sources **631**, 236233 (2025). https://doi.org/10.1016/j.jpowsour.2025.236233
254. M. El-Alouani, O. Kharbouch, K. Dahmani, M. Galai, N. Dkhireche et al., Probing corrosion protective mechanism of 2- (4-nitrobenzylidene) malononitrile on anode for enhanced alkaline (4 M NaOH) aluminum-air battery performance. J. Alloys Compd. **1010**, 178239 (2025). https://doi.org/10.1016/j.jallcom.2024.178239
255. Y. Wan, Y. Qiang, S. Liu, Y. Gao, Y. Jin et al., Multi-center corrosion inhibition strategy for enhanced interfacial stability and longevity of aluminum-air batteries. Chem. Eng. J. **521**, 166814 (2025). https://doi.org/10.1016/j.cej.2025.166814
256. C. Pan, Z. Wang, S. Cai, Y. Zhu, D. Zhang, Inhibition effect of cashew phenol polyoxyethylene ether on self-corrosion of anode of alkaline aluminum-air batteries. Ind. Crops Prod. **228**, 120925 (2025). https://doi.org/10.1016/j.indcrop.2025.120925
257. Z. Wang, C. Pan, J. Yang, D. Zhang, Z. Xin, Enhanced inhibition for anode self-corrosion in alkaline aluminum-air battery by synergy of cetyltrimethyl ammonium bromide and 8-hydroxyquinoline-5-sulfonic acid. Colloids Surf. A Physicochem. Eng. Aspects **725**, 137506 (2025). https://doi.org/10.1016/j.colsurfa.2025.137506
258. I.B. Obot, A.A. Bahraq, M. Qamar, R. Ahmad, Sustainable additives to mitigate the self-corrosion of aluminium metal in alkaline solution: electrochemical and theoretical investigations. Mater. Today Commun. **42**, 111325 (2025). https://doi.org/10.1016/j.mtcomm.2024.111325
259. A. Perumal, V. Elumalai, M. Perumalsamy, A. Sathyaseelan, R.P. Sivasankaran et al., Complexation chemistry as a corrosion control of aluminum anode in neutral aluminum-based electrochemical energy systems. Energy Storage Mater. **81**, 104540 (2025). https://doi.org/10.1016/j.ensm.2025.104540
260. M.A. Deyab, 1-Allyl-3-methylimidazolium bis(trifluoromethylsulfonyl)imide as an effective organic additive in aluminum-air battery. Electrochim. Acta **244**, 178–183 (2017). https://doi.org/10.1016/j.electacta.2017.05.116
261. D. Gelman, I. Lasman, S. Elfimchev, D. Starosvetsky, Y. Ein-Eli, Aluminum corrosion mitigation in alkaline electrolytes containing hybrid inorganic/organic inhibitor system for power sources applications. J. Power. Sources **285**, 100–108 (2015). https://doi.org/10.1016/j.jpowsour.2015.03.048
262. M.A. Deyab, Effect of nonionic surfactant as an electrolyte additive on the performance of aluminum-air battery. J. Power Sources **412**, 520–526 (2019). https://doi.org/10.1016/j.jpowsour.2018.11.086
263. Y. Liu, H. Zhang, Y. Liu, J. Li, W. Li, Inhibitive effect of quaternary ammonium-type surfactants on the self-corrosion of the anode in alkaline aluminium-air battery. J. Power Sources **434**, 226723 (2019). https://doi.org/10.1016/j.jpowsour.2019.226723
264. C. Hou, S. Chen, Z. Wang, G. Wang, G. Dong, Effect of 6-thioguanine, as an electrolyte additive, on the electrochemical behavior of an Al–air battery. Mater. Corros. **71**(9), 1480–1487 (2020). https://doi.org/10.1002/maco.202011542
265. Y. Nie, J. Gao, E. Wang, L. Jiang, L. An et al., An effective hybrid organic/inorganic inhibitor for alkaline aluminum-air fuel cells. Electrochim. Acta **248**, 478–485 (2017). https://doi.org/10.1016/j.electacta.2017.07.108
266. Q.X. Kang, Y. Wang, X.Y. Zhang, Experimental and theoretical investigation on calcium oxide and L-aspartic as an effective hybrid inhibitor for aluminum-air batteries. J. Alloys Compd. **774**, 1069–1080 (2019). https://doi.org/10.1016/j.jallcom.2018.09.391
267. S. Wu, Q. Zhang, D. Sun, J. Luan, H. Shi et al., Understanding the synergistic effect of alkyl polyglucoside and potassium stannate as advanced hybrid corrosion inhibitor for alkaline aluminum-air battery. Chem. Eng. J. **383**, 123162 (2020). https://doi.org/10.1016/j.cej.2019.123162
268. E. Grishina, D. Gelman, S. Belopukhov, D. Starosvetsky, A. Groysman et al., Improvement of aluminum–air battery performances by the application of flax straw extract. ChemSusChem **9**(16), 2103–2111 (2016). https://doi.org/10.1002/cssc.201600298
269. S. Li, D. Miao, Y. Liu, J. Qu, W. Yan, Constructing composite protective interphase *in situ* for high-performance aluminum-air batteries. J. Power Sources **640**, 236750 (2025). https://doi.org/10.1016/j.jpowsour.2025.236750
270. J. Ma, W. Li, G. Wang, Y. Li, F. Ren et al., Influences of L-cysteine/zinc oxide additive on the electrochemical behavior of pure aluminum in alkaline solution. J. Electrochem. Soc. **165**, A266 (2018). https://doi.org/10.1149/2.1071802jes
271. C. Zhu, H. Yang, A. Wu, D. Zhang, L. Gao et al., Modified alkaline electrolyte with 8-hydroxyquinoline and ZnO complex additives to improve Al-air battery. J. Power. Sources **432**, 55–64 (2019). https://doi.org/10.1016/j.jpowsour.2019.05.077
272. A.P. Sinha, T.S. Thomas, D. Mandal, An inorganic-organic protective anode interface towards high-performance Al-air battery. Energy Storage Mater. **63**, 102988 (2023). https://doi.org/10.1016/j.ensm.2023.102988
273. P. Zhang, W. Peng, J. Miao, G. Ren, Y. Wang et al., Evolution of the solid-liquid interface using a novel hybrid corrosion inhibitor to improve Al-air battery performance. J. Energy Chem. **104**, 69–78 (2025). https://doi.org/10.1016/j.jechem.2024.12.041
274. Y. Gao, Q. Zhao, W. Liu, F. Guo, Y. Yin et al., A green electrolyte additive based on *To ona sinensis* extract for enhanced performance of alkaline Al-air battery. Corros. Sci. **252**, 112952 (2025). https://doi.org/10.1016/j.corsci.2025.112952
275. L. Guo, Y. Huang, A. Su, T. Shang, M. Qu et al., Boosting the performance of alkaline Al-air batteries by interfacial

reconstruction *via* N-doped carbon quantum dots. J. Energy Storage **127**, 117136 (2025). https://doi.org/10.1016/j.est.2025.117136

276. Y. Li, Z. Guo, W. Zhang, S. Ramakrishna, Y. Qiang, Interfacial regulation of aluminum-air batteries by biomass carbon quantum dots: corrosion inhibition and electrochemical enhancement. J. Mater. Sci. Technol. **255**, 318–328 (2026). https://doi.org/10.1016/j.jmst.2025.08.029
277. M. Wei, K. Wang, Y. Zuo, L. Zhong, A. Züttel et al., A Prussian-blue bifunctional interface membrane for enhanced flexible Al–air batteries. Adv. Funct. Mater. **33**(37), 2302243 (2023). https://doi.org/10.1002/adfm.202302243
278. Y. Chung, S. Lee, S. Yoon, W.-K. Choi, S.-K. Jeong, Mitigating anodic corrosion in aluminum–air batteries: effects of alkali metal cation size on electrochemical performance. Appl. Surf. Sci. **681**, 161533 (2025). https://doi.org/10.1016/j.apsusc.2024.161533
279. M. El-Alouani, O. Kharbouch, K. Dahmani, M. Galai, N. Dkhireche et al., Corrosion protection mechanism of maltoheptaose on aluminum anodes for enhanced performance in alkaline aluminum-air batteries. J. Energy Storage **131**, 117538 (2025). https://doi.org/10.1016/j.est.2025.117538
280. L. Li, L. He, N. Han, Y. Wang, M. Wang et al., Effects ofl-cysteine inhibitor on the electrochemical properties of an aluminum alloy anode used for an aluminum-air battery. ChemistrySelect **10**(12), e202405409 (2025). https://doi.org/10.1002/slct.202405409
281. H. Moghanni-Bavil-Olyaei, J. Arjomandi, Performance of Al–1Mg–1Zn–0.1Bi–0.02In as anode for the Al–AgO battery. RSC Adv. **5**(111), 91273–91279 (2015). https://doi.org/10.1039/c5ra15567c
282. H. Xiong, X. Yin, Y. Yan, Y. Dai, S. Fan et al., Corrosion and discharge behaviors of Al-Mg-Sn-Ga-In in different solutions. J. Mater. Eng. Perform. **25**(8), 3456–3464 (2016). https://doi.org/10.1007/s11665-016-2172-7
283. R.N. Mutlu, B. Yazıcı, Copper-deposited aluminum anode for aluminum-air battery. J. Solid State Electrochem. **23**(2), 529–541 (2019). https://doi.org/10.1007/s10008-018-4146-1
284. J. Ren, J. Ma, J. Zhang, C. Fu, B. Sun, Electrochemical performance of pure Al, Al–Sn, Al–Mg and Al–Mg–Sn anodes for Al-air batteries. J. Alloys Compd. **808**, 151708 (2019). https://doi.org/10.1016/j.jallcom.2019.151708
285. E. Ghali, in Corrosion of Magnesium Alloys, Woodhead Publishing Series in Metals and Surface Engineering(Woodhead Publishing, Cambridge, 2011), pp. 66–114. https://doi.org/10.1533/9780857091413.1.66
286. S.H. Salleh, S. Thomas, J.A. Yuwono, K. Venkatesan, N. Birbilis, Enhanced hydrogen evolution on Mg $(OH)_2$ covered Mg surfaces. Electrochim. Acta **161**, 144–152 (2015). https://doi.org/10.1016/j.electacta.2015.02.079
287. J. Ma, G. Wang, Y. Li, F. Ren, A.A. Volinsky, Electrochemical performance of Mg-air batteries based on AZ series magnesium alloys. Ionics **25**(5), 2201–2209 (2019). https://doi.org/10.1007/s11581-018-2705-1
288. J. Ma, G. Wang, Y. Li, C. Qin, F. Ren, Electrochemical investigations on AZ series magnesium alloys as anode materials in a sodium chloride solution. J. Mater. Eng. Perform. **28**(5), 2873–2880 (2019). https://doi.org/10.1007/s11665-019-04035-w
289. Y. Zhou, X. Lu, M.L. Zheludkevich, F. Wang, Tailoring corrosion and discharge performance of Mg anode by corrosion inhibitor. Electrochim. Acta **436**, 141471 (2022). https://doi.org/10.1016/j.electacta.2022.141471
290. A. Atrens, X. Chen, Z. Shi, Mg corrosion: recent progress. Corros. Mater. Degrad. **3**(4), 566–597 (2022). https://doi.org/10.3390/cmd3040031
291. M.A. Deyab, Decyl glucoside as a corrosion inhibitor for magnesium–air battery. J. Power. Sources **325**, 98–103 (2016). https://doi.org/10.1016/j.jpowsour.2016.06.006
292. J. Xu, Q. Yang, C. Huang, M.S. Javed, M.K. Aslam et al., Influence of additives fluoride and phosphate on the electrochemical performance of Mg–MnO_2 battery. J. Appl. Electrochem. **47**(7), 767–775 (2017). https://doi.org/10.1007/s10800-017-1074-1
293. Y. Zhao, G. Huang, C. Zhang, C. Peng, F. Pan, Effect of phosphate and vanadate as electrolyte additives on the performance of Mg-air batteries. Mater. Chem. Phys. **218**, 256–261 (2018). https://doi.org/10.1016/j.matchemphys.2018.07.037
294. Y. Li, J. Ma, G. Wang, F. Ren, Y. Zhu et al., Investigation of sodium phosphate and sodium dodecylbenzenesulfonate as electrolyte additives for AZ91 magnesium-air battery. J. Electrochem. Soc. **165**, A1713 (2018). https://doi.org/10.1149/2.0581809jes
295. W. Zhao, R. Wan, X. Sun, Z. Wang, Z. Gong et al., Inhibition mechanism of phosphorus-doped carbon quantum dots on anodic corrosion in neutral Mg-air batteries. J. Alloys Compd. **1037**, 182609 (2025). https://doi.org/10.1016/j.jallcom.2025.182609
296. P. Jiang, K. Li, R. Hou, D. Mei, J. Yang et al., Boosting discharge performance of primary Mg-air batteries *via* adopting sodium citrate as electrolyte to suppress self-corrosion of Mg anode during discharge. Chem. Eng. J. **511**, 162200 (2025). https://doi.org/10.1016/j.cej.2025.162200
297. P. Wang, J. Li, Y. Guo, Z. Yang, F. Xia et al., Effect of tin addition on microstructure and electrochemical properties of rolled AZ61-Sn magnesium anodic materials. Rare Met. **30**(6), 639–643 (2011). https://doi.org/10.1007/s12598-011-0442-y
298. G. Williams, H.A. Dafydd, H.N. McMurray, N. Birbilis, The influence of arsenic alloying on the localised corrosion behaviour of magnesium. Electrochim. Acta **219**, 401–411 (2016). https://doi.org/10.1016/j.electacta.2016.10.006
299. R.L. Liu, J.R. Scully, G. Williams, N. Birbilis, Reducing the corrosion rate of magnesium *via* microalloying additions of group 14 and 15 elements. Electrochim. Acta **260**, 184–195 (2018). https://doi.org/10.1016/j.electacta.2017.11.062
300. R.L. Liu, J.R. Scully, G. Williams, N. Birbilis, Reducing the corrosion rate of magnesium via microalloying additions of group 14 and 15 elements. Electrochim. Acta **260**, 184–195 (2018). https://doi.org/10.1016/j.electacta.2017.11.062

 https://doi.org/10.1007/s40820-026-02178-9

301. R.L. Liu, Z.R. Zeng, J.R. Scully, G. Williams, N. Birbilis, Simultaneously improving the corrosion resistance and strength of magnesium *via* low levels of Zn and Ge additions. Corros. Sci. **140**, 18–29 (2018). https://doi.org/10.1016/j.corsci.2018.06.027
302. T.W. Cain, C.F. Glover, J.R. Scully, The corrosion of solid solution Mg-Sn binary alloys in NaCl solutions. Electrochim. Acta **297**, 564–575 (2019). https://doi.org/10.1016/j.electacta.2018.11.118
303. M. Deng, D. Höche, S.V. Lamaka, D. Snihirova, M.L. Zheludkevich, Mg-Ca binary alloys as anodes for primary Mg-air batteries. J. Power Sources **396**, 109–118 (2018). https://doi.org/10.1016/j.jpowsour.2018.05.090
304. Q. Lu, A. Omar, M. Hantusch, S. Oswald, L. Ding et al., Dendrite-free and corrosion-resistant sodium metal anode for enhanced sodium batteries. Appl. Surf. Sci. **600**, 154168 (2022). https://doi.org/10.1016/j.apsusc.2022.154168
305. P. Phogat, S. Rawat, S. Dey, M. Wan, Advancements and challenges in sodium-ion batteries: a comprehensive review of materials, mechanisms, and future directions for sustainable energy storage. J. Alloys Compd. **1020**, 179544 (2025). https://doi.org/10.1016/j.jallcom.2025.179544
306. M. Li, Elevating the practical application of sodium-ion batteries through advanced characterization studies on cathodes. Energies **16**(24), 8004 (2023). https://doi.org/10.3390/en16248004
307. J.-Y. Hwang, S.-T. Myung, Y.-K. Sun, Sodium-ion batteries: present and future. Chem. Soc. Rev. **46**(12), 3529–3614 (2017). https://doi.org/10.1039/c6cs00776g
308. L.-F. Zhao, Z. Hu, W.-H. Lai, Y. Tao, J. Peng et al., Hard carbon anodes: fundamental understanding and commercial perspectives for Na-ion batteries beyond Li-ion and K-ion counterparts. Adv. Energy Mater. **11**, 2002704 (2021). https://doi.org/10.1002/aenm.202002704
309. H. Huang, X. Wu, Y. Gao, Z. Li, W. Wang et al., Polyanionic cathode materials: a comparison between Na-ion and K-ion batteries. Adv. Energy Mater. **14**(14), 2304251 (2024). https://doi.org/10.1002/aenm.202304251
310. R. Shang, Y. Ma, K. Anduaga-Quiros, G. Briseno, Y. Ning et al., Powering the future: unveiling the potential of Na, K, and Mg solid-state batteries. Nanomaterials **15**(11), 859 (2025). https://doi.org/10.3390/nano15110859
311. S. Sandhiya, P. Elumalai, Stability challenges in non-aqueous Li–O_2 batteries and their protective strategies: a comprehensive review on electrode and electrolyte engineering. J. Mater. Chem. A **14**(5), 2565–2612 (2026). https://doi.org/10.1039/d5ta06153a
312. C.-L. Liu, S.-H. Luo, H.-B. Huang, Y.-C. Zhai, Z.-W. Wang, Layered potassium-deficient P2- and P3-type cathode materials $KxMnO_2$ for K-ion batteries. Chem. Eng. J. **356**, 53–59 (2019). https://doi.org/10.1016/j.cej.2018.09.012
313. Y. Kim, G. Oh, J. Lee, H. Kang, H. Kim et al., Stabilization of layered-type potassium manganese oxide cathode with fluorine treatment for high-performance K-ion batteries. J. Power. Sources **588**, 233729 (2023). https://doi.org/10.1016/j.jpowsour.2023.233729
314. X.-C. Wang, L.-K. Zhao, Z.-M. Liu, Q. Gu, X.-W. Gao et al., Interface chemistry engineering toward layer-structured oxide for potassium-ion batteries. ACS Energy Lett. **10**(1), 48–57 (2025). https://doi.org/10.1021/acsenergylett.4c03191
315. B. Xiao, T. Rojo, X. Li, Hard carbon as sodium-ion battery anodes: progress and challenges. ChemSusChem **12**(1), 133–144 (2019). https://doi.org/10.1002/cssc.201801879
316. F.N. Shafiee, S.A. Mohd Noor, M.A.A. Mohd Abdah, S.H. Jamal, A. Samsuri, Recent progress on hard carbon and other anode materials for sodium-ion batteries. Heliyon **10**(8), e29512 (2024). https://doi.org/10.1016/j.heliyon.2024.e29512
317. F. Xie, Z. Xu, Z. Guo, M.-M. Titirici, Hard carbons for sodium-ion batteries and beyond. Progr. Energy **2**, 042002 (2020). https://doi.org/10.1088/2516-1083/aba5f5
318. Z. Wu, J. Zou, S. Shabanian, K. Golovin, J. Liu, The roles of electrolyte chemistry in hard carbon anode for potassium-ion batteries. Chem. Eng. J. **427**, 130972 (2022). https://doi.org/10.1016/j.cej.2021.130972
319. H. Zhang, H. Wang, W. Li, Y. Wei, B. Wen et al., Enabling high-performance potassium-ion batteries by manipulating interfacial chemistry. Adv. Funct. Mater. **34**(21), 2312368 (2024). https://doi.org/10.1002/adfm.202312368
320. J. Wei, P. Zhang, Y. Liu, M. Zhu, T. Dai et al., Wide-voltage-window amphiphilic supramolecule excluded-volume electrolytes for ultra-durable full-cell aqueous potassium-ion batteries. Chem. Eng. J. **459**, 141623 (2023). https://doi.org/10.1016/j.cej.2023.141623
321. W. Lee, H. Li, D. Biswas, Z. Du, W. Ren et al., A cost-effect Na and K ion-conducting amorphous covalent organic framework with high ion conductivity. ACS Appl. Energy Mater. **8**(1), 569–580 (2025). https://doi.org/10.1021/acsaem.4c02760
322. H. Wang, D. Zhai, F. Kang, Solid electrolyte interphase (SEI) in potassium ion batteries. Energy Environ. Sci. **13**(12), 4583–4608 (2020). https://doi.org/10.1039/d0ee01638a
323. T. Hosaka, T. Matsuyama, K. Kubota, S. Yasuno, S. Komaba, Development of KPF_6/KFSA binary-salt solutions for long-life and high-voltage K-ion batteries. ACS Appl. Mater. Interfaces **12**(31), 34873–34881 (2020). https://doi.org/10.1021/acsami.0c08002
324. N.S. Katorova, S.S. Fedotov, D.P. Rupasov, N.D. Luchinin, B. Delattre et al., Effect of concentrated diglyme-based electrolytes on the electrochemical performance of potassium-ion batteries. ACS Appl. Energy Mater. **2**(8), 6051–6059 (2019). https://doi.org/10.1021/acsaem.9b01173
325. M. Salado, M. Amores, C. Pozo-Gonzalo, M. Forsyth, S. Lanceros-Méndez, Advanced and sustainable functional materials for potassium-ion batteries. Energy Mater. (2023). https://doi.org/10.20517/energymater.2023.36
326. R. Verma, P.N. Didwal, J.-Y. Hwang, C.-J. Park, Recent progress in electrolyte development and design strategies for next-generation potassium-ion batteries. Batter. Supercaps

4(9), 1428–1450 (2021). https://doi.org/10.1002/batt.202100029

327. S. Lv, J. Wang, Y. Zhai, Y. Chen, J. Yang et al., Lithium-ion dynamic interface engineering of nano-charged composite polymer electrolytes for solid-state lithium-metal batteries. Nano-Micro Lett. **18**(1), 46 (2025). https://doi.org/10.1007/s40820-025-01899-7
328. Y. Tian, T. Shi, W.D. Richards, J. Li, J.C. Kim et al., Compatibility issues between electrodes and electrolytes in solid-state batteries. Energy Environ. Sci. **10**(5), 1150–1166 (2017). https://doi.org/10.1039/c7ee00534b
329. N. Boaretto, I. Garbayo, S. Valiyaveettil-SobhanRaj, A. Quintela, C. Li et al., Lithium solid-state batteries: state-of-the-art and challenges for materials, interfaces and processing. J. Power. Sources **502**, 229919 (2021). https://doi.org/10.1016/j.jpowsour.2021.229919
330. M. Liu, A. Song, X. Zhang, J. Wang, Y. Fan et al., Interfacial lithium-ion transportation in solid-state batteries: challenges and prospects. Nano Energy **136**, 110749 (2025). https://doi.org/10.1016/j.nanoen.2025.110749
331. S. Liu, L. Zhou, K. Neyts, From promise to production: strategy for halide-based all-solid-state battery pilot lines. Adv. Energy Mater. **16**(4), e05286 (2026). https://doi.org/10.1002/aenm.202505286
332. J. Huang, C. Li, D. Jiang, J. Gao, L. Cheng et al., Solid-state electrolytes for lithium metal batteries: state-of-the-art and perspectives. Adv. Funct. Mater. **35**, 2411171 (2025). https://doi.org/10.1002/adfm.202411171
333. E. Biçer, A. Aksöz, R. Bakar, Ç. Odabaşı, W. Vonk et al., Solid-state batteries: chemistry, battery, and thermal management system, battery assembly, and applications: a critical review. Batteries **11**(6), 212 (2025). https://doi.org/10.3390/batteries11060212
334. A. Machín, C. Morant, F. Márquez, Advancements and challenges in solid-state battery technology: an in-depth review of solid electrolytes and anode innovations. Batteries **10**(1), 29 (2024). https://doi.org/10.3390/batteries10010029
335. K. Kerman, A. Luntz, V. Viswanathan, Y.-M. Chiang, Z. Chen, Practical challenges hindering the development of solid state Li-ion batteries. J. Electrochem. Soc. **164**, A1731 (2017)
336. H. Chen, Research on the application and the interface problem of solid-state batteries. Highlights Sci. Eng. Technol. **157**, 33–38 (2025). https://doi.org/10.54097/kkdyst24
337. J. Zhu, J. Zhao, Y. Xiang, M. Lin, H. Wang et al., Chemo-mechanical failure mechanism study in NASICON-type $Li_{1.3}Al_{0.3}Ti_{1.7}(PO_4)_3$ solid-state lithium batteries. Chem. Mater. **32**(12), 4998–5008 (2020). https://doi.org/10.1021/acs.chemmater.9b05295
338. P. Du, Q. Song, Z. Ning, H. Xie, D. Wang et al., A metal oxide coating to suppress the corrosion of aluminum current collectors for high-voltage LiTFSI-based batteries. Energy Storage Mater. **82**, 104569 (2025). https://doi.org/10.1016/j.ensm.2025.104569
339. D. Yang, Y. Liu, T. Yang, R. Fang, Z. Xiao et al., Anti-corrosion lithium anode interface by $Li_{6.4}La_3Zr_{1.4}Ta_{0.6}O_{12}$ modified buffer layer for stable cycling of room-temperature solid-state lithium metal batteries. J. Colloid Interface Sci. **689**, 137225 (2025). https://doi.org/10.1016/j.jcis.2025.03.014
340. A. Morchhale, Z. Tang, C. Yu, R. Farahati, J.-H. Kim, Coating materials and processes for cathodes in sulfide-based all solid-state batteries. Curr. Opin. Electrochem. **39**, 101251 (2023). https://doi.org/10.1016/j.coelec.2023.101251
341. Z. Zhang, X. Xue, Z. Mo, X. Lei, X. Xie et al., Silicon-based anodes for solid-state batteries: challenges, opportunities, and multiscale strategies. RSC Adv. **15**(40), 33561–33585 (2025). https://doi.org/10.1039/d5ra05126f
342. K. Tuo, C. Sun, S. Liu, Recent progress in and perspectives on emerging halide superionic conductors for all-solid-state batteries. Electrochem. Energy Rev. **6**(1), 17 (2023). https://doi.org/10.1007/s41918-023-00179-5
343. J. Wu, J. Li, X. Yao, Exploring the potential of halide electrolytes for next-generation all-solid-state lithium batteries. Adv. Funct. Mater. **35**(10), 2416671 (2025). https://doi.org/10.1002/adfm.202416671
344. T.A. Manfo, M.E. Şahin, D.B. Altuntaş, Development of quasi-flexible solid polymer blend electrolytes and boron carbide reinforced tea waste electrodes for supercapacitors. J. Energy Storage **111**, 115442 (2025). https://doi.org/10.1016/j.est.2025.115442
345. M. Kabir, D.E. Demirocak, Degradation mechanisms in Li-ion batteries: a state-of-the-art review. Int. J. Energy Res. **41**, 1963–1986 (2017). https://doi.org/10.1002/er.3762
346. J. Cabana, B.J. Kwon, L. Hu, Mechanisms of degradation and strategies for the stabilization of cathode–electrolyte interfaces in Li-ion batteries. Acc. Chem. Res. **51**(2), 299–308 (2018). https://doi.org/10.1021/acs.accounts.7b00482
347. I.B. Mansir, P.C. Okonkwo, Component degradation in lithium-ion batteries and their sustainability: a concise overview. Sustainability **17**(3), 1000 (2025). https://doi.org/10.3390/su17031000
348. Y. Zhang, Z.-Z. Shen, Y. Zhang, M. Niu, L. Dong et al., Insights into the electrolyte hydrolysis and its impacts on the interfacial chemistry of a Li^+-intercalated anode during high-temperature calendar aging. Angew. Chem. Int. Ed. **64**(15), e202425491 (2025). https://doi.org/10.1002/anie.202425491
349. M. Liu, J. Vatamanu, X. Chen, L. Xing, K. Xu et al., Hydrolysis of $LiPF_6$-containing electrolyte at high voltage. ACS Energy Lett. **6**(6), 2096–2102 (2021). https://doi.org/10.1021/acsenergylett.1c00707
350. Z. Zhang, S. Said, A.J. Lovett, R. Jervis, P.R. Shearing et al., The influence of cathode degradation products on the anode interface in lithium-ion batteries. ACS Nano **18**(13), 9389–9402 (2024). https://doi.org/10.1021/acsnano.3c10208
351. S. Kim, S.O. Park, M.-Y. Lee, J.-A. Lee, I. Kristanto et al., Stable electrode–electrolyte interfaces constructed by fluorine- and nitrogen-donating ionic additives for high-performance lithium metal batteries. Energy Storage Mater. **45**, 1–13 (2022). https://doi.org/10.1016/j.ensm.2021.10.031
352. T. Deng, Q. Han, H. Liu, J. Hu, J. Wang et al., Fluorine- and nitrogen-donating gel polymer electrolytes enabling LiF- and Li_3N-enriched SEI for stabilizing lithium metal anodes. ACS

Sustain. Chem. Eng. **12**(1), 192–204 (2024). https://doi.org/10.1021/acssuschemeng.3c05371

353. R. Zhang, C. Li, B. Yang, R. Cao, Y. Chen et al., Fluorinated gel polymer electrolytes for high performance lithium metal batteries: a mechanism analysis and systematic review. Sci. China Chem. **68**(10), 4712–4732 (2025). https://doi.org/10.1007/s11426-025-2593-1
354. X. Zhao, Q. Liu, W. He, D. Mu, L. Li et al., Uniform Al_2O_3 coating for improved cycling stability of O_3 type sodium-ion batteries cathode: mechanisms and performance insights. J. Energy Storage **131**, 117548 (2025). https://doi.org/10.1016/j.est.2025.117548
355. E. Hüger, L. Riedel, J. Zhu, J. Stahn, P. Heitjans et al., Lithium niobate for fast cycling in Li-ion batteries: review and new experimental results. Batteries **9**(5), 244 (2023). https://doi.org/10.3390/batteries9050244
356. P. Wang, H. Qing, R. Zhang, W. Li, Fluorine-free electrolytes for sustainable lithium batteries: a review. npj Mater. Sustain. **3**, 32 (2025). https://doi.org/10.1038/s44296-025-00074-8
357. A. Raulo, S. Lateef, H. McRay, K.R. Ilancheran, F. Albano et al., Fluorinated electrolytes for lithium–sulfur and beyond-lithium metal–sulfur batteries. Energy Storage Mater. **82**, 104600 (2025). https://doi.org/10.1016/j.ensm.2025.104600
358. S. Priyadarsini, A.P. Das, Analytical and structural characterization of waste lithium-ion batteries for their effective recycling strategy. Environ. Chem. Ecotoxicol. **7**, 182–191 (2025). https://doi.org/10.1016/j.enceco.2024.12.004
359. M. Rezaei, A. Nekahi, A.K. M R, A. Nizami, X. Li et al., A review of lithium-ion battery recycling for enabling a circular economy. J. Power. Sources **630**, 236157 (2025). https://doi.org/10.1016/j.jpowsour.2024.236157
360. O. Kwon, J. Kang, S. Kim, T. Yoon, Impact of electrolyte decomposition on copper corrosion in Li_6PS_5Cl-based all-solid-state batteries. Adv. Funct. Mater. **35**(20), 2420474 (2025). https://doi.org/10.1002/adfm.202420474
361. P. Pahari, S. Ramakrishnan, Interfacial passivation in anodeless solid-state batteries enabled by a porous, Li_2O-rich interphase generated from a corrosion-conversion reaction. ACS Electrochem. **1**(11), 2364–2375 (2025). https://doi.org/10.1021/acselectrochem.5c00203
362. A.T. Dąbrowska, N. Izdebska, E. Żero, M. Smolarek, D. Jastrzębski et al., Corrosion investigation of current collector in solid state lithium sulphur batteries. Appl. Phys. A **131**(3), 173 (2025). https://doi.org/10.1007/s00339-024-08187-y
363. A. Mauger, C. Julien, A. Paolella, M. Armand, K. Zaghib, Recent progress on organic electrodes materials for rechargeable batteries and supercapacitors. Materials **12**(11), 1770 (2019). https://doi.org/10.3390/ma1211770
364. M. Li, R.P. Hicks, Z. Chen, C. Luo, J. Guo et al., Electrolytes in organic batteries. Chem. Rev. **123**(4), 1712–1773 (2023). https://doi.org/10.1021/acs.chemrev.2c00374
365. S. Kim, J.H. Lee, T. Lim, M.J. Lee, J. Panda et al., Biodegradable redox-active organic radical cathode material for lithium-ion batteries. ACS Appl. Energy Mater. **8**(17), 12929–12939 (2025). https://doi.org/10.1021/acsaem.5c02086
366. Y. Zhang, Y. Fu, Y. Lv, Z. Song, L. Gan et al., Carbonyl-rich organic cathodes for advanced aqueous batteries: progress and perspectives. Chem. Commun. **61**(76), 14611–14624 (2025). https://doi.org/10.1039/d5cc04203h
367. X. Chen, H. Zhang, C. Luo, C. Gao, C. Sun et al., Game changers: scavenging materials for nonaqueous rechargeable battery applications. eScience **5**(5), 100411 (2025). https://doi.org/10.1016/j.esci.2025.100411
368. D.H. Jeon, S. Kim, R. Hempelmann, Degradation factors of commercial lithium-ion batteries. Appl. Phys. Rev. **12**(3), 031320 (2025). https://doi.org/10.1063/5.0255290
369. W. Li, C. Shen, Z. Wu, Y. Wang, D. Ma et al., Pyridine functionalized phenothiazine derivatives as low-cost and stable hole-transporting material for perovskite solar cells. Mater. Today Energy **23**, 100903 (2022). https://doi.org/10.1016/j.mtener.2021.100903
370. T. Patranika, K. Märker, S. Paul, A.J. Naylor, J. Mindemark et al., Interaction of boron-based cross-linkers with polymer binders for silicon anodes in lithium-ion batteries. ACS Appl. Polym. Mater. **6**(20), 12429–12440 (2024). https://doi.org/10.1021/acsapm.4c01523
371. S. Muench, A. Wild, C. Friebe, B. Häupler, T. Janoschka et al., Polymer-based organic batteries. Chem. Rev. **116**(16), 9438–9484 (2016). https://doi.org/10.1021/acs.chemrev.6b00070
372. X. Pan, W. Li, X. Lai, Y. Liang, Z. Jiang et al., Electrolyte design strategies for next-generation supercapacitors and metal-ion batteries. Emerg. Mater. **8**(8), 6843–6917 (2025). https://doi.org/10.1007/s42247-025-01284-5
373. R.-S. Kühnel, M. Lübke, M. Winter, S. Passerini, A. Balducci, Suppression of aluminum current collector corrosion in ionic liquid containing electrolytes. J. Power Sources **214**, 178–184 (2012). https://doi.org/10.1016/j.jpowsour.2012.04.054
374. K. Matsumoto, K. Inoue, K. Nakahara, R. Yuge, T. Noguchi et al., Suppression of aluminum corrosion by using high concentration LiTFSI electrolyte. J. Power Sources **231**, 234–238 (2013). https://doi.org/10.1016/j.jpowsour.2012.12.028
375. I. Stoševski, A. Bonakdarpour, S.R. Smith, A. Jacobs, B. Way et al., Corrosion of lithium-ion battery cylindrical cell hardware: understanding the mechanisms and exploring effective solutions. J. Electrochem. Soc. **171**, 081502 (2024). https://doi.org/10.1149/1945-7111/ad6713
376. R. Amin, U. Nisar, M.M. Rahman, M. Dixit, A. Abouimrane et al., Prospects of polymer coatings for all solid-state and emerging Li-ion batteries. J. Mater. Chem. A **12**(24), 14186–14205 (2024). https://doi.org/10.1039/d4ta01061b
377. C. Ren, Y. Dong, Y. Lei, High-voltage cathode materials for sodium-ion batteries: advances and challenges. Small **22**(12), 2501262 (2026). https://doi.org/10.1002/smll.202501262
378. S. Guo, M. Yao, S. Liang, G. Fang, Failure mechanisms and practical optimizations for ah-scale aqueous zinc-ion pouch cells. Adv. Mater. **37**(44), e12364 (2025). https://doi.org/10.1002/adma.202512364

379. A. Gabryelczyk, S. Ivanov, A. Bund, G. Lota, Corrosion of aluminium current collector in lithium-ion batteries: a review. J. Energy Storage **43**, 103226 (2021). https://doi.org/10.1016/j.est.2021.103226
380. M. Deguchi, Y.M. Todorov, K. Abe, Functional electrolyte: design of corrosion inhibition additives to protect Cu current collectors in over-discharged state. J. Power. Sources **625**, 235613 (2025). https://doi.org/10.1016/j.jpowsour.2024.235613
381. S.-L. Lee, Y.-C. Chiu, T.-A. Pan, M.-C. Chen, Effects of trace amounts of Mn, Zr and Sc on the recrystallization and corrosion resistance of Al-5Mg alloys. Crystals **11**(8), 926 (2021). https://doi.org/10.3390/cryst11080926
382. F. Birol, Y. Birol, Corrosion behavior of twin-roll cast Al–Mg and Al–Mg–Si alloys. InL Proc. 9th Int. Conf. Aluminium Alloys **2024**, 338–344 (2004).
383. E. Yoon, J. Lee, S. Byun, D. Kim, T. Yoon, Passivation failure of Al current collector in $LiPF_6$-based electrolytes for lithium-ion batteries. Adv. Funct. Mater. **32**(22), 2200026 (2022). https://doi.org/10.1002/adfm.202200026
384. H. Jeong, J. Jang, C. Jo, A review on current collector coating methods for next-generation batteries. Chem. Eng. J. **446**, 136860 (2022). https://doi.org/10.1016/j.cej.2022.136860
385. C. Yang, J. Zhang, S. Cui, K. Wang, Y. Zhang, Optimizing coating layer to construct corrosion resistant current collectors for highly stable magnesium-air batteries. Surf. Interfaces **57**, 105739 (2025). https://doi.org/10.1016/j.surfin.2025.105739
386. Z. Chen, Q. Zhang, Q. Liang, Carbon-coatings improve performance of Li-ion battery. Nanomaterials **12**(11), 1936 (2022). https://doi.org/10.3390/nano12111936
387. A.W. Zia, S.A. Hussain, S. Rasul, D. Bae, S. Pitchaimuthu, Progress in diamond-like carbon coatings for lithium-based batteries. J. Energy Storage **72**, 108803 (2023). https://doi.org/10.1016/j.est.2023.108803
388. E. Feyzi, M. Rezaei, A. Nekahi, A.K. M R, M.B. Armand et al., Carbon in lithium-ion battery technology and beyond; Tribute to Kim Kinoshita. Energy Storage Mater. **79**, 104348 (2025). https://doi.org/10.1016/j.ensm.2025.104348
389. E.D. García-Bustos, D. Maxemin-Lugo, N. Diez-Torres, N. López-Perrusquia, M.A. Doñu-Ruiz et al., Electrochemical and tribocorrosion study of D2 steel coated with TiN with C or Cr addition films in 3.5 wt.% of NaCl in bi-distillated water solution. Materials **18**(12), 2733 (2025). https://doi.org/10.3390/ma18122733
390. H.C. Barshilia, M.S. Prakash, A. Poojari, K.S. Rajam, Corrosion behavior of nanolayered TiN/NbN multilayer coatings prepared by reactive direct current magnetron sputtering process. Thin Solid Films **460**(1–2), 133–142 (2004). https://doi.org/10.1016/j.tsf.2004.01.096
391. R. Gracia, D. Mecerreyes, Polymers with redox properties: materials for batteries, biosensors and more. Polym. Chem. **4**(7), 2206 (2013). https://doi.org/10.1039/c3py21118e
392. M.R. Yazdani McCord, A. Seppälä, M. Pourakbari-Kasmaei, J.B. Zimmerman, O.J. Rojas, From low conductivity to high energy efficiency: the role of conductive polymers in phase change materials. Chem. Eng. J. **508**, 160804 (2025). https://doi.org/10.1016/j.cej.2025.160804
393. H. Jo, J.-W. Ok, Y.-S. Lee, Y. Je, S. Kim et al., Ag-coated super duplex stainless steel AISI2507 with or without crystallization of secondary phase as advanced Li-ion battery case material. Crystals **14**(7), 653 (2024). https://doi.org/10.3390/cryst14070653
394. Y. Wang, Y. Pan, X. Xu, W. Zhang, R. Feng et al., Improving corrosion and wear resistances of 2195 Al–Li alloy by PEO and LDHs composite coating. J. Mater. Res. Technol. **28**, 1044–1061 (2024). https://doi.org/10.1016/j.jmrt.2023.12.067
395. W. Wang, C. Xin, Z. Feng, G. Li, R. Zhang et al., Ceramic coatings by microarc oxidation of Ti and Al alloys. Surf. Interfaces **33**, 102260 (2022). https://doi.org/10.1016/j.surfin.2022.102260
396. Y. Zhang, J. Wang, Stabilizing the cathode-electrolyte interphase for superior Li-ion batteries. Green Chem. Eng. **6**(4), 447–455 (2025). https://doi.org/10.1016/j.gce.2025.05.010
397. Y. He, Z. Chen, Y. Zhang, Strategies for improving cathode electrolyte interphase in high-performance dual-ion batteries. iScience **27**(8), 110491 (2024). https://doi.org/10.1016/j.isci.2024.110491
398. E.J. Cheng, H. Duan, M.J. Wang, E. Kazyak, H. Munakata et al., Li-stuffed garnet solid electrolytes: current status, challenges, and perspectives for practical Li-metal batteries. Energy Storage Mater. **75**, 103970 (2025). https://doi.org/10.1016/j.ensm.2024.103970
399. Z. Wang, H. Zhang, B. Cao, X. Zhao, H. Liu et al., Inhibition strategies of the hydrogen evolution reaction on zinc metal anodes in aqueous zinc-ion batteries: a review. J. Mater. Sci. Technol. **265**, 283–302 (2026). https://doi.org/10.1016/j.jmst.2025.11.040
400. W. Shin, D.-S. Kwon, M. Kim, J. Woo, H.-G. Jung et al., Fluorine-free binder strategies for high-nickel cathodes: toward PFAS-free lithium-ion batteries. ChemSusChem **19**, e202501943 (2026). https://doi.org/10.1002/cssc.202501943
401. Y. Cai, Y. Li, B. Jin, A. Ali, M. Ling et al., Dual cross-linked fluorinated binder network for high-performance silicon and silicon oxide based anodes in lithium-ion batteries. ACS Appl. Mater. Interfaces **11**(50), 46800–46807 (2019). https://doi.org/10.1021/acsami.9b16387
402. M. Das, K. Ghosh, M.W. Raja, Flexible ceramic based 'paper separator' with enhanced safety for high performance lithium-ion batteries: probing the effect of ceramics impregnation on electrochemical performances. J. Power Sources **606**, 234573 (2024). https://doi.org/10.1016/j.jpowsour.2024.234573
403. A.E.A.S. Fouda, S.E.H. Etaiw, S. Sobhy, Metal-organic frameworks based on heterocyclic ligands and some transition metals as effective carbon steel corrosion inhibitors in aqueous environment. J. Mol. Liq. **348**, 118402 (2022). https://doi.org/10.1016/j.molliq.2021.118402
404. R. Narayan, C. Laberty-Robert, J. Pelta, J.-M. Tarascon, R. Dominko, Self-healing: an emerging technology for

 https://doi.org/10.1007/s40820-026-02178-9

next-generation smart batteries. Adv. Energy Mater. **12**(17), 2102652 (2022). https://doi.org/10.1002/aenm.202102652

405. X. Yang, Z. Zhang, X. Xu, L. Wang, Y. Zhou et al., Self-healing functional materials for advanced batteries: mechanisms, dynamics, and applications. Energy Storage Mater. **75**, 103992 (2025). https://doi.org/10.1016/j.ensm.2024.103992
406. Y. Cheng, X. Xiao, K. Pan, H. Pang, Development and application of self-healing materials in smart batteries and supercapacitors. Chem. Eng. J. **380**, 122565 (2020). https://doi.org/10.1016/j.cej.2019.122565
407. A. Cordoba, F.A. Gutiérrez-Mejía, G. Cepeda-Granados, J.V. Cauich-Rodríguez, K. Esquivel Escalante, Self-healing polymer-based coatings: mechanisms and applications across protective and biofunctional interfaces. Polymers **17**(23), 3154 (2025). https://doi.org/10.3390/polym17233154
408. Z. Quan, X. Xiu, M. Li, L. Song, X. Jin et al., Recent progress and challenges of self-healing batteries. Energy Mater. Devices **3**(1), 9370058 (2025). https://doi.org/10.26599/emd.2025.9370058
409. S. B. Syed, M. H. Rashid, M. Rahman, Self-healing strategies for battery electrolytes: a review of recent breakthroughs and future prospects. Self-healing strategies for battery electrolytes: a review of recent breakthroughs and future prospects (unpublished). https://papers.ssrn.com/sol3/papers.cfm?abstract_id=4954895
410. H. Wang, P. Wang, Y. Feng, J. Liu, J. Wang et al., Recent advances on self-healing materials and batteries. ChemElectroChem **6**(6), 1605–1622 (2019). https://doi.org/10.1002/celc.201801612
411. V.-P. Vu, H.-M. So, A. Kim, J.Y. Lee, M. Oh et al., Self-healing polymer binders: next-generation battery applications. J. Mater. Chem. A **13**(45), 38541–38571 (2025). https://doi.org/10.1039/d5ta04403k
412. Y.-M. Zhao, F.-S. Yue, S.-C. Li, Y. Zhang, Z.-R. Tian et al., Advances of polymer binders for silicon-based anodes in high energy density lithium-ion batteries. InfoMat **3**(5), 460–501 (2021). https://doi.org/10.1002/inf2.12185
413. A. Marinow, Z. Katcharava, W.H. Binder, Self-healing polymer electrolytes for next-generation lithium batteries. Polymers **15**(5), 1145 (2023). https://doi.org/10.3390/polym15051145
414. X. Li, S. Deng, M.N. Banis, K. Doyle-Davis, D. Zhang et al., Suppressing corrosion of aluminum foils *via* highly conductive graphene-like carbon coating in high-performance lithium-based batteries. ACS Appl. Mater. Interfaces **11**(36), 32826–32832 (2019). https://doi.org/10.1021/acsami.9b06442
415. J. Chen, Z. Bai, X. Li, Q. Wang, J. Du et al., Reduced graphene oxide-modified aluminum foils as highly conductive and corrosion-resistant cathode current collectors for Li-ion batteries. Appl. Surf. Sci. **606**, 155002 (2022). https://doi.org/10.1016/j.apsusc.2022.155002
416. G.Y. Uzunoglu, S. Coskun, R. Yuksel, The role of hexagonal boron nitride (h-BN) in enhancing electrolytes for safer and efficient lithium-based batteries. ChemElectroChem **12**(11), e202500011 (2025). https://doi.org/10.1002/celc.202500011
417. X. Yu, A. Manthiram, A review of composite polymer-ceramic electrolytes for lithium batteries. Energy Storage Mater. **34**, 282–300 (2021). https://doi.org/10.1016/j.ensm.2020.10.006
418. M. Kannadasan, K. Sathiasivan, I. Pandurangan, M. Balakrishnan, Synergistic nanocomposite polymer electrolytes for advanced all-solid-state sodium-ion batteries. Int. J. Hydrog. Energy **78**, 634–641 (2024). https://doi.org/10.1016/j.ijhydene.2024.06.305
419. K.S. Randhawa, Advanced ceramics in energy storage applications: batteries to hydrogen energy. J. Energy Storage **98**, 113122 (2024). https://doi.org/10.1016/j.est.2024.113122
420. S. Wang, J. Liu, X. Song, H. Xu, Y. Gu et al., Artificial intelligence empowers solid-state batteries for material screening and performance evaluation. Nano-Micro Lett. **17**(1), 287 (2025). https://doi.org/10.1007/s40820-025-01797-y
421. A.H. Khalaf, Y. Xiao, N. Xu, B. Wu, H. Li et al., Emerging AI technologies for corrosion monitoring in oil and gas industry: a comprehensive review. Eng. Fail. Anal. **155**, 107735 (2024). https://doi.org/10.1016/j.engfailanal.2023.107735
422. Y. Liu, J. Sun, Y. Shang, X. Zhang, S. Ren et al., A novel remaining useful life prediction method for lithium-ion battery based on long short-term memory network optimized by improved Sparrow Search Algorithm. J. Energy Storage **61**, 106645 (2023). https://doi.org/10.1016/j.est.2023.106645
423. Z. Wei, Q. He, Y. Zhao, Machine learning for battery research. J. Power Sources **549**, 232125 (2022). https://doi.org/10.1016/j.jpowsour.2022.232125
424. Z. Nozarijouybari, H.K. Fathy, Machine learning for battery systems applications: progress, challenges, and opportunities. J. Power Sources **601**, 234272 (2024). https://doi.org/10.1016/j.jpowsour.2024.234272
425. D. Winkler, Predicting the performance of organic corrosion inhibitors. Metals **7**(12), 553 (2017). https://doi.org/10.3390/met7120553
426. R. van der Laag, A. Rizzato, T. Bäck, Y. Fan, Machine learning for hydrogen technologies: a comprehensive review of challenges, opportunities, and emerging trends. Int. J. Hydrog. Energy **197**, 152556 (2026). https://doi.org/10.1016/j.ijhydene.2025.152556